

SPONSORED BY



# 8<sup>th</sup> UHMWPE

## INTERNATIONAL MEETING PROGRAM

OCTOBER 19-20, 2017

THURSDAY & FRIDAY

“UNIONE INDUSTRIALE” CONGRESS CENTER  
UNIVERSITY OF TORINO & DREXEL UNIVERSITY  
TORINO, ITALY





**THE PURPOSE OF THE MEETING** is to bring together engineers, scientists, and clinicians from academia and industry and present leading edge research on advancements in medical grade UHMWPE technology and clinical applications.

Focus areas of this year's meeting are:

- advances in processing, crosslinking, and sterilization of UHMWPE
- structural composites and woven fiber applications of medical grade UHMWPE
- new methods of processing clinical and retrieval studies of highly crosslinked UHMWPE (HXLPE), with a special emphasis on the performance of thin acetabular liners and knee arthroplasty
- HXLPE performance in upper extremity, ankle, and spine
- international registry outcomes for HXLPE in hip and knee
- novel UHMWPE articulations with ceramic and PEEK bearing surfaces
- developments in Vitamin E and new antioxidant technologies for UHMWPE
- progress in thermal processing of HXLPE
- advancements in biologic aspects of UHMWPE wear debris

**SCIENTIFIC AND ORGANIZING COMMITTEE AND INVITED SPEAKERS:**

**President:** Pierangiola Bracco, Ph.D.

**Honorary President:** Steven Kurtz, PhD

Ebru Oral, Ph.D.

Elizabeth Walton-Paxton

Mark Tapšák, Ph.D.

Mark Allen

Rainer Walkenhorst, Ph.D.

**Organizer:** Jaclyn Schachtner

**Sponsorship:** We are pleased to announce that Celanese is supporting the 8th International Meeting as a Platinum Sponsor. We also welcome the involvement of Lima Corporate, Orthoplastics, Quadrant Meditech and Stryker Orthopaedics as Bronze Sponsors. We would also like to acknowledge Zzyzx as a Copper Sponsor.

# DAY ONE

UHMWPE Meeting Agenda Thursday, October 19, 2017

7:00 AM

**On-Site Registration Opens**

8:00 AM

**Opening Remarks**

[Steven Kurtz, Ph.D.](#)

8:15 AM

**Welcome**

[Isaac Khalil, Celanese](#)

8:20 AM

**Invited Talk 1: GUR 1001 - A New Injection Moldable GUR to Extend the Celanese Medical Materials Portfolio**

[Presenter: Rainer Walkenhorst, Ph.D.](#)

## **SESSION I: Oxidation, Stabilization, Biology and HXLPE**

[Session Co-Moderators: Pierangiola Bracco, Ph.D. and Orhun Muratoglu, Ph.D.](#)

8:50 AM

**Podium Talk 1:** The Role of Lamellar Morphology on the Oxidation Resistance of Post-Irradiated Aged UHMWPE

[Presenter: Anuj Bellare, Ph.D.](#)

9:05 AM

**Podium Talk 2:** The Roles of Stress, Lipids, and Reactive Oxygen Species in the Oxidation of UHMWPE: In Vitro Results Support Retrieval Findings

[Presenter: Douglas Van Citters, Ph.D.](#)

9:20 AM

**Podium Talk 3:** Effect of Vitamin E on the decay of UHMWPE Radicals for 10 Years

[Presenter: M. Shah Jahan, Ph.D.](#)

9:35 AM

**Podium Talk 4:** New Stabilization System for UHMWPE Based on Vitamin E and Tetracycline Antibiotic: Synergistic Increase in Oxidation Resistance

[Presenter: Mirek Slouf, Ph.D.](#)

9:50 AM

**Podium Talk 5:** The Properties of Accelerated Aged Highly Crosslinked UHMWPE Manufactured Using High Power X-Ray

[Presenter: Mark Allen](#)

10:05 AM

**Morning Coffee Break**

# DAY ONE

UHMWPE Meeting Agenda Thursday, October 19, 2017

## **SESSION II: Structure and Properties of UHMWPE Biomaterials**

Session Co-Moderators: Anuj Bellare, Ph.D., and Lisa Pruitt, Ph.D.

10:45 AM

**Podium Talk 6:** Shape memory effect in UHMWPE with different structures

Presenter: Fedor Senatov, Ph.D.

11:00 AM

**Podium Talk 7:** An investigation on the surface and bulk mechanical properties of clinically relevant UHMWPE formulations using nanoindentation and compression testing

Presenter: Sofia Arevalo

11:15 AM

**Podium Talk 8:** Different Consolidation and Sterilization Methods have No Impact on Highly Crosslinked UHMWPE Properties

Presenter: Lin Song, Ph.D.

11:30 AM

**Podium Talk 9:** The Effect of Sequential Gamma Radiation on Crosslinking of UHMWPE with Vitamin E

Presenter: Mark Allen

11:45 AM

**Podium Talk 10:** Characterization Methods for Structure-Property Relationships in Clinical Formulations of UHMWPE

Presenter: Louis Malito

12:00 PM

**Buffet Lunch and POSTER SESSION**

# DAY ONE

UHMWPE Meeting Agenda Thursday, October 19, 2017

## SESSION III: Advances in Processing, Crosslinking, and Additives

Session Co-Moderators: Ebru Oral, Ph.D., and Rainer Walkenhorst, Ph.D.

1:30 PM

### **Invited Talk 2: Primer on Drug Delivery from UHMWPE Biomaterials with Applications in Safe and Efficacious Release of Pain Medication**

Presenter: Ebru Oral, Ph.D.

2:00 PM

### **Podium Talk 11: Pressure-Induced Recrystallization of UHMWPE**

Presenter: Lin Song, Ph.D.

2:15 PM

### **Podium Talk 12: Influencing UHMWPE Molecular Weight Distribution by High Shear Polymer Modification**

Presenter: Mark Tapšák, Ph.D.

2:30 PM

### **Invited Talk 3: Chemically crosslinked UHMWPE: A comparison of different peroxides**

Presenter: Pierangiola Bracco, Ph.D.

3:00 PM

### **Podium Talk 13: Rifampin and vancomycin-eluting UHMWPE for long-term infection treatment**

Presenter: Orhun Muratoglu, Ph.D.

3:15 PM

### **Afternoon Coffee Break**

# DAY ONE

UHMWPE Meeting Agenda Thursday, October 19, 2017

## SESSION IV: Clinical Performance of HXLPE Biomaterials

Session Co-Moderators: Steven Kurtz, Ph.D. and Tim Wright, Ph.D.

3:45 PM

### **Invited Talk 4: Short-Term Clinical Outcomes of Vitamin E- and Covernox-Containing HXLPE in TKA**

Presenter: Elizabeth Paxton

4:15 PM

### **Podium Talk 14: Clinical and Radiographic Outcomes of a Novel Polyethylene Glenosphere in Reverse Shoulder Arthroplasty**

Presenter: Carlo Felice De Biase, Ph.D.

4:30 PM

### **Podium Talk 15: Clinical mid-term results for vitamin enhanced HXLPE**

Presenter: Daniel Delfosse, Ph.D.

4:45 PM

### **Podium Talk 16: Clinical Wear and Oxidative Performance of Long-Term Duration Polyethylene Acetabular Retrievals**

Presenter: Francisco Medel, Ph.D.

5:00 PM

### **Podium Talk 17: Long-term In Vivo Degradation of 1st Generation Highly Crosslinked Polyethylene in THA**

Presenter: Jaclyn Schachtner

5:15 PM

### **Podium Talk 18: Antioxidant Stabilized Highly Crosslinked Polyethylene in TKA: A Retrieval Analysis**

Presenter: Timothy Wright, Ph.D.

5:30 PM

**Day 1 Meeting Adjourns**

6:00 PM

**Bus Departs for Reception and Dinner Begins at Venaria Reale**

# DAY TWO

UHMWPE Meeting Agenda Friday, October 20, 2017

8:00 AM

**On Site Registration Opens**

## **SESSION V: New Tribological Applications of UHMWPE Biomaterials**

Session Co-Moderators: Francisco Medel, Ph.D. and Ryan Siskey

8:30 AM

**Podium Talk 19:** Edge Loading Properties of Glenoids Articulating against a Ceramic Humeral Head: Comparative Wear Study of Conventional and Highly Cross-Linked Vitamin E polyethylene

Presenter: [Reto Lerf, Ph.D.](#)

8:45 AM

**Podium Talk 20:** The Tribological Performance of Crosslinked UHMWPE on Coated Titanium

Presenter: [Ryan Siskey](#)

9:00 AM

**Podium Talk 21:** The Tribological Performance of UHMWPE on Pyrolytic Carbon

Presenter: [Hideyuki Sakoda, Ph.D.](#)

9:15 AM

**Podium Talk 22:** Influence of radiation conditions and aging duration on the wear behaviour of a vitamin E stabilized TKA bearing

Presenter: [Jens Schwiesau](#)

9:30 AM

**Invited Talk 5:** Tribology of PEEK-on-UHMWPE Bearings and Applications in TKA

Presenter: [Steve Kurtz, Ph.D.](#)

10:00 AM

**Morning Coffee Break and POSTER SESSION**

# DAY TWO

UHMWPE Meeting Agenda Friday, October 20, 2017

## SESSION VI: New Frontiers in UHMWPE

Session Co-Moderators: Steve Kurtz, Ph.D., and Pierangiola Bracco, Ph.D.

10:45 AM

**Podium Talk 23:** UHMWPE Compounding with High Shear Polymer Modification and Challenging Examples

Presenter: Mark Tapšák, Ph.D.

11:00 AM

**Podium Talk 24:** Biomimetic UHMWPE structures for restoration of osteochondral defects

Presenter: Fedor Senatov, Ph.D.

11:15 AM

**Podium Talk 25:** Ultrahigh Molecular Weight Polyethylene Membrane for Use in Vascular Stent Graft Applications - Preliminary Evidence From an Ovine Peripheral Implantation Model

Presenter: Wei Cheng, Ph.D.

11:30 AM

**Podium Talk 26:** Preparation of Medical Ultra High Molecular Weight Polyethylene Fiber via Dry Spinning

Presenter: Xinwei Wang, Ph.D.

11:45 AM

**Podium Talk 27:** Micro injection molding Processing of UHMWPE using ultrasonic vibration energy

Presenter: Marcelo Hernandez Avila, Ph.D.

12:00 PM

**Closing Remarks**

Presenter: Steven Kurtz, Ph.D.

12:15 PM

**Meeting Adjourn**

WITH  
SPECIAL  
THANKS  
TO:





# MATERIAL OF CHOICE FOR IMPROVED PATIENT COMFORT

**For more than 50 years, GUR® UHMWPE has been the material of choice among orthopedic surgeons for joint replacements. Our durable and abrasion resistant UHMWPE improves patient comfort, and delivers excellent impact strength and lubricity. Contact us today and discover the benefits of GUR UHMWPE.**

## GUR UHMWPE benefits:

- Low wear
- Excellent lubricity
- Exceptional impact strength
- High energy absorption
- High purity
- Biocompatible
- ASTM F648, ISO 5834-1 approval
- FDA compliant
- Drug and device master file listed

## GUR UHMWPE applications

- Hip, knee, and shoulder arthroplasty
- Other joint replacements
- Spine applications and replacements

### CELANESE

222 West Las Colinas Boulevard  
Suite 900N  
Irving, TX 75039  
(800) 833-4882

[celanese.com/UHMWPE](http://celanese.com/UHMWPE)



# An investigation on the surface and bulk mechanical properties of clinically relevant UHMWPE formulations using nanoindentation and compression testing

Arevalo, SE and Pruitt, L

Department of Mechanical Engineering, University of California Berkeley, CA

Correspondence: searevalo94@berkeley.edu

**Introduction:** Ultra High Molecular Weight Polyethylene (UHMWPE) was introduced in the early 1960s as the articulating bearing surface for total joint replacements [1,2]. Since its introduction to the orthopedic industry, UHMWPE has become the gold-standard material due to its biocompatibility, low coefficient of friction and desirable mechanical properties [2]. However, adhesive/abrasive wear and subsequent implant loosening have challenged this polymer as an implant material [3]. It was observed that crosslinking UHMWPE improved wear resistance but at the expense of ductility [4,5]. It is well known that radiation associated with sterilization or crosslinking of UHMWPE can compromise mechanical properties owing to free radicals and associated oxidation degradation [6,7]. Antioxidants such as Vitamin E were introduced to improve oxidation resistance and mechanical properties [8,9]. An ongoing challenge in assessing clinical performance of UHMWPE formulations is correlation of structure-property relationships in retrievals; Kurtz et al validated the use of small punch testing to measure the mechanical properties of retrieved UHMWPE components and to elucidate oxidation degradation schemes that occur in-vivo across clinical formulations of UHMWPE [2,10,11]. While there is a plethora of research into local tensile properties obtained using small punch tests, there is a paucity of studies addressing nanoscale properties and their correlation to compressive properties for clinical formulations of UHMWPE. Little is known about the influence of antioxidants on the surface mechanical properties (elastic modulus and hardness) of UHMWPE infused with different types of antioxidants (Vitamin E and AO) across different crosslinking dosages. Understanding the effect of crosslinking in the presence of various antioxidants on the surface mechanical properties may elucidate wear mechanisms in contemporary formulations of UHMWPE. The use of nanoindentation can be used to distinguish the surface mechanical properties across different formulations and to assess correlation with bulk compression properties.

We investigated the nanomechanical and bulk compression properties of two clinically relevant antioxidants at various crosslinking dosages using nanoindentation and compression testing. We show that the nanomechanical properties are strongly correlated with the bulk properties; we suggest nanoindentation as an efficient and nondestructive alternative to compression testing for locally analyzing the surface mechanical properties of retrievals.

**Methods and Materials:** We studied the nanomechanical and bulk mechanical properties of UHMWPE Type GUR 1020 for two types of antioxidants at different

crosslinking dosages. The following two material groups were tested: (1) UHMWPE infused with Vitamin E (VE) from Orthoplastics at 0 kGy (control), 50 kGy, 75 kGy, 100 kGy, 125 kGy and (2) UHMWPE infused with COVERNOX™ antioxidant (AO) from Depuy at 0 kGy (control) and 80 kGy.

**Sample preparation:** Nanoindentation samples were fabricated into 4 mm cube samples from stock material and then microtomed with a glass blade to obtain optically smooth surfaces [2]. Compression samples were machined into cylinders with a 10 mm diameter and 15 mm height [12,13].

**Nanoindentation-Tip Area Calibration:** A tip area calibration was performed to account for deviations from the ideal tip geometry [14,15]. The tip-area function, shown in Equation 1, relates the contact area and contact depth during indentation.

$$A_c(h_c) = C_0 h_c^2 + C_1 h_c + C_2 h_c^{1/2} + C_3 h_c^{1/4} \quad [1]$$

The coefficients of Equation 1 were obtained experimentally by making a series of indentations on a standard calibration polymer: polycarbonate (2.95 GPa) [16]. A series of 36 indents were performed on polycarbonate for a load range of 100-10000 uN [14]. The area as a function of penetration depth was fitted to Equation 1 and provided the values of the coefficients.

**Nanoindentation- Testing Parameters & Data Analysis:** A TI 900 TriboIndenter (Hysitron, Minneapolis, MN) was used to perform indentations at ambient temperature using a conospherical diamond tip with a nominal 20 um radius. The indentations were load-controlled with a rate of 30 uN/s. A trapezoidal loading-unloading function was used [14,15,17]. Five specimens (n=5) were tested for each material group. Three groups of fifteen indentations per specimen were performed. Each sample group comprised of 15 indentations with a maximum load prescribed as 150-650 uN in equally spaced intervals [14].

We developed a custom MATLAB function to calculate the stiffness, S, elastic modulus, E, and contact hardness, H, of the material from the force-displacement curves [18]. A MATLAB built-in function (polyfit.m) was used to perform a linear regression on the initial region of the unloading curve in order to capture the elastic stiffness of the polymer (Equation 2) [14,17,18].

$$S = \frac{dP}{dh} = \frac{2\sqrt{A_c(h_c)}}{\sqrt{\pi}} E_r \quad [2]$$

The elastic modulus (E) was then obtained by applying Equation 3.

$$\frac{1}{E_r} = \frac{1-\nu^2}{E} + \frac{1-\nu_i^2}{E_i} \quad [3]$$

The contact hardness of the material is defined as the maximum load applied over the contact area (Equation 4).

$$H_c = \frac{P_{\max}}{A_c(h_c)} \quad [4]$$

#### Compression - Testing Parameters & Data Analysis:

Compression tests were performed using a servohydraulic Instron machine at a displacement rate of 18 mm/min. Five (5) specimens were tested for each material group. The slope of the linear region was used to determine the elastic modulus and a 0.2% offset method was used to determine the yield strength (ASTM D695-15).

**Statistics and property correlations:** Spearman's correlation ( $\rho$ ) was used to determine the relationship between the mechanical properties (Figure 1, 2) obtained from nanoindentation and compression tests. Additionally, an analysis of variance (ANOVA) was used to determine statistical significance ( $p < 0.05$ ) across different formulations (crosslinking dosage and type of antioxidant) of medical-grade UHMWPE.

**Results:** The mechanical properties obtained from nanoindentation and compression testing is shown in Table 1. Our findings indicate a very strong positive correlation between the elastic modulus of nanoindentation and compression tests. As expected, an increase in nanoindentation elastic modulus results in an increase in hardness. Similarly, an increase in compressive elastic modulus results in an increase in yield strength (Figure 2).

**Table 1:** The surface and bulk mechanical properties obtained from nanoindentation and compression testing, of clinically relevant UHMWPE formulations.

	Nano-indentation		Compression	
	Elastic Modulus [MPa]	Hardness [MPa]	Elastic Modulus [MPa]	Yield Strength [MPa]
<b>AO</b>	745.33 ±187.46	34.95 ±9.28	646.12 ±72.27	21.55 ±1.70
<b>AO-80 kGy</b>	918.38 ±240.12	43.83 ±13.45	802.97 ±28.29	23.39 ±0.36
<b>VE</b>	611.16 ±205.43	29.62 ±9.88	629.18 ±28.51	21.81 ±0.26
<b>VE-50 kGy</b>	815.09 ±141.60	33.51 ±5.27	696.33 ±47.96	22.06 ±1.18
<b>VE-75 kGy</b>	912.84 ±147.41	41.10 ±9.66	756.62 ±10.69	23.94 ±0.29
<b>VE-100 kGy</b>	717.08 ±95.91	32.55 ±4.95	669.18 ±22.40	22.27 ±0.68
<b>VE-125 kGy</b>	880.66 ±129.73	36.16 ±7.79	718.98 ±31.35	23.02 ±0.87
<b>GUR 1020</b>	728.46 ±110.65	36.99 ±9.02	619.66 ±36.45	20.59 ±0.72

**Discussion:** This study uniquely provides correlation of surface mechanical properties to bulk compression properties of contemporary formulations of UHMWPE. Our findings show a very strong positive correlation ( $\rho > 0.8$ ) between nanoindentation and compression testing. Furthermore, nanoindentation is sensitive to different material formulations. When different crosslinking dosages were tested, nanoindentation was better able

discriminate across different materials ( $p < 0.05$ ) as opposed to compression testing. This finding concludes that nanoindentation has the ability to detect local surface mechanical changes at the nanometer length scale, an advantage over compression testing and punch testing. Nanoindentation is thus validated as an alternate method for calculating the mechanical properties of explants.

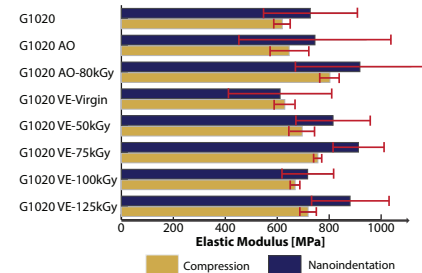


**Figure 1:** Compression and nanoindentation elastic modulus (assuming a Poisson ratio of 0.46) for different formulation of medical-grade UHMWPE GUR 1020.

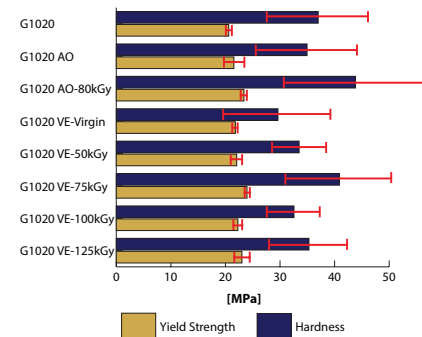


**Figure 2:** Yield strength from compression testing and contact hardness results from nanoindentation for different formulation of medical-grade UHMWPE GUR 1020.

#### Reference:

- [1] R.G. Voltz (1987). *Drug Therapy Hosp.* 35-46.
- [2] S.M. Kurtz (2009). *UHMWPE Biomaterials Handbook*.
- [3] Dumbleton (2002). *J of Arthroplasty*. 17: 649-661.
- [4] McKellop et al. (1990). *J of Orthopaedic Research*. 17:157-167.
- [5] O.K. Muratoglu (1999). *Biomaterials*. 20(16):1463-70.
- [6] Jahan et al. (1991). *J Biomed Mater Res*. 25:1005-17
- [7] E. Oral, O.K. Muratoglu (2007). *Nucl Instrum Methods Phys Res B*. 265:18-22.
- [8] N. Tomita et al. (1999). *J Biomed Mater Res (Appl Biomat)*. 48:474-8.
- [9] E. Oral et al. (2006). *J of Arthroplasty*. 21:580-91.
- [10] S.M. Kurtz et al. (1997). *Biomaterials*. 18: 1659-1663.
- [11] S.M. Kurtz et al. (2009). *J of Biomed Mat Res Part A*. 90A.2: 549-563.
- [12] K. Masayoshi et al. (1988). *J of Mat Sci*. 23:4085-4090.
- [13] S.M. Kurtz et al. (1998). *Biomaterials*. 19: 1989-2003.
- [14] C.K. Klapperich et al. (2001). *J of Tribo*. 123: 624.
- [15] *Probe Calibration*. 1st ed. Minneapolis: Hysitron.
- [16] L. Pruitt et al. (1996). *Poly Eng & Sci*. 36: 1300-1305.
- [17] A.C Fischer-Cripps. Nanoindentation.
- [18] G.M. Pharr et al (1992). *J Mater. Res*.7: 613-617.

## The Effect of Sequential Gamma Radiation on Crosslinking of UHMWPE with Vitamin E

Allen M.D<sup>1</sup>

<sup>1</sup>Orthoplastics Ltd, Grove Mill, Todmorden Road, Bacup, Lancashire, OL13 9EF.

[mallen@orthoplastics.com](mailto:mallen@orthoplastics.com)

**Introduction:** Crosslinking of Ultra High Molecular Weight Polyethylene (UHMWPE) has been utilised for some time to improve the wear performance of medical devices. Sequential crosslinking of UHMWPE using gamma irradiation was introduced as a measure to maintain mechanical properties of crosslinked UHMWPE, whilst improving the oxidative stability, and has been in use for over a decade. It is reported that the effectiveness of the sequential dose of irradiation is reduced compared to the original exposure [1]. Vitamin E blended UHMWPE also aims to improve oxidative stability of the material without requiring a thermal stabilisation process that may reduce the mechanical performance [2]. These materials are currently sterilised using non ionizing methods.

The purpose of this study was to evaluate the effect of a second dose of gamma irradiation on the crosslinking and mechanical properties of UHMWPE with and without blended vitamin E.

**Materials and Methods:** Orthoplastics crosslinked production batches were sent for a second exposure of gamma radiation at two separate doses (24.35 kGy and 38.6 kGy). Materials included both standard GUR 1020 (Celanese, USA) and vitamin E blended GUR 1020 UHMWPEs.

**Table 1 - List of materials included in the study and their sequential and cumulative irradiation doses.**

Project Material Ref <sup>a</sup>	Polymer	Initial Irradiation Dose (kGy)	Sequential Irradiation Dose (kGy)	Total Irradiation Dose (kGy)
Material 1	GUR1020-E	49.2	N/A	49.2
Material 1a	GUR1020-E	49.2	24.35	73.55
Material 1b	GUR1020-E	49.2	38.6	87.8
Material 2	GUR1020-E	81.2	N/A	81.2
Material 2a	GUR1020-E	81.2	24.35	105.55
Material 2b	GUR1020-E	81.2	38.6	119.8
Material 3	GUR1020	50.91	N/A	50.91
Material 3a	GUR1020	50.91	24.35	75.26
Material 3b	GUR1020	50.91	38.6	89.51
Material 4	GUR1020	74.96	N/A	74.96
Material 4a	GUR1020	74.96	24.35	99.31
Material 4b	GUR1020	74.96	38.6	113.56

Crosslink properties of the materials were evaluated according to swell ratio testing methods outlined in ASTM F2214.

Mechanical properties of the materials were evaluated using IZOD impact strength in accordance with methods outlined in ASTM D256/F648.

**Results:** IZOD impact strength decreased with increasing irradiation dose. The decrease in impact strength was reduced between the initial irradiation dose and the second irradiation doses (**Fig. 1**).

Increasing irradiation dose resulted in a decrease in the swell ratio (**Fig. 2**).

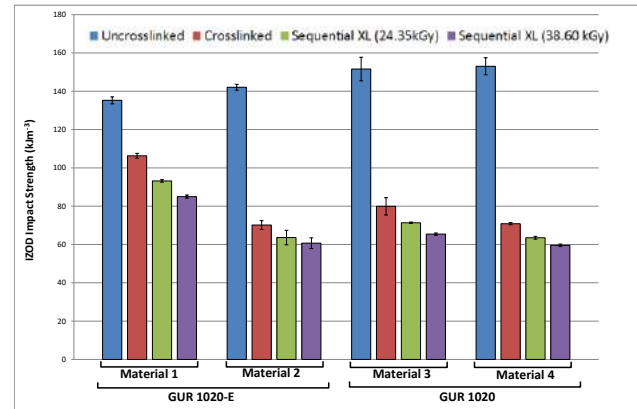


**Figure 1:** IZOD impact strength of all materials (Mean  $\pm$  SD, n=5).

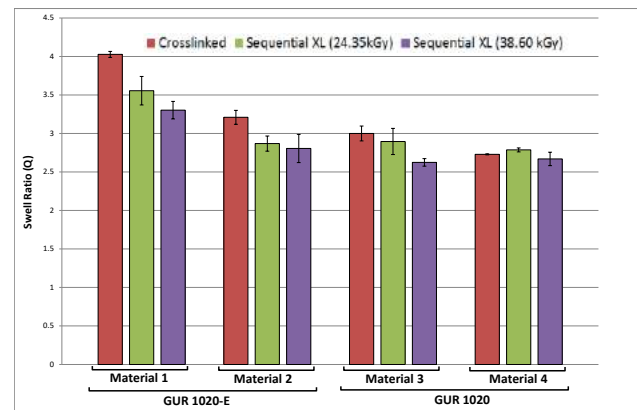


**Figure 2:** Swell ratio of all materials (Mean  $\pm$  SD, n=3).

**Discussion:** The reduction in the change in impact strength between the crosslinked and sequentially crosslinked groups for all materials suggests that the second dose of irradiation is not as effective in crosslinking the material as the first dose; this is supported by the reduction in impact strength not being proportional to the irradiation dose seen at each step.

**Conclusions:** This study concludes that sequential doses of gamma radiation are less effective at crosslinking UHMWPE than the first dose. This would suggest that crosslinked vitamin E UHMWPE can be sterilized using low irradiation doses (up to 25kGy) without affecting the crosslink density of the material significantly. This provides a cost benefit compared to non-ionizing methods of sterilization currently in use.

**Further Studies:**

- Additional studies are required with larger sample sizes to confirm the hypothesis.
- Further sequential irradiation doses.

**References**

- [1] A. Wang *et al.*, J. Phys D Appl Phys., 39, pp 3213-19, (2006).  
[2] E. Oral *et al.*, Int Orthop., 35(2), pp 215-23, (2011).

## The Properties of Accelerated Aged Highly Crosslinked UHMWPE Manufactured Using High Power X-Ray

Allen M.D

([mallen@orthoplastics.com](mailto:mallen@orthoplastics.com))

Orthoplastics Ltd, Grove Mill, Todmorden Road, Bacup, Lancashire, OL13 9EF.

### Introduction

Commercial X-ray processing techniques have been developed at Synergy healthcare (Daniken, Switzerland) utilizing high energy electron beam accelerator. Previous studies have shown that dose distribution and attenuation are reduced significantly when compared to Gamma and e-Beam technologies; in addition studies have shown that X-Ray processing is comparable to conventional Gamma processing. Highly crosslinked Ultra High Molecular Weight Polyethylene (UHMWPE) for orthopaedic applications, are characterized by physical/mechanical test methods outlined in both ISO and ASTM international standards.

The purpose of this study was to evaluate the physical mechanical characteristics of UHMWPE processed through X-ray and Gamma (Co<sub>60</sub>) irradiation processes at different administered doses and after accelerated ageing.

### Materials and Methods

Processing was completed on a small scale development with product 84mm Ø x 500mm.

Compression molded (Celanese GUR1020) was evaluated at five nominal irradiation doses (50, 75, 100, 125 and 150kGy), test samples were manufactured and accelerated aged in a pressure vessel at 70°C and 5.033bar for 14 days in accordance with ASTM F2003. Table 1 shows the material variants.

TP0483-3 14 day aged	21016M GAMMA	50kGy
	20909M XRAY	
TP0483-4 14 day aged	21016M GAMMA	75kGy
	21036M XRAY	
TP0483-5 14 day aged	21016M GAMMA	100kGy
	20994M XRAY	
TP0483-6 14 day aged	21064M GAMMA	125kGy
	20994M XRAY	
TP0483-7 14 day aged	21064M GAMMA	150kGy
	20994M XRAY	

Table 1

### Analysis

Processed materials were analyzed in accordance with the principle guidance of ASTM F2565, namely the characterization of Extensively Irradiation-Crosslinked Ultra-High Molecular Weight Polyethylene Fabricated Forms for Surgical Implant Applications. Testing of the materials included:

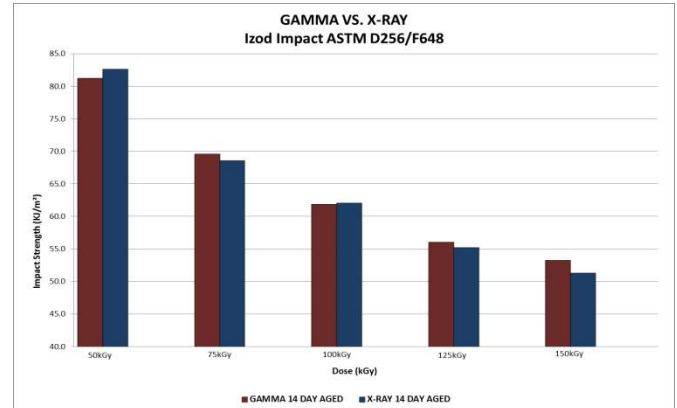
Izod Impact Strength	ASTM D256/ F648
Tensile Testing	ASTM D638
Small Punch Testing	ASTM F2183
Thermal Properties (DSC)	ASTM F2625
TVI	ASTM F2183
Oxidation Index	ASTM F2102

### Results and Discussion

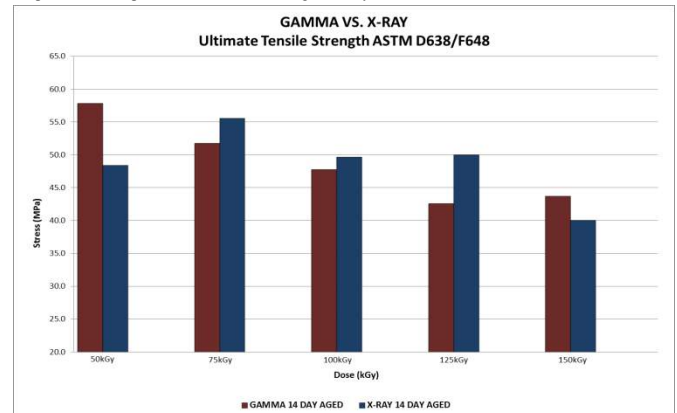
Irradiation Dose (kGy)	Tensile UTS (mPa)	Tensile Yield (mPa)	Tensile Elong. (%)	Izod Impact (J/m <sup>2</sup> )	TVI
50	0.01	0.18	0.07	0.11	1.00
75	0.17	0.00	0.47	0.18	0.10
100	0.03	0.36	0.47	0.80	0.89
125	0.02	0.72	0.22	0.13	0.98
150	0.14	0.57	0.13	0.00	0.04

Table 2 – Table of P-Values for associated materials and methods

One way ANOVA analysis of variance was completed on the data sets with a  $P \leq 0.05$  considered statistically significant (Table 2). Limited statistical analysis indicated that the variation between X-Ray and Gamma processing on the properties of accelerated aged HXL UHMWPE was, in most cases, not significant.



Graph 1 – Izod Impact data of Accelerated Aged X-Ray V.s Gamma Materials



Graph 2 – Ultimate Tensile Strength data of Accelerated Aged X-Ray V.s Gamma Materials

The hypothesis of the study was that X-Ray crosslinking is comparable to Gamma crosslinking in terms of mechanical and physical properties of UHMWPE. The results show that even with small sample sets the variance between Gamma and X-Ray is in most cases not significant.

Significant values could be attributed to the very small data sets for the products tested and the difference in Dose administered in the processes.

### Conclusions

X-Ray crosslinking is comparable to conventional Gamma processing. Further studies are required with larger data sets to confirm the findings of this study.

### Further Studies

- Additional studies are required with larger sample sizes to confirm the hypothesis.

# The Role of Lamellar Morphology on the Oxidation Resistance of Post-Irradiated Aged UHMWPE

Mollazadeh-Moghaddam, K<sup>1</sup>; D'Angelo, F<sup>2</sup>; Bracco, P<sup>2</sup>; Bellare, A<sup>1\*</sup>

<sup>1</sup>Department of Orthopedic Surgery, Brigham & Women's Hospital, Harvard Medical School, Boston, MA

<sup>2</sup>Department of Chemistry, University of Turin, Turin, Italy

Anuj@alum.mit.edu

**Introduction:** Joint replacement components of Ultrahigh Molecular Weight Polyethylene (UHMWPE) have historically been subjected to sterilization by gamma radiation in air. It is well documented that the long-lived free radicals produced after irradiation with ionizing radiation decrease the mechanical strength and ductility of UHMWPE [1, 2]. The clinical impact of oxidative degradation involving delamination wear of tibial inserts and rim cracking of acetabular components are also well documented, as well as accelerated particulate wear that leads to osteolysis, all of which result in early revision surgery to replace the implant [3, 4]. Consequently, ionizing radiation treatment to sterilize or to induce crosslinking in UHMWPE is followed by post-radiation thermal treatment to quench free radicals or by incorporation of antioxidants to react to the free radicals as they migrate to lamellar surfaces before they can result in oxidation by reaction with dissolved oxygen available in the amorphous phase of the polymer [5]. The lamellar morphology of UHMWPE must affect the extent of oxidative degradation since higher crystallinity would mean more trapped free radicals while lower crystallinity would result in more of the free radicals being used to form crosslinks or induce chain scission in the amorphous regions. Yet, to date, the quantitative relationship between the crystalline morphology and oxidation has not been established. In this study, we prepared UHMWPE rods with several lamellar morphologies, each associated with a unique lamellar surface area, and subjected them to an identical radiation dose followed by accelerated aging and oxidation measurement to develop a quantitative relationship between lamellar surface area and oxidation. We hypothesized that higher lamellar surface area would result in a lower extent of oxidation in post-irradiated aged UHMWPE.

**Methods and Materials:** Rod stock of GUR 1050 UHMWPE (MediTECH Medical Polymers, Fort Wayne, IN) were machined into rods of 25mm length and 12.5mm diameter to fit snugly into a custom built high pressure cell. The specimens were heated to 140°C, 160°C, 180°C, 200°C, 220°C, 240°C, and 260°C, respectively, in the high-pressure cell followed by application of 500 MPa pressure using a Carver hydraulic press and then slow cooled to room temperature under pressure followed by depressurization. The degree of crystallinity ( $n = 3$ ) in the pre-irradiation samples were measured using a Q1000 calorimeter (TA Instruments, New Castle, DE) differential scanning calorimeter (DSC), using a heat of fusion of 293 J/g. Ultra-small angle x-rays scattering (USAXS) was performed at the UNICAT beamline of the Advanced Photon Source, Argonne National Laboratory, Argonne, IL and used to measure the specific surface area of lamellae using a previously established method [6]. The UHMWPE

specimens were subjected to gamma radiation to a 50 kGy dose (Steris Inc, Northborough, MA) with no post-thermal treatment. Accelerated aging was performed in accordance with ASTM standard F2003-02. A Parr bomb reactor has filled with oxygen gas and maintained at 5 Atmosphere pressure and 70°C temperature for a period of 14 days. Fourier Transform Infrared (FTIR) spectroscopy was performed using a Nicolet Magna 860 spectrometer on a 100-200 $\mu$ m thickness sections of the samples ( $n=6$ ). The oxidation index (OI) was defined to be the ratio of the area under carbonyl peak at 1740  $\text{cm}^{-1}$  to the area under methylene stretching absorbance at 1370  $\text{cm}^{-1}$ .

**Results:** High pressure crystallization of UHMWPE showed a systematic increase in crystallinity with an increase in the crystallization temperature from 140°C to 180°C and thereafter there was no statistically significant difference ( $p>0.05$ , ANOVA) in the observed crystallinity over a temperature range of 180°C-200°C (see Table 1). The lamellar thickness calculated from a combination of USAXS and DSC measurements, however, showed a monotonic increase under high pressure crystallization from 140-240°C and then it decreased slightly at 260°C. The crystallinity and lamellar thickness of the 500 MPa pressure crystallized specimens at 140°C and 160°C were lower than the corresponding crystallinity and lamellar thickness of the ram extruded, untreated control UHMWPE.

**Table 1.** Crystallinity and lamellar thickness (average  $\pm$  standard deviation) of the control and crystallized samples at various temperatures (pressure = 500MPa).

Crystallization Temperature (°C)	Crystallinity percentage (%)	Lamellar Thickness (nm)
Control	51.8 $\pm$ 0.8	23.8 $\pm$ 0.3
140	44.7 $\pm$ 3.1	20.6 $\pm$ 1.4
160	48.3 $\pm$ 0.3	21.7 $\pm$ 0.1
180	68.9 $\pm$ 0.3	106.7 $\pm$ 0.4
200	69.4 $\pm$ 1.4	125.6 $\pm$ 2.4
220	70.3 $\pm$ 0.3	226.4 $\pm$ 0.9
240	68.5 $\pm$ 3.0	264.4 $\pm$ 11.6
260	66.8 $\pm$ 4.8	235.1 $\pm$ 16.9

The Lorentz corrected USAXS scattering intensity plotted against the scattering vector,  $q$  where  $q=(2\pi/\lambda)(\sin\theta)$ ,  $\lambda$  is the wavelength of x-rays and  $\theta$  is one-half the scattering angle showed a wide range of scattering peaks for the various UHMWPEs (Figure 1). The scattering peak was below the scattering vector of 0.1 [ $\text{nm}^{-1}$ ] for the control UHMWPE as well as the 140°C and 160°C high pressure crystallized UHMWPE whereas at higher temperatures the main scattering peak was at lower values of scattering vectors, corresponding to a larger inter-lamellar spacing.

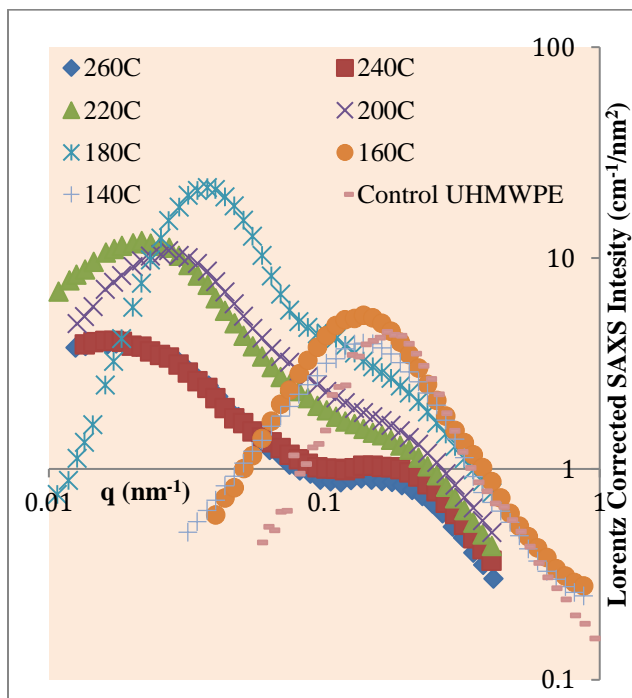


**Figure 1.** A log-log plot of Lorentz corrected SAXS Intensity versus scattering vector “q” for various UHMWPE specimens.

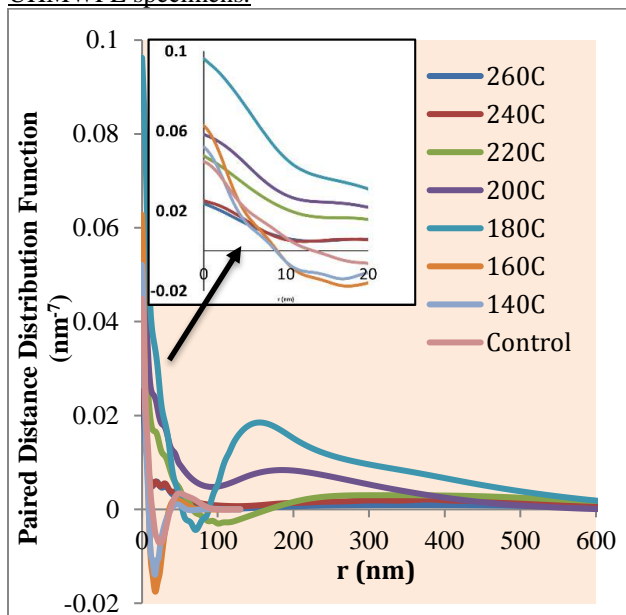


**Figure 2.** Paired distance distribution functions (PDDF) of UHMWPE specimens as a function of radial distance “r”.

The PDDF of UHMWPE specimens showed a variation in both inter-lamellar spacing (represented by the first maximum) and specific surface area of lamellae which is equal to  $-2 \times \text{slope of the initial linear decay in PDDF}$  divided by the electron density difference between

amorphous and lamellar regions (Figure 2). FTIR experiments showed that the bomb aged 50 kGy irradiated PE had a substantially higher OI compared to air aged PE at all subsurface depths, with the maximum OI just below the surface. The bomb aged 50 kGy PE had a maximum OI of  $1.68 \pm 0.13$  compared to  $0.29 \pm 0.09$  for control PE. The OI decreased exponentially with increase in the specific surface area of the lamellae ( $R^2=0.96$ ) over the range of surface areas studied (Figure 3).

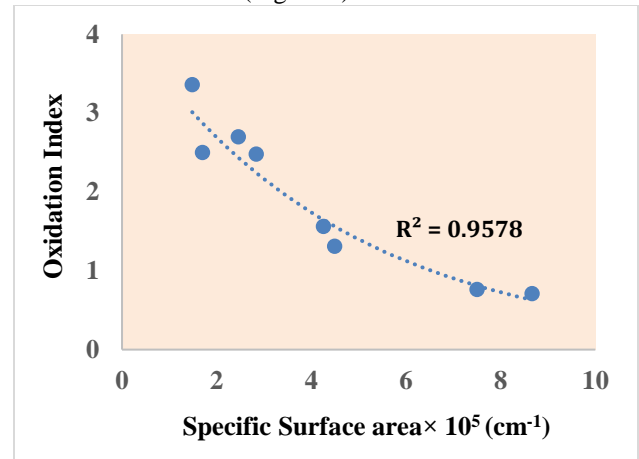


**Figure 3.** Oxidation index versus specific surface area of lamellae for various UHMWPE specimens.

**Discussion:** This post-irradiation accelerated aging study on UHMWPE specimens with different lamellar surface areas and lamellar thicknesses, showed that the pre-irradiation lamellar surface area strongly affected oxidation resistance. This is likely due to a small lamellar surface area associated with high pressure crystallized, high crystallinity UHMWPEs compared to lower crystallinity UHMWPEs due to the higher nucleation density in the latter. The lower crystallinity UHMWPEs not only have a larger number of thin lamellae but the total content of lamellae is less than in high pressure crystallized UHMWPEs that are crystallized at temperatures exceeding 160°C. Therefore, they trap less free radicals than high pressure crystallized UHMWPEs and induce a lower extent of long-term oxidation. Further investigation of UHMWPEs of identical crystallinity but with different lamellar thicknesses (and consequently surface area) would provide further insight into the quantitative relationship between the lamellar surface area of UHMWPE and its oxidation resistance. It would also be useful to investigate their effect on mechanical and wear performance of irradiated UHMWPEs in joint replacement prostheses.

**References:** [1] Premnath V, et al. *Biomaterials*. 1996; 17(18): 1741-53. [2] Kurtz SM, et al. *Biomaterials*, 1999; 20: 1659-88 [3] Sutula LC, et al. *Clin Orthop Relat Res*. 1995; (319): 28-40. [4] Besong AA, et al. *J Bone Joint Surg Br*. 1998; 80(2): 340-4. [5] Bracco P, et al. *Clin Orthop Rel Res*. 2011; 469:2286-93 [6] Turell ME, et al. *Biomaterials*, 2004; 25:3389-98.

# Chemically crosslinked UHMWPE: A comparison of different peroxides

Sciarra, G<sup>1</sup>; Bellare, A<sup>2</sup>; Bracco, P<sup>1\*</sup>

<sup>1</sup>Department of Chemistry, University of Turin, Turin, Italy

<sup>2</sup>Department of Orthopedic Surgery, Brigham & Women's Hospital, Harvard Medical School, Boston, MA

pierangiola.bracco@unito.it

**Introduction:** The wear of the ultra-high molecular weight polyethylene (UHMWPE) components and wear debris induced osteolysis are still among the major causes of failure in total joint replacements. Crosslinking has been shown to improve the wear resistance of UHMWPE by creating a network structure that increases the resistance of the surface layer to plastic deformation. Crosslinking can be achieved by introducing free radicals on the polymer chains either by physical (high energy ionizing radiation) or by chemical (peroxides or silanes) methods. Crosslinking by organic peroxides is a convenient and effective process as compared to radiation crosslinking as it does not require specialized equipment and it allows a nearly complete suppression of chain scission. Furthermore, the degree of crosslinking can be easily manipulated by changing the amount of peroxides added [1-3]. Several studies have been conducted on peroxide crosslinking of polyethylenes and it has been demonstrated that differences in the decomposition temperatures and rates are the main factors in selecting a particular peroxide for an intended application [4, 5]. The present study compared the crosslinking performance of different contents of three different peroxides and their effects on the physico-chemical and mechanical properties of medical grade UHMWPE GUR 1020 resin.

**Methods and Materials:** Ten samples were prepared as follows: benzoyl peroxide (BP), 1-1-bis(tertbutylperoxy)-3,3,5-trimethylcyclohexane (Luperox 231<sup>®</sup> - LUP) or Dicumyl peroxide (DCP) respectively (Table 1), were dissolved in the appropriate solvent (acetone or cyclohexane), blended with GUR 1020 powder (Celanese, Germany) and immediately consolidated into blocks (approx. 10x7.5x1.5 cm) containing 0 (Control), 0.75, 1.00 or 1.50 wt % of each peroxide. Compression molding was performed at a temperature of 200°C and 10 MPa pressure, and slow cooled to room temperature.

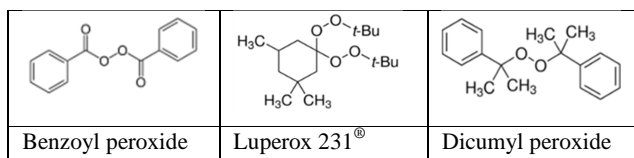


Table 1: Chemical structure of the peroxides studied

The cross-link density of each sample was determined gravimetrically, according to ASTM D2765. Crystallinity was assessed by DSC (Pyris 6, Perkin Elmer, Waltham, MA), using a heat of fusion of 293 J/g (n=3). Small angle x-rays scattering (SAXS) was performed using a laboratory CuK $\alpha$  rotating anode SAXSLAB instrument equipped with a DECTRIS PILATUS 300K detector measuring scattering over an angular range of  $q_{min}=0.032$

[nm<sup>-1</sup>] and  $q_{max}=2.5$  [nm<sup>-1</sup>], where  $q$  is defined as  $q=(4\pi/\lambda)\sin\theta$ ,  $\lambda$  is the wavelength of the x-ray used (0.154 nm) and  $\theta$  is one-half the scattering angle. A combination of SAXS and DSC measurements was used to calculate the lamellar thickness [6]. Tensile mechanical properties were measured according to ASTM D638: Type V dogbone specimens (n = 5) were subjected to tensile testing at room temperature using a universal tensile tester operating at a crosshead speed of 10 mm/min.

**Results:** The cross-link density of all peroxide containing samples increased with the peroxide content. DCP showed the highest crosslinking efficiency among the different peroxides, followed by BP and LUP (Figure 1).

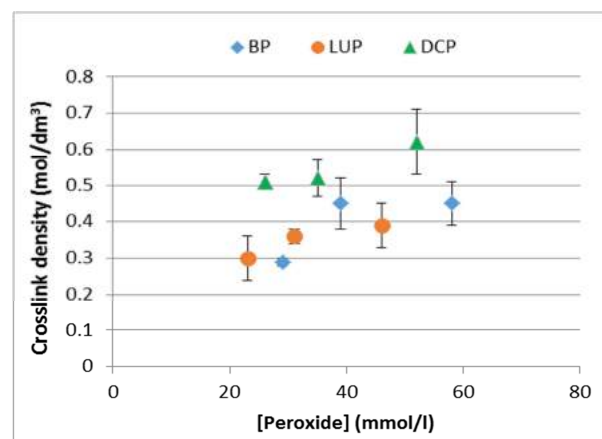


Figure 1: Crosslinking densities of the peroxide crosslinked UHMWPEs

Sample	Crystallinity (%)	Lamellar thickness (nm)
Control	52.3 ± 1.7	26.3
BP_0.75	51.2 ± 0.4	25.7
BP_1.00	49.8 ± 1.4	24.4
BP_1.50	49.6 ± 1.3	25.5
LUP_0.75	46.9 ± 1.6	25.1
LUP_1.00	47.6 ± 1.2	24.6
LUP_1.50	47.5 ± 0.5	23.9
DCP_0.75	44.8 ± 1.2	18.6
DCP_1.00	44.2 ± 0.5	17.7
DCP_1.50	42.6 ± 0.6	15.2

Table 2: Crystallinity and lamellar thickness of the control and crosslinked samples.

The crystallinity of all crosslinked samples slightly decreased with increasing peroxide content (Table 2). The crystallinity of LUP and DCP was lower than that of the control, with DCP showing the lowest crystallinity. The

lamellar thicknesses of all LUP and BP samples were not significantly different from that of the control, while those of the DCP series were significantly lower and decreased with the peroxide content.

The tensile tests showed that the elastic modulus and strain at break of all crosslinked samples were lower than those of the control and decreased with increasing peroxide content. The ultimate tensile strength (UTS) of all crosslinked samples also decreased with peroxide content. However, UTS of the BP samples was higher than that of the control, that of LUP showed no significant differences and that of DCP was statistically lower.

Sample	UTS (MPa)	Strain at break (mm/mm)	Tensile modulus (MPa)
Control	42.5 ± 1.0	9.10 ± 0.30	201 ± 9
BP_0.75	49.3 ± 2.1	6.62 ± 0.31	193 ± 15
BP_1.00	48.0 ± 1.1	6.57 ± 0.14	166 ± 5
BP_1.50	44.2 ± 3.2	5.24 ± 0.08	169 ± 18
LUP_0.75	45.0 ± 1.3	4.67 ± 0.20	170 ± 3
LUP_1.00	43.6 ± 0.8	5.43 ± 0.14	128 ± 9
LUP_1.50	40.5 ± 1.1	4.51 ± 0.20	134 ± 9
DCP_0.75	37.0 ± 1.1	3.92 ± 0.23	134 ± 6
DCP_1.00	35.2 ± 1.3	3.61 ± 0.27	130 ± 8
DCP_1.50	32.7 ± 0.9	3.18 ± 0.19	120 ± 3

Table 3: Tensile properties of the control and crosslinked samples

**Discussion:** DCP showed the highest crosslinking efficiency. This was surprising since one LUP molecule is the origin of four radical species upon decomposition. Thus, one could have expected it to be more efficient in promoting crosslinking. Conversely, the observed trend may be explained on the basis of the different decomposition temperatures ( $T_d$ ) of the peroxides: DCP has the highest one-hour half-life of 135°C, very close to the UHMWPE peak melting temperature. This means that most dicumyl peroxy radicals are released when the UHMWPE powder is almost entirely melted and the bulk of the polymer is in the amorphous phase, allowing the radicals enough mobility to provide more efficient crosslinking. In contrast, LUP had a one-hour half-life of 115°C and BP had the lowest one-hour half-life of 93°C.

The crystallinity of the crosslinked samples decreased with the increase of peroxide content and crosslink density since the crosslinks hinder recrystallization of the molten polymer. The highly crosslinked DCP samples showed the lowest crystallinity, accompanied by a significant decrease in the lamellar thickness, again because the larger the number of crosslinks originated in the melted and completely amorphous phase, the more impeded will be the chain mobility during recrystallization, thus leading to a lower number of thinner lamellae.

The decrease in crystallinity appeared to be the dominant factor in determining the reduction in the elastic modulus of the peroxide containing samples, while the increase in crosslink density is likely responsible for a high strain hardening rate and decrease in elongation at break. The UTS trend can be explained on the basis of two concurrent phenomena: UTS is generally expected to increase due to the increased resistance of chemical crosslinks to molecular mobility at large deformations, while it is expected to decrease with the decrease in the number of crystallites, which act as physical entanglements.

The peroxides used here had different crosslinking efficiency and different impact on the polymer morphology, thus resulting in a different influence on two opposite factors: the effect of crosslinking predominates in the BP samples, whose variation in crystallinity and lamellar morphology were limited; a balance of the two phenomena occurred in the LUP samples, so there was no significant variation in the overall UTS compared to that of the control sample, while the significant decrease in crystallinity and lamellar thickness of the DCP samples predominated over crosslinking in determining a reduced UTS. The primary reason for these variations is the difference in their decomposition temperatures. When the decomposition temperature was low, as is the case of BP, one can expect crosslinking to have occurred on the surfaces of the UHMWPE powder particles where the chemical crosslinking agents resided upon coating with their solvents. Thus, in the case of BP, crosslinking was effectively a process of “stitching” of powder particles with not much crosslinking in the interior of the powder particles. In contrast, DCP released free radicals when the powder was almost completely melted, and the higher thermal energy would also have promoted diffusion into the interior of the powder particles to provide a more uniform crosslinking rather than crosslinking confined to the surface region of the powders, as in the case of BP. LUP had an intermediate decomposition temperature, and thereby showed intermediate physico-chemical effects.

These results suggest that chemical crosslinking with organic peroxides can be used to produce crosslinked UHMWPE with tunable physico-chemical and mechanical properties, by varying the type and amount of peroxide.

#### References:

- 1) Gul, RM. J Mat Sci: Mat Med, 2008, 19 (6), 2427
- 2) Liu S et al. J Macromol Sci Phys, 2014, 53 (1): 67
- 3) Gul RM et al. IOP Conf. Ser. Mater. Sci. Eng., 2014, 60(1) 012015
- 4) Gul RM. Eur Polym J, 1999, 35: 2001
- 5) Bremner T et al. J. Appl. Polym. Sci. 1993, 49: 785.
- 6) Turell ME, et al. Biomaterials, 2004; 25:3389-98

# **Ultrahigh Molecular Weight Polyethylene Membrane for Use in Vascular Stent Graft Applications — Preliminary Evidence From an Ovine Peripheral Implantation Model**

W. Cheng<sup>1</sup>, H. Smelt<sup>1</sup>, <sup>2</sup>James Joye, <sup>2</sup>Steven Tyler, <sup>2</sup>Ziad Rouag, <sup>3</sup>Renu Virmani

<sup>1</sup> DSM Biomedical B.V., Urmonderbaan 22, 6167 RD , Geleen, The Netherlands

<sup>2</sup> PQ Bypass, Inc., 169 N Mathilda Avenue, Sunnyvale, CA 94086

<sup>3</sup> CV Path Institute, Inc., 19 Fristfield Road, Gaithersburg, MD 20878

[wei.cheng@dsm.com](mailto:wei.cheng@dsm.com)

**Introduction:** Despite many years of efforts, the commercial availability of graft material suitable for stent graft application is rather limited and ePTFE (expanded polytetrafluoroethylene) remains almost the only choice for small profile stent grafts. Here we demonstrate that a commercially available ultra-high molecular weight polyethylene (UHMWPE) membrane, Dyneema Purity® Membrane, shows great promise as an alternative graft material for use in vascular stent graft applications. In comparison to typical ePTFE, this thin and highly porous UHMWPE membrane is mechanically strong and isotropic with a breaking strength of ~20 MPa, and hence is particularly suitable for making low profile stent grafts. In addition, it can be processed at a much lower temperature than ePTFE, therefore allows for easier stent covering process. A 90 days animal study based on ovine model peripheral artery stenting reveals equivalent performance between stent graft covered by this UHMWPE membrane without special surface treatment and a commercial stent graft (Gore® Viabahn®) covered by ePTFE with CARMEDA® bioactive heparin-bonded surface.

**Methods and Materials:** Dyneema Purity® Membrane is manufactured via a proprietary gel-extrusion and bi-axially stretching process which leads to a highly porous and thin (3 g/m<sup>2</sup> and < 20 µm thick) membrane as shown in left panel of Figure 1.



Figure 1 Left: Typical SEM image of Dyneema Purity® Membrane (scale bar is 50 µm), Right: Dyneema Purity® Membrane covered-stent wrapped around a coin.

The Dyneema Purity® Membrane covered-stents used in this study were produced via a proprietary lamination process that encapsulates the nitinol stent. The right panel of Figure 1 shows the appearance of a typical Dyneema Purity® Membrane covered-stent.

Four sheep (*Ovis aries*) weighing 50-60 kg were used for the current animal study. For each sheep, one test article (Dyneema Purity® Membrane covered-stent) and one control article Gore® Viabahn® covered-stent with CARMEDA® bioactive heparin surface (Gore-CA) were introduced via femoral access to the carotid or iliofemoral artery. On the day of termination (day 90) angiography was performed, where after animals were sacrificed and the

target artery segments containing the test articles or the control articles were explanted. Before processing samples for further histological analysis, explanted arteries were grossly radiographed and photographed for macroscopic evaluation of vessel intactness and stent expansion.

**Results:** Angiography shows that all implanted stent grafts, both test articles and control articles, in all four sheep were widely patent at 90 days. The corresponding photographic and radiographic images show that each of the vessels is intact and contains well-expanded struts of the implanted stent graft, as evidenced by the images from the right carotid and left iliofemoral arteries in Figure 2.

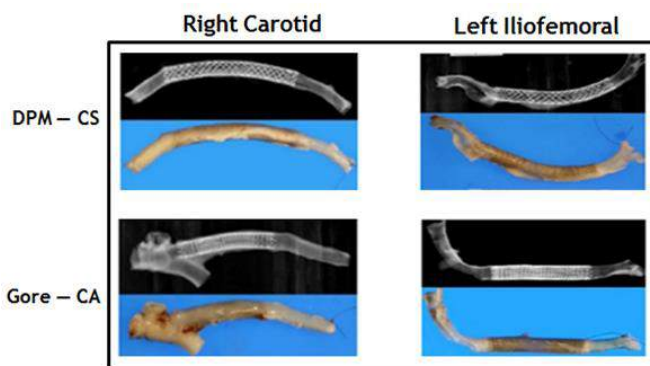


Figure 2 Radiographic and optical images of explanted and stented right carotid and left iliofemoral arteries

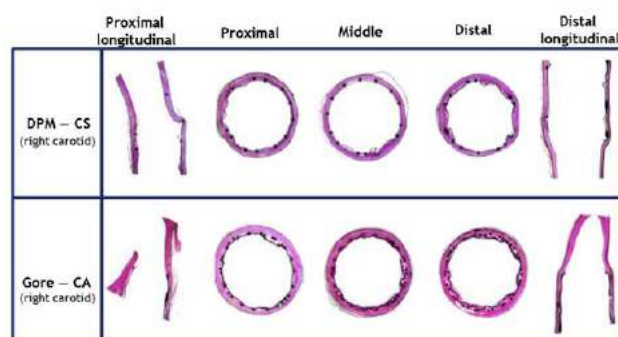


Figure 3 Images of longitudinal and transverse sections of the stent grafts implanted in the right carotid arteries

Histological analysis of both longitudinal and transverse sections of all implanted stent grafts, both test articles (Dyneema Purity® Membrane covered-stent) and control articles (Gore-CA), show comparable graft apposition, tissue reaction and inflammatory response. In addition, histological results corroborate the widely patent status of

the implanted stent graft at 90 days. Figure 3 gives an example of the histological images of longitudinal and transverse sections of the stent graft in the right carotid artery for both Dyneema Purity® Membrane covered-stent and Gore-CA.

**Discussion:** The objective of this animal study was to evaluate the safety and performance of the Dyneema Purity® Membrane covered-stent compared to the commercially available Gore-CA. Note that Gore-CA has a heparin-coated surface while Dyneema Purity® Membrane covered-stent does not involve any surface treatment.

The results from angiographical, radiographical and histological analyses performed on all implanted stent grafts show that the Dyneema Purity® Membrane covered stent does not exhibit inferior performance when compared to Gore-CA. Such findings suggest great promise of Dyneema Purity® Membrane to be used as an alternative synthetic graft material for vascular covered-stent, particularly low profile covered-stent applications.

## Clinical mid-term results for vitamin enhanced HXLPE

Delfosse D<sup>1</sup>, Röthlisberger M<sup>1</sup>, Münger P<sup>1</sup>

<sup>1</sup>Mathys Ltd Bettlach, Switzerland

daniel.delfosse@mathysmedical.com

**Introduction:** The 2nd generation of highly crosslinked UHMWPE, called VEPE (vitamin E enhanced highly cross-linked polyethylene), was introduced to maintain the superior wear resistance of the HXLPE while also retaining the mechanical properties and fatigue resistance of the un-crosslinked material and providing improved stability against oxidation over time.

The first VEPE was introduced for hip arthroplasty in 2007 as E1-poly (Biomet Inc., Warsaw, IN) using an infusion process to add the vitamin E. In 2009, vitamys (Mathys Ltd Bettlach, Switzerland) was the second VEPE in clinical application – and the first using a blending technique to add the vitamin E. In the meantime, from 2010 to today, many orthopaedic companies have followed the example of Mathys, introducing their own brands of a blended VEPE. Still today, VEPE is regarded as a novel material with good pre-clinical data, short-term clinical follow-up and unknown potential side effects. It is therefore of utmost importance to follow the clinical results with these early patients very closely.

**Methods and Materials:** With the first clinical introduction of vitamys in the RM Pressfit vitamys cup (Fig. 1), several PMCFs were started, either initiated by the company or by independent medical investigators. In addition, the registry data was analysed using the latest published reports or separate ad hoc reports from the Registry. For the RM Pressfit vitamys cup, registry data is available from the Swiss SIRIS (5'342 cups, max. FU 3 years), the New Zealand NZJR (2'374 cups, max. FU 5 years), the Australian AOANJRR (1'148 cups, max. FU 4 years) and the NJR for England, Wales and Northern Ireland (629 cups, max. FU 3.5 years).



Figure 1: The RM Pressfit vitamys cup

**Results:** Clinical follow-up data for the RM Pressfit vitamys cup is already available in a number of publications [1-5] as listed in table 1.

A RSA analysis [5] shows clearly the difference between vitamys VEPE and standard UHMWPE, using the same RM Pressfit cup. The head penetration in the vitamys material is significantly slower (after the initial creep phase) than in the UHMWPE (fig. 2).

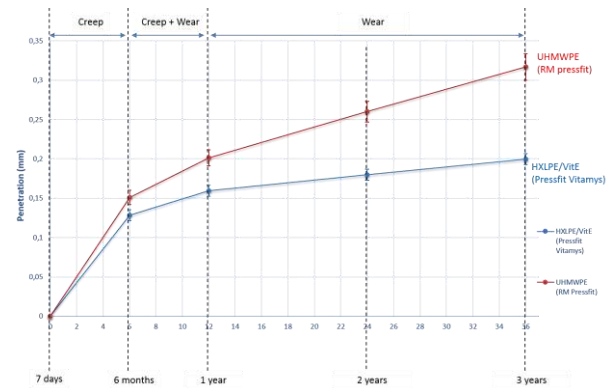


Figure 2: In vivo head penetration for RM Pressfit vitamys and UHMWPE cup, measured with RSA [5]

An overview of the available registry data for the RM Pressfit vitamys cup is given in table 2. The survival rate of the vitamys cup is within or even above the state-of-the-art. In the NZJR, the survival rate at 3 years was 99.1% for all revisions. This is the same rate as in the NJR report where the cumulative revision rate for acetabular revision as endpoint was reported as 0.9% at 3 years, a rate comparable to the 1.2% for all uncemented cups in the NJR registry.

Reference	Number of Implants	FU time	Revisions of RM Pressfit vitamys	Survival rate of RM Pr. vitamys	Steady-state wear rate (mm/y)
[1]	164	1 y	1	99.3 %	n.a.
[2]	112	2 y	2	98.3%	0.035 (year 2)
[3]	38	min. 3y	0	100%	-0.008
[4]	92	5 y	0	100%	n.a.
[5]	33	3 y	0	100%	0.020

Table 1: Summary of published clinical data for the RM Pressfit vitamys cup

The RM Pressfit vitamys cup has recently received a 5A\* ODEP rating, based on sufficient 5 year FU data from NZJR and [4].

Registry	Number of Implants	RR for RM cup (all rev.)	Average RR (all rev.)	RR for RM cup (cup rev. only)	Average RR (cup rev. only)
SIRIS	5342	-	-	0.26	0.39
NZJR	4724	0.52	0.68 – 0.87	0.20	n.a.

Table 2: Summary of clinical data for the RM Pressfit vitamys cup in National Joint Registries

(RR = revision rate, in revision per 100 component years)

Comparing the different head sizes in the SIRIS, the revision rate for the 28mm head size was higher than for all uncemented cups (fig. 3) The reason for this higher

number of cup revisions is due to dislocations. In contrast, the rate per 100 component years for the RM Pressfit vitamys cup 32mm was significantly lower than for all uncemented cups.

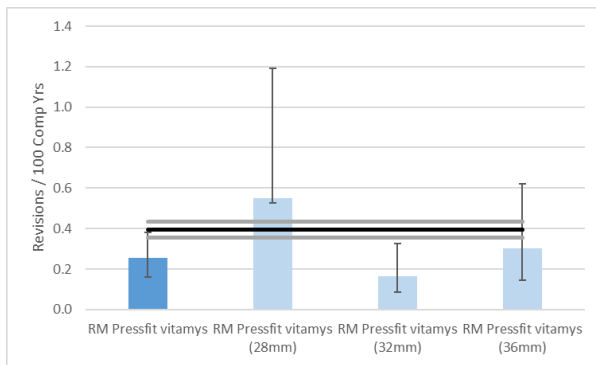


Figure 3: Revisions per 100 component years of the RM Pressfit vitamys cup in the SIRIS registry, 2016 (black line: all uncemented cups in SIRIS)

**Discussion:** The vitamys VEPE material has shown excellent short to mid-term clinical follow-up. The revision rates of the RM Pressfit vitamys hip cup are low. The wear rate of this VEPE material in vivo is around 0.02 mm/year. This compares favorably to a review article by Kurtz [6] that determined the linear in vivo head penetration for conventional UHMWPE and HXLPE as 0.137 mm/year (based on 18 studies, N=695 hips) and 0.042 mm/year (based on 28 studies, N=1503 hips), respectively, with values ranging from 0.023 mm/year for Durasul to 0.063 mm/year for Aeonian HXLPE.

VEPE has a short-term advantage for THA compared to UHMWPE: Because of the lower wear rate, larger articulation diameters are allowed, thus reducing the dislocation risk.

VEPE also has a long-term advantage compared to UHMWPE: Due to the stabilization with vitamin E, the properties of VEPE are not influenced by the oxidative environment during shelf life and in situ. VEPE is the only polyethylene that keeps its mechanical properties over time. Therefore, we expect the difference in the clinical outcome to become even more pronounced with longer follow-up times.

**References:** [1] Beck et al. in K. Knahr (Ed.): Total Hip Arthroplasty, 2012. [2] Halma et al. JoA 2015. [3] Scemama et al. Int. Orthop. 2016. [4] Wyatt et al. Hip Int. 2016. [5] Rochcongar et al. Accepted for publication by JBJS Am. 2017. [6] Kurtz et al. CORR 2011.

# Combining Retrieval Research with Epidemiology to Understand the Role of Periprosthetic Joint Infection on the Oxidative Degradation of Total Hip Replacements

<sup>1</sup>Genymphas B. Higgs; <sup>1</sup>Carina Gerveshi, <sup>1</sup>Loni Tabb, <sup>1</sup>Alison Evans <sup>1,2</sup>Steven M. Kurtz

<sup>1</sup>Drexel University, Philadelphia, PA; <sup>2</sup>Exponent, Philadelphia, PA

gbh26@drexel.edu

**Introduction:** Database and registry research in orthopedic surgery provide invaluable insight into patient outcomes, but lack the rich information about device performance and material behavior that retrieval analysis provides. The purpose of this study was to identify the potential of epidemiological techniques in retrieval analysis by examining the survival behavior of hip and knee implants with regard to the development of periprosthetic joint infection. We hypothesized that trends observed among retrievals would reflect those found using large-scale national databases. A secondary goal of this work was to understand the role of immune system secretions in the degradation of polymeric components used in total hip arthroplasty. We assessed whether patients with periprosthetic joint infection (PJI) are associated with increased oxidative degradation of the polyethylene liner.

**Methods and Materials:** The study cohort included 3097 hips and 2724 knees consecutively revised between 1992 and 2017. Any device revised for infection within 10 years was modeled as an event (failure) with all other cases considered censored. Kaplan-Meier curves of survival until infection, stratified on procedure (knee vs. hip), were generated for a global overview of the variable of interest. Univariate Cox semi-parametric proportional hazards models were created for each of the covariates to determine their relationship with survival time until infection. Parametric exponential, Weibull, and log-logistic models with and without frailty, were compared using AIC to determine which was the most appropriate for the data. To assess the effect of PJI on polyethylene degradation, oxidation analysis was conducted on 533 retrieved liners. Thin slices (200 um) were taken depth-wise from the center of each specimen, and analyzed under Fourier Transform Infrared Spectroscopy (FTIR) to calculate an oxidation index (OI). Implants revised for PJI (n=133) were compared to those revised for all other reasons (n=440). Differences in OI between the PJI and control groups were initially assessed cross-sectionally using the Wilcoxon test. Oxidation index was also dichotomized as minimal ( $0 \leq \text{OI} \leq 1$ ), or significant ( $\text{OI} > 1$ ) and logistic regression was used to model the effect of the available clinical variables on the probability of significant OI. Univariate models were first used to assess the individual effect of each variable. Significant predictors were then modeled together to assess their effect in the context of a multivariable analysis. For all analyses, significance was assessed at  $\alpha=0.05$ .

**Results:** In From the univariate survival analysis, having a knee procedure ( $p<0.001$ ), having a previous revision

( $p<0.001$ ), male gender ( $p<0.001$ ), non-white race ( $p=0.04$ ), and increased age ( $p<0.001$ ) were found to increase the hazard of failure due to infection. The final model was a log-logistic parametric survival model with frailty to accommodate the variation among hospitals. In this multivariable model, having a previous revision ( $p<0.001$ ), male gender ( $p<0.001$ ), and increased age ( $p<0.001$ ) increased the hazard of failure due to infection. From the cross-sectional analysis of oxidative degradation, PJI was associated with lower OI ( $p=0.002$ ). The univariate regression analysis identified non-PJI diagnosis ( $p=0.008$ ), time in situ ( $p<0.001$ ) and non-white race ( $p<0.001$ ) as predictors of significant OI. Cases of PJI were 54% less likely to have significant oxidation than the controls ( $\text{OR}=0.44$ ; 95%  $\text{CI}=0.24-0.80$ ;  $p=0.008$ ). Each year of implantation was associated with a 16% increase in the odds of significant oxidation ( $\text{OR}=1.16$ ; 95%  $\text{CI}=1.10-1.22$ ;  $p<0.001$ ). Implants from non-white patients were 133% more likely to have significant oxidation ( $\text{OR}$ , 2.33; 95%  $\text{CI}$ , 1.46 – 3.73;  $p<0.001$ ) than those from white patients. In the final multivariable model, the effect of PJI was not significant ( $p=0.08$ ) in the context of time in situ ( $p<0.001$ ) and race ( $p<0.001$ ).

**Discussion:** These results support the hypothesis that retrieval analysis can accommodate epidemiological techniques that are usually relegated to registry-based studies. Though this study is limited to a collection of failed THAs and TKAs retrieved at revision surgery, the trends observed are consistent with those identified in studies using large-scale national databases. Furthermore, this study demonstrates the potential for retrieval analysis metrics such as taper corrosion and polyethylene oxidation, to be readily incorporated into database and registry research techniques. The results from the cross-sectional analysis of OI contradicts the central hypothesis that the immune system, activated in cases of PJI, causes increased oxidative degradation of hip replacements. However, summary statistics revealed differences between the comparison groups for other variables as well, with PJI cases having shorter implantation times, a higher prevalence of previous revision history, and a greater proportion done in teaching hospitals, as compared to the controls. The potential of this homogeneity for confounding was confirmed in the regression analyses that identified implantation time as a significant predictor of OI. Subsequent multivariable analysis revealed that the apparent protective effect of PJI fails to remain significant when modeled along with implantation time. Thus, while the final results of this investigation fail to support the initial hypothesis, they do not provide evidence in favor of a counter hypothesis that PJI leads to lower OI values.

## References:

Bongartz, T., Halligan, C.S., Osmon, D.R., Reinalda, M.S., Bamlet, W.R., Crowson, C.S., Hanssen, A.D. and Matteson, E.L., 2008. Incidence and risk factors of prosthetic joint infection after total hip or knee replacement in patients with rheumatoid arthritis. *Arthritis Care & Research*, 59(12), pp.1713-1720.

Kurtz SM, Lau E, Schmier J, Ong KL, Zhao K, Parvizi J. Infection burden for hip and knee arthroplasty in the United States. *The Journal of arthroplasty* 23(7): 984, 2008

SooHoo NF, Farnig E, Lieberman JR, Chambers L, Zingmond DS. Factors that predict short-term complication rates after total hip arthroplasty. *Clinical Orthopaedics and Related Research*® 468(9): 2363, 2010

## Investigation of Free Radicals in Conventional UHMWPE for 18 Years

Jahan M. Shah<sup>1</sup>, Walters, Benjamin M<sup>1</sup>, Gomrok, S<sup>1</sup> and Sharmin, A<sup>1</sup>

<sup>1</sup>Biomaterials Research Lab, Dept. of Physics and Materials Science, The University of Memphis, Memphis TN, USA

Corresponding author email: [mjahan@memphis.edu](mailto:mjahan@memphis.edu)

**Introduction:** Free radical analyses were performed using electron spin resonance (ESR) technique for two UHMWPE resins, GUR 4150 and Hylamer (Himont 1900). These materials were provided by the medical-device industry members of the NSF-Industry/University Center for Biosurfaces (IUCB), a partnership program between the State University of New York at Buffalo (SUNY Buffalo) and the University of Memphis (1997-2011). The primary objective of the IUCB program at the University of Memphis Site was to understand free radical reaction mechanisms and consequences in UHMWPE components over the lifetime of total hip and knee replacement units. The second objective was to determine the long-term effects of storage temperature (23°C, 37°C and 75°C) and environment (inert or open air) upon the radical reactions. This was to address further whether or not free radicals could be quenched at or below 75°C. The third objective was to compare and contrast GUR4150 and Hylamer (Himont 1900) resins so far as the free radical reactions were concerned. This project was undertaken in 1998, and free radical measurements have been conducted on a regular basis since then.

**Methods and Materials:** The test samples (10 mm long and 2 mm in diameter) were machine-cut to fit the ESR (electron spin resonance) sample tubes (thin-wall suprasil quartz with 3 mm inner diameter). For inert environment storage, the tubes (one sample per tube) were sealed under vacuum or partial nitrogen pressure. All samples were  $\gamma$ -irradiated (30 kGy) at room temperature (23°C) using a Cobalt-60 source. Following irradiation, the samples were divided into groups and stored at 23°C (shelf), and in 37°C and 75°C ovens. To maintain constant operation throughout the lifetime of this project, the ovens were/are connected to the emergency power line of the laboratory. For ESR tests, a sample tube was/is taken out from an oven and returned immediately after measurement. All measurements were/are performed at room temperature using a Bruker EMX 300 Biospin spectrometer operating at X-band frequency (~9 GHz).

**Results:** Since 1998 (t=0), free-radical test results have been reported (1), the present report focusses on the measurements performed at t = 18 years. The samples stored at 23°C or 37°C in open air show the presence of oxygen-induced polyenyle radicals, with a greater concentration at 23°C. At 75°C, there were still small quantities of radicals detected in inert-stored samples, and no detectable radicals in those stored in air. While the total concentration of radicals in all samples decreased by two orders of magnitude in 18 years, the present data showed that, at 37°C, it decreased less in Hylamer than in GUR 4150, by a factor of 2/3. In inert environments (nitrogen or

vacuum), both GUR 4150 and Hylamer showed similar concentrations (slightly higher at 23°C than at 37°C). Compared to GUR 4150, Hylamer showed the presence of 0.6, 0.9, 1.0, 1.1, and 1.3 times more radicals at 23°C (air), 37°C (air), 23°C (inert), 37°C (inert) and 75°C (inert), respectively. In terms of radical type (alkyl, allyl, polyenyle, dienyle, and trienyle), no significant difference was found between GUR 4150 and Hylamer at 23°C (inert), but at 37°C (inert) Hylamer showed the presence of more alkyl (20/13), allyl (51/40) and less polyenyle (28/46). No dienyle or trienyle was observed at 23°C (inert) or 37°C (inert). At 75°C (inert), Hylamer (compared to GUR 4150) showed a lower concentration of alkyl (6/15), higher concentration of allyl (24/10), no polyenyle (0/0), approximately equal number of dienyle (68/74), and no trienyle (0/0). Analyses of the ESR data of the open-air samples further revealed that, compared to GUR 4150, Hylamer contained lower concentrations, 0.6x and 0.5x, of carbon-centered polyenyle (R1:  $\text{—}\cdot\text{CH—[CH=CH—]}_m\text{—}$ , polyenyl with  $m>3$ ) and oxygen-centered-polyenyle (R2:  $\text{—}\cdot\text{OCH—[CH=CH—]}_m\text{—}$ ) (OIR) with  $m=2$  or  $3$ , respectively. A summary of these results is presented in Figure 1.

**Discussion and Summary:** Although a significant decrease in radical concentration took place in all samples, quantifiable radicals remain most samples after 18 years. At 23°C, Hylamer and GUR 4150 both show equal amount of radicals in inert environment, but in open air the former contains 10% less. This reduction might occur due to an increased level of reaction with oxygen, producing more oxygen-induced non-radical species. At 37°C, the higher concentration in Hylamer could be attributed to its higher molecular weight. Again, a significant lower concentration of R1 (carbon centered polyenyle) and R2 (oxygen centered polyenyle) radicals in Hylamer suggest that this resin has a better protection from oxygen than GUR 4150. At 75°C in open air, no radicals were detected in Hylamer or GUR 4150 because of thermal recombination/oxidation reactions. In inert environments at 75°C, both Hylamer and GUR 4150 lost about the same amount radicals because of thermal recombination. As a result, the ESR spectra recorded at t=18 years do exhibit the characteristic feature of the combined primary radicals (allyl, alkyl, polyenyle). This result confirms that, in an inert environment, complete annihilation or recombination of radicals cannot occur even when the material is heated for 18 years at or below 75°C. When exposed to oxygen (breaking the sample tube or package, for example), oxidation process would occur and the magnitude of oxygen-induced radicals produced would be proportional to the number of radicals present at the time of exposure.

**Reference:**

1. M.S. Jahan, Ch. 35, ESR Insights into Macroradicals in UHMWPE, In UHMWPE Biomaterials Handbook (3<sup>rd</sup> Ed.), edited by Steven M. Kurtz, William Andrew Publishing, Oxford, 2016, 668-692.

**Acknowledgements:** Work was supported in parts by the NSF Industry/University Cooperative Center for Biosurfaces (IUCB) at the University of Memphis.

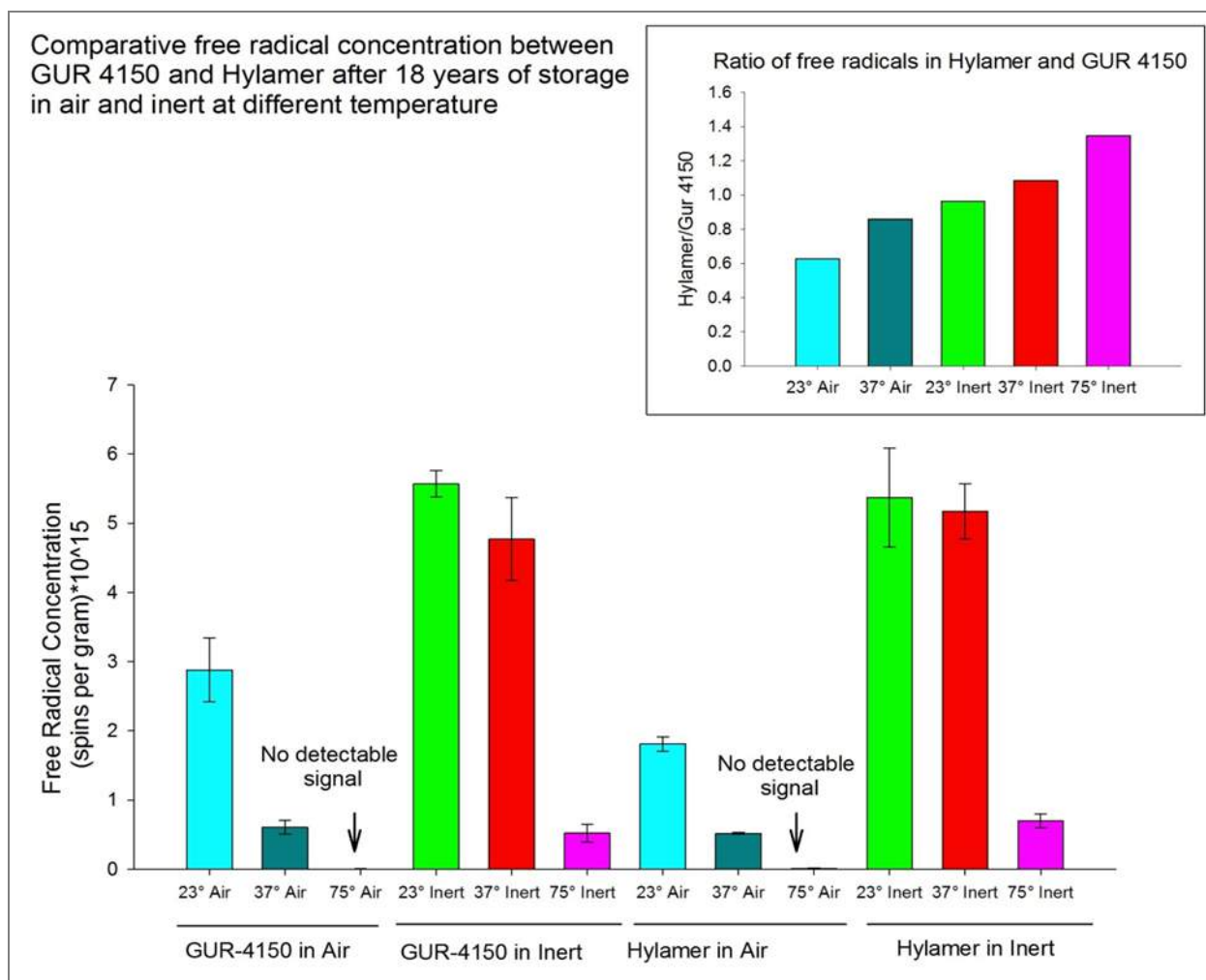


**Figure 1:** Summary of Results

## Effect of Vitamin E on the decay of UHMWPE Radicals for 10 Years

Jahan, M. Shah<sup>1</sup>, Walters, Benjamin M.<sup>1</sup>, Gomrok, S.<sup>1</sup>, and Sharmin, A.<sup>1</sup>

<sup>1</sup>Biomaterials Research Lab, Dept. of Physics and Materials Science, The University of Memphis, Memphis TN, USA

Corresponding author email: [mjahan@memphis.edu](mailto:mjahan@memphis.edu)

**Introduction:** Polyethylene (PE) radicals generated in ultra-high molecular weight polyethylene (UHMWPE) by radiation sterilization and/or cross-linking processes can be quenched or stabilized, and oxidative degradation of the joint components eliminated or reduced, by adding vitamin E (alpha tocopherol,  $\alpha$ -T) to UHMWPE (1). However, in a more recent study (2) when UHMWPE powder containing 20%  $\alpha$ -T was gamma-irradiated in nitrogen ( $N_2$ ) with a dose of 32-kGy, PE radicals were produced which subsequently transformed to oxygen-induced residual radicals (OIR) in the presence of oxygen (air); the presence of vitamin E radicals (tocopheroxyl ( $\alpha$ -T-O $\cdot$ )) was also observed. Although there are no clinical data, to our knowledge, the residual radicals may have long-term oxidation potential as well; they decay very slowly with an estimated half-life of about 10 years [estimated from the Bessel function fitting parameters as reported by Jahan et al. (3)]. The commonly observed ESR (electron spin resonance) signal due to these residual radicals has normally resembled a single-line spectrum or a singlet. In another study, the singlet was split into two lines, one due to radical R1 and the other R2 (4): R1 is a singlet due to a carbon centered polyenyl ( $\cdot\text{CH}[-\text{CH}=\text{CH}]_m$ ,  $m \geq 3$ ); R2 is a sextet due to an oxygen-centered di- or tri-enyl radical ( $\cdot\text{OCH}[-\text{CH}=\text{CH}]_m$ ,  $m \leq 3$ ). The ESR spectral parameters for these residual radicals were found as follows. R1:  $\Delta H_{pp} = 5.5$  G and  $g = 2.0044$  and R2:  $a_H = 4.8$  G and  $g = 2.0056$ . Better understanding of the behavior or the properties of the residual radicals can be important in the field of orthopedic science and medicine. The primary objective of this study was to determine whether or not vitamin E had any effect on the PE radicals during shelf storage in room environment. In particular, the dependence of the recently observed R1 and R2 radicals (so called residual radicals) on the presence of vitamin E was explored. The secondary objective was to measure the vitamin E radical as a function of aging time. Because vitamin E radical ( $\alpha$ -T-O $\cdot$ ) is a stable radical, one should be able to detect it. However, its signal generally remains overlapped by that due to the relatively strong PE-radical. Therefore, spectral analysis is employed to extract the embedded spectrum due to  $\alpha$ -T-O $\cdot$ .

**Methods and Measurements:** In this study, free radical analyses were performed on vitamin E-containing UHMWPE (GUR 1020) following post-gamma (30 kGy) shelf aging for 10 years at 23°C (room temperature) in open air. Vitamin E ( $\alpha$ -Tocopherol) was consolidated with GUR 1020 at concentration levels varying between 0% (no Vitamin E) and 20% in 2006. The purpose of using high concentrations of  $\alpha$ -T was to facilitate the detection of  $\alpha$ -T-O $\cdot$ . For ESR measurements, a Bruker EMX 300 Biospin spectrometer was used. Gamma irradiation (32 kGy) was

performed at 23°C using a Cobalt-60 source. Free radical concentrations (FRC spin/g) were determined by the spectral double integration method (5) using a NIST standard along with the test sample.

**Results:** ESR measurements conducted immediately after gamma irradiation in 2006 showed a decrease in free radical concentration by an order of magnitude due to vitamin E. In 10 years (2016), the radical concentration was reduced by another order of magnitude; i.e., from  $\sim 10^{17}$  to  $\sim 10^{15}$  radicals per gram in all samples, with or without vitamin E. No measurable difference between radical concentrations was found as a function of vitamin E (different vitamin E concentrations). Decays of the remaining radicals followed very similar pattern, and the oxygen-induced radicals (R1 and R2) were formed in all samples tested. Free radical concentrations (FRC) are shown in Fig. 1.

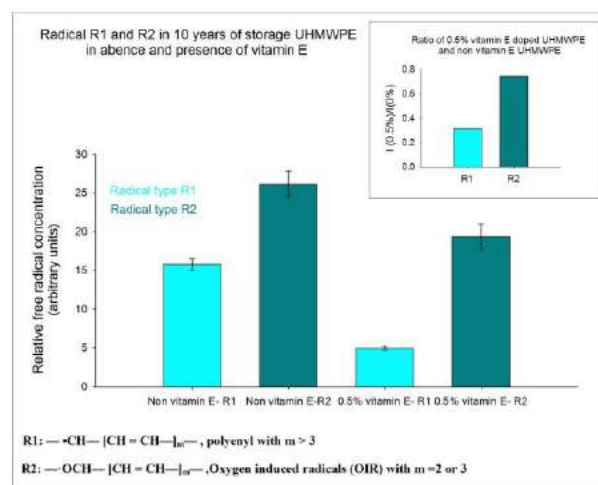


**Figure 1:** R1 and R1 in UHMWPE, with and without vitamin E, after 10-years.

**Discussion and Conclusions:** The fact that the ratio of R1 vs. R2 radicals, in UHMWPE and UHMWPE- $\alpha$ -T, remained about the same in 10 years suggests that vitamin E played a lesser role in radical quenching during this time. In other words, vitamin E molecules did not participate in any reaction, thermal recombination or oxygen-induced reduction of the radicals in the ambient environment. Lower concentration of the radicals R1 and R2 in vitamin E-containing samples, shown in the figure, could be due to the presence of lower concentrations found at  $t=0$ . While the presence of vitamin E radical was not apparent in the ESR spectra, a project is undertaken to conduct further analyses of the ESR spectra.

**Reference:**

1. E. Oral, B.W. Ghali, O. K. Muratoglu, The elimination of free radicals in irradiated UHMWPEs with and without vitamin E stabilization by annealing under pressure, *Biomed. Mater. Res. Part B Appl. Biomater*, 97B (1), 167–174 (2011).
2. M.D. Ridley, M.S. Jahan, Effects of packaging environments on free radicals in  $\gamma$ -irradiated UHMWPE resin powder blend with vitamin E, *Biomed. Mater. Res. Part A*, 88A (4), 1097–1103 (2009).
3. M.S. Jahan, J. Durant, Investigation of the oxygen-induced radicals in ultra-high molecular weight polyethylene. *Nucl. Instr. Meth. Phys. Res.* 236B, 166–171 (2005).
4. M.S. Jahan, M. Fuzail, Examination of the long-lived oxygen-induced radicals in irradiated ultra-high molecular weight polyethylene, *Nucl. Instr. Meth. Phys. Res. B* (265), 67–71 (2007)
5. M.S. Jahan, Ch. 35, ESR Insights into Macroradicals in UHMWPE, In *UHMWPE Biomaterials Handbook* (3<sup>rd</sup> Ed.), edited by Steven M. Kurtz, William Andrew Publishing, Oxford, 2016, 668-692.

**Acknowledgements:** Work was supported in parts by the NSF Industry/University Cooperative Center for Biosurfaces (IUCB) at the University of Memphis.

## Does cross-linked polyethylene reduce wear debris in total knee arthroplasty?

Sandra Lasurt-Bachs<sup>1</sup>, Pere Torner-Pifarré<sup>2</sup>, Francisco Maculé-Beneyto<sup>3</sup>, Eva Prats-Miralles<sup>4</sup>, Francisco Menéndez-García<sup>4</sup>, José Ríos-Guillermo<sup>5</sup>

1. Consorci Sanitari Integral, Sant Joan Despí, Barcelona. University of Barcelona. Spain.
2. Hospital Parc Taulí, Sabadell, Barcelona, University autonomaof Barcelona. Spain.
3. Hospital Clínic i Universitari de Barcelona, University of Barcelona, Spain.
4. Scientific and Technological Centres of the University of Barcelona (CCiTUB). Spain.
5. UASP. IDIBAPS Statistics Department. Hospital Clínic, University of Barcelona. Spain  
*slasurtb@yahoo.es*

### Introduction:

Ultra-high molecular weight polyethylene is currently the material of choice for the bearing surfaces of total knee arthroplasties. Cross-linked polyethylene was developed as an alternative to conventional Ultra-high molecular weight polyethylene as it has been hypothesised to reduce wear debris.

### Methods and Materials:

A prospective non-randomized controlled pilot blinded evaluation was carried out on twenty-five patients implanted with a staged bilateral total knee replacement, six months apart. Synovial fluid was extracted from the patients' knees at six months, one and three years.

A modified HCl digestion technique combined with a methanol dilution was used. This method was presented at the Sixth World Biomaterials Congress in May 2000 and has been used by several other authors such as Michael D. Ries and Marcus L. Scott.

To assess the production of polyethylene wear debris particles in vivo, we performed: validation of our isolation technique, characterization of wear debris particles using scanning electron microscopy, confirmation of our findings by imaging analysis and spectrometry, in vivo study of

polyethylene particles in patients with total knee prosthesis, and comparison of the results obtained with two different types of polyethylene.

### Results:

The technique used in this study allows an appropriate characterization of in vivo-generated polyethylene wear particles in synovial fluid by scanning electron microscopy and imaging analysis in patients who underwent total knee replacement.

At three years from total knee arthroplasty, no significant reduction in the number of wear particles was observed comparing ultra high molecular weight and cross-linked polyethylene inserts in vivo.

### Discussion:

The characteristics of polyethylene debris particles (number, size and shape) have been described as critical in the appearance of osteolysis. Increased macrophage activation is more likely to be stimulated in the presence of greater particle volumes, sub-micrometre size and an elongated shape.

The biological effects of polyethylene depend not only on the total volume of wear debris and the number of generated particles, but also on the proportion of biologically active particles. It has been suggested that the

particles generated by cross-linked polyethylene in revision hip surgeries tend to be more biologically active due to their size.

Several methods of tissue sampling have been described in the literature but none of them has demonstrated its superiority among the others.

Longer-term studies (ten or fifteen years post-implantation) should be performed to assess the efficiency of cross-linked inserts despite their high manufacturing complexity and elevated cost.

A great advantage of our study is that all surgical procedures were performed by the same team using the same procedure, prosthetic design and materials implanted, except for polyethylene liner. The results obtained are consequently reliable and suitable for the evaluation of the two types of inserts.

In conclusion, the technique used in this study allows an appropriate characterization of in vivo-generated polyethylene wear particles in synovial fluid by scanning electron microscopy and imaging analysis in patients who underwent total knee replacement.

At three years from TKR, no reduction in the number of wear particles was observed comparing ultra high molecular weight and cross-linked polyethylene inserts in vivo.

# Different Consolidation and Sterilization Methods have No Impact on Highly Crosslinked UHMWPE Properties

Le, K-P.<sup>1</sup>; Blitz, J.<sup>1</sup>; Song, L.<sup>1</sup>

<sup>1</sup>Stryker, Mahwah, New Jersey, USA

Kim-Phuong.Le@stryker.com

## Introduction:

Ultra-high molecular weight polyethylene (UHMWPE) used in joint replacement prostheses is typically consolidated using compression molding (CM) or ram extrusion (RE). The consolidated stock is then crosslinked, machined into final parts, cleaned, packaged and sterilized. Sterilization methods for UHMWPE include gamma radiation, gas plasma (GP), and Ethylene Oxide (ETO). Currently, sequentially-crosslinked UHMWPE (SXL) is produced from CM stock material and sterilized by GP.

The goal of the study is to determine if changes in (1) consolidation (CM to RE) and (2) sterilization (GP to ETO) have any impact on the resulting SXL mechanical and physical properties. Three material groups made from different consolidation and sterilization methods, namely CM-GP, CM-ETO, and RE-ETO, were evaluated in the study. Post-accelerated-aging mechanical properties were also assessed for the two ETO-sterilized test groups.

## Materials and Methods:

### Materials:

GUR1020 resin from Celanese (Germany) was either compression molded or ram extruded at Quadrant Mediatech (IN, USA). The consolidated materials were sequentially crosslinked with 3 cycles of 30-kGy gamma irradiation and 130 °C thermal annealing by Quadrant Mediatech. The test preforms were machined, cleaned, packaged, and sterilized with gas-plasma at Stryker (NJ, USA) or ethylene-oxide at Steris (NJ, USA).

ETO sterilized material groups were subjected to 2-week accelerated aging at 75 psi and 70 °C in oxygen according to ASTM F2003.

**Methods:** A comprehensive battery of material characterization (Table 1) was carried out according to 2016 FDA guidance<sup>1</sup> and ASTM F2565<sup>2</sup>.

**Statistical analysis:** 2-sample equivalency hypothesis testing ( $\alpha = 0.05$ ) were performed on pairs of material groups, namely (1) RE-ETO versus CM-ETO, (2) CM-ETO versus CM-GP, (3) RE-ETO versus CM-GP, and (4) un-aged versus 2-week-accelerated-aged (CM-ETO versus CM-ETO-A and RE-ETO versus RE-ETO-A).

## Results:

All material properties were statistically equivalent ( $p > .05$ ) for each pair of unaged test groups, RE-ETO versus CM-ETO, CM-ETO versus CM-GP, and RE-ETO versus CM-GP.

ETO-sterilized groups (RE-ETO and CM-ETO) showed no reduction in mechanical properties post accelerated aging.

**Table 1:** List of the mechanical and physical tests performed

Physical Test	Mechanical Test
Density	Compression
Differential scanning calorimetry	Fatigue crack propagation
Electron spin resonance	Izod impact
Fourier-transform infrared spectroscopy	Small punch
Swell ratio	Tensile

## Discussion:

Mechanical properties and performance of SXL PE are influenced by the PE microstructure, crystallinity, and crosslinking.

Ram extrusion and ETO sterilization did not change the SXL PE microstructure as evidenced by the equivalent percentage of crystallinity and peak melting temperature. The crosslinking level was also not affected by the consolidation and sterilization as evidenced by the equivalent small punch ultimate load and swell ratio. In addition, the fatigue behavior remained the same as all three material groups showed equivalent Delta K inception, Exponent and Coefficient in the fatigue crack propagation test.

Furthermore, the consolidation and sterilization change did not impact the stability of the SXL PE as the mechanical properties of CM-ETO and RE-ETO remained the same post accelerated aging.

## Conclusion:

Changes in consolidation and sterilization method did not impact the properties of sequentially-crosslinked UHMWPE.

## References:

1. FDA Guidance 2016 “Characterization of Ultrahigh Molecular Weight Polyethylene (UHMWPE) Used in Orthopedic Devices - Draft Guidance for Industry and Food and Drug Administration Staff”, FDA, Silver Spring, MD, [www.fda.gov](http://www.fda.gov)
2. ASTM F2565-13 “Standard Guide for Extensively Irradiation-Crosslinked Ultra-High Molecular Weight Polyethylene Fabricated Forms for Surgical Implant Applications”, ASTM International, West Conshohocken, PA, [www.astm.org](http://www.astm.org)

# Edge Loading Properties of Glenoids Articulating against a Ceramic Humeral Head: Comparative Wear Study of Conventional and Highly Cross-Linked Vitamin E Polyethylene

Reto Lerf<sup>1</sup>, Simon Bell<sup>2</sup>, Frank Dallmann<sup>3</sup>

<sup>1</sup>: Mathys Ltd Bettlach, Bettlach, Switzerland; <sup>2</sup>: Melbourne Shoulder and Elbow Centre, Australia;

<sup>3</sup>: Mathys Orthopaedie GmbH, Moersdorf, Germany  
reto.lerf@mathysmedical.com

**Introduction:** Polyethylene wear resulting in glenoid loosening is the main reason for long-term failure of total shoulder replacement. Edge loading is a specific wear regime which must be addressed when considering shoulder arthroplasty. The significant translation that occurs between the humeral head and the glenoid components results in rim contact and edge loading, with potentially detrimental effects on polyethylene glenoid components. This study was done to compare the wear behaviour under edge loading of a ceramic humeral head on conventional polyethylene (CPE) glenoid components and vitamin E enhanced highly cross-linked (VEPE) polyethylene glenoids.

**Methods and Materials:** Wear tests were performed using a shoulder wear simulator set up for roll-glide with edge loading of  $\pm 1.5$  mm. The tests were run for 0.5 million cycles (Mc) with four samples per pairing at IMA GmbH, Dresden, Germany. Gravimetric measurements were according to ISO 14242-3. Commercial, sterile implants from the Affinis<sup>®</sup> Shoulder System were tested (Mathys Ltd Bettlach, Switzerland). All test cohorts used size 51/19 Affinis<sup>®</sup> ceramic ( $\text{Al}_2\text{O}_3$ ) humeral heads. On the glenoid side Affinis<sup>®</sup> components size 4 were used, in CPE and VEPE. The vitamin E enhanced highly cross-linked PE by Mathys, trade name vitamys<sup>®</sup>, is manufactured from GUR 1020 UHMWPE and contains 0.1% blended Vitamin E. Glenoids in non-aged condition and with accelerated ageing according to ASTM F2003 were compared. Photo-optical documentation of the worn surfaces were completed on all specimens before, and at the conclusion of testing.

**Results:** The unaged VEPE glenoid showed a wear rate of  $9.97 \pm 0.95$  mg/Mc, a 36% reduction compared to the unaged CPE glenoid ( $15.54 \pm 2.08$  mg/Mc;  $p=0.003$ ). Ageing significantly increased the polyethylene wear rate,  $26.44 \pm 3.01$  mg/Mc for CPE and  $13.61 \pm 1.37$  mg/Mc for VEPE. Compared to the corresponding unaged cohorts, both aged cohorts demonstrated increased wear rates after artificial ageing. However, the advantage of VEPE over CPE is more pronounced with a 49% reduction in wear in the VEPE group ( $p=0.0002$ ). Figure 1 displays these results graphically. The optical appearance after the test showed no signs of wear on the ceramic heads and typical wear patterns on the glenoid components. On the articulating surfaces of the glenoids, the transition between loaded and unloaded regions was clearly visible. Evidence of wear around the rim of the prosthesis confirmed that edge loading had occurred during the simulation (Figure 2). No back-side wear was observed.

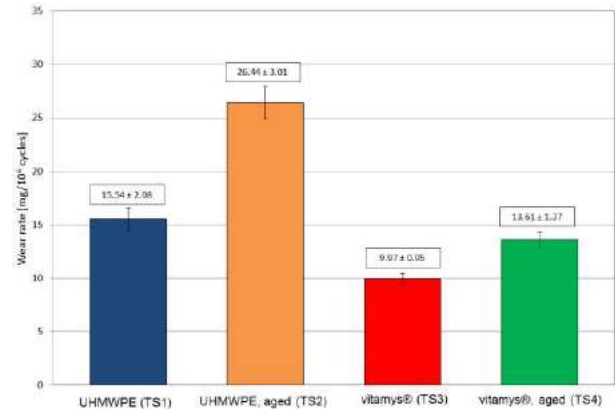


Figure 1

Wear rates of the Affinis<sup>®</sup> Glenoids



Figure 2

Typical wear pattern created by edge loading, Affinis<sup>®</sup> Glenoid vitamys<sup>®</sup>

**Discussion:** The distinct worst-case edge loading on the rim of the glenoids did not lead to abnormal wear behaviour for any group of implants. However, this study demonstrates in vitro superior wear properties of the VEPE glenoid compared to conventional polyethylene when articulating with a ceramic head under edge loading conditions. The addition of vitamin E to polyethylene was shown to decrease polyethylene degradation related to oxidation, resulting in less wear in the artificially aged VEPE glenoid compared to the corresponding CPE component.

# Characterization Methods for Structure-Property Relationships in Clinical Formulations of UHMWPE

Malito, L<sup>1\*</sup>; Kozak, A<sup>2</sup>; Spiegelberg, S<sup>2</sup>; Bellare, A<sup>3</sup>; Pruitt, L<sup>1</sup>

<sup>1</sup>University of California, Berkeley, Berkeley, CA; <sup>2</sup>Cambridge Polymer Group, Cambridge, MA; <sup>3</sup>Department of Orthopaedic Surgery, Brigham and Women's Hospital, Harvard Medical School Boston, MA

\*lmalito@berkeley.edu

## Introduction:

Mechanical properties such as elastic modulus, Poisson's ratio, yield stress, yield strain, as well as ultimate strength and fracture strain are fundamental parameters in assessing ultra high molecular weight polyethylene (UHMWPE) for orthopedics [1]. Yet, there is ongoing discrepancy in the methodology employed in characterizing these structure-property relationships that are critical for constitutive modeling and clinical predictions. Tensile properties are known to be correlated with Hertzian contact stresses, resistance to wear, fatigue, fracture, and are important for implant design.

The standardized tensile test methods for plastic materials, ASTM D638 and ISO 527, offer broad guidance in analyzing tensile properties and specify measurements based on engineering stress rather than true stress that result in variations in the reported properties for UHMWPE depending on methodology employed [2]. Such broad guidance may not sufficiently characterize the structural properties needed in understanding clinical performance of UHMWPE. This work presents a comprehensive structural characterization analysis of twelve clinically relevant formulations of UHMWPE. Microstructure, elastic, yield and post-yield behavior are analyzed along with assessment of property variations that are owed to methodology utilized.

## Methods and Materials:

### Material Formulations:

For this study, twelve clinically relevant UHMWPE material formulations were investigated (**table 1**). Material was sourced from three different UHMWPE consolidators Orthoplastics (Lancashire, UK), Depuy (Warsaw, IN), and Quadrant EPP (Fort Wayne, IN). Variations to two molecular weight resins, GUR 1020 and GUR 1050 were investigated. These variations consisted of irradiation cross-linking, antioxidant addition, as well as coupled antioxidant irradiation cross-linking. The antioxidants used were 0.1 wt% Vitamin E and Depuy's COVERNOX<sup>TM</sup> (AO) which were blended into GUR 1020 resin before consolidation. All UHMWPE formulations were compression molded. Lastly, irradiation cross-linking dosages at 75kGy in base resin materials were re-melted (RM) to alleviate free-radicals.

### Microstructural Characterization:

The microstructure of the UHMWPE formulations was measured through DSC and SAXS. DSC measurements were obtained according to ASTM F2625-10 using a Q2000 DSC (TA Instruments). SAXS data was collected using a laboratory CuK $\alpha$  rotating anode SAXSLAB instrument that used a Rigaku 002 microfocus x-ray source with Osmic staggered parabolic multilayer optics to focus the beam crossover at the second pinhole

and two sets of JJ x-ray 5 jaw collimation slits. The SAXS scattering intensity was collected by a DECTRIS PILATUS 300K detector placed at a distance that corresponds to an angular scattering range of  $q_{min}=0.032$  [nm<sup>-1</sup>] and  $q_{max}=2.5$  [nm<sup>-1</sup>], where  $q$  is defined as

$$q = (4\pi/\lambda) \sin \theta \quad (1)$$

where  $\lambda$  is the wavelength of the x-ray used (0.154 nm) and  $\theta$  is half the scattering angle. The x-ray source was operated at 45kV and 30mA. Based on beam diameter and sample thickness, the sampling volume associated with each x-ray measurement was estimated to be 0.06 mm<sup>3</sup>. Data was analyzed using a custom MATLAB script.

**Table 1: UHMWPE Formulations**

UHMWPE Material Type and Manufacturer			
1020 (Orthoplastics)	1020 AO (Depuy)	1020 0.1wt% Vit E (Orthoplastics)	1050 (Orthoplastics)
1020 35kGy (Orthoplastics)	1020 AO 80kGy (Depuy)	1020 0.1wt% Vit E 50 kGy (Orthoplastics)	1050 75kGy RM (Quadrant)
1020 75kGy RM (Orthoplastics)		1020 0.1wt% Vit E 75kGy (Orthoplastics)	
		1020 0.1wt% Vit E 100 kGy (Orthoplastics)	
		1020 0.1wt% Vit E 125kGy (Orthoplastics)	

### Uniaxial Stress-Strain:

Engineering and true tensile stress-strain testing for the determination of elastic modulus, yield stress, yield strain, non-linear hardening coefficients, engineering ultimate stress, true ultimate stress, true ultimate strain, and energetic toughness was performed per ASTM D638 and Kurtz et al 1998 [1]. Type IV tensile bar specimens, approximately 3.2 mm thick, were CNC machined from stock perpendicular to the compression molding direction with  $n=5$  specimens per UHMWPE group. Testing was performed on a Shimadzu AGS-X electromechanical load frame (Kyoto, Japan) with a 1kN load cell at  $23 \pm 2$  °C and 50mm/min displacement rate. Material deformation was measured by a non-contact video extensometer (based around a Point Grey FL3-U3-88S2C-C camera) validated to the criteria outlined in ASTM E83 for a class B-2 extensometer. Data was analyzed using a custom MATLAB script.

### Poisson's Ratio:

Tensile testing for the determination of Poisson's Ratio was performed per ASTM D638, Appendix A3. Type IV specimens were prepared in the same way as the uniaxial stress-strain group. Poisson's Ratio testing was performed using an MTS Mini-Bionix II load frame (Eden Prairie, MN) using a 5 kN load cell at  $23 \pm 2$  °C and 5mm/min displacement rate per ASTM standard. The same

non-contact video extensometer setup was used for the Poisson's ratio testing.

The Poisson's ratio was determined based on measured true axial and transverse strains as defined by ASTM D638 Appendix A3:

$$\mu = \frac{\frac{d\epsilon_t}{dP}}{\frac{d\epsilon_a}{dP}} \quad (2)$$

where  $d\epsilon_t$  is the absolute change in transverse strain,  $d\epsilon_a$  is the absolute change in axial strain, and  $dP$  is the change in the applied load. Finally the data was analyzed using a custom MATLAB script.

## Results:

Microstructure:

**Table 2: Summary of microstructural properties for non-irradiated samples of UHMWPE.** Xc is % crystallinity, L is interlamellar spacing, D is lamellar thickness, and A is amorphous thickness.

Material Type	Xc [%]	L [nm]	D [nm]	A [nm]
GUR 1020	52.2	25.7	13.4	12.3
GUR 1020 AO	51.9	26.3	13.6	12.6
GUR 1020 Vit E	52.9	26.8	14.2	12.6
GUR 1050	49.8	25.7	12.8	12.9

## Uniaxial Stress-Strain:

The elastic modulus was calculated in several ways across all UHMWPE formulations. First the modulus was calculated from the engineering stress-strain curve using a 2% secant line. It is known that UHMWPE does not conform to Hooke's law throughout the elastic range; hence, calculating a secant modulus from a certain strain can provide useful information [3,4]. It should be noted that the secant modulus values vary based on the strain value chosen. Modulus was also calculated from the true stress-strain data using a linear regression from 0.05% to several strain thresholds: 0.9%, 2.5%, and 4%. The relative standard deviation was compared across all methods along with  $R^2$  values from the linear regression fits.

A linear regression to 0.9% strain on the true stress-strain curve gave the highest  $R^2$  values across materials (0.96-0.99) without sacrificing relative standard deviation. As a result this was the chosen method moving forward to analyze the stress-strain data specifically the true stress-strain data.

Yield stress is typically agreed upon to be the local maximum on the engineering stress-strain curve. To use this information in conjunction with a model, a yield strain is required which is often reported as the true strain recorded from an extensometer at the given engineering yield stress [5]. The corresponding values of true yield strain range from 10% to 22%; it should be noted full elastic recoverability is not possible in UHMWPE from these strains and that plastic deformation occurs above 2% strains [1]. True stress-strain data accounts for change in cross sectional areas owing to the large deformations in UHMWPE and is more appropriate for mechanical characterization and constitutive modeling. In conjunction with the 0.9% regression threshold method analysis of the true stress-strain data, a 0.2% offset was performed to

calculate yield stress and strain values across the different formulations. Kurtz et al. found this method to accurately predict the onset of plastic deformation in UHMWPE [1].

Poisson's Ratio:

Poisson's ratio was calculated using a linear regression of the true axial and transverse strains over the load as described in equation 2. ASTM D638 Appendix A3 outlines a regression from 0.05% to 0.25% true axial strains however due to the noise in the data at these low strains, it made it nearly impossible to calculate Poisson's Ratio. As a result regression was taken from true axial strains of 0.05% to yield strain from the 0.2% offset line for the different UHMWPE materials. After the regression was taken, the absolute ratio of the true axial and transverse strains was calculated for Poisson's ratio. Some tensile results are listed in table 3.

**Table 3: Summary of material properties for non-irradiated samples of UHMWPE**

Material Type	GUR 1020	GUR 1020 AO	GUR 1020 Vit E	GUR 1050
True Elastic Modulus [MPa]	799.5 ± 26.2	925.9 ± 64.5	921.2 ± 13.6	810.6 ± 26.2
R <sup>2</sup> Range	0.98 - 0.99	0.97 - 0.99	0.97 - 0.98	0.98 - 0.99
Poisson's Ratio	0.459 ± 0.015	0.544 ± 0.056	0.633 ± 0.042	0.540 ± 0.076
0.2% Offset Yield Stress [MPa]	10.8 ± 1.2	12.5 ± 1.0	13.5 ± 0.4	13.2 ± 0.7
0.2% Offset Yield Strain [mm/mm]	0.016 ± 0.002	0.016 ± 0.001	0.017 ± 0.001	0.018 ± 0.001
Ultimate True Tensile Stress [MPa]	184.3 ± 17	156.4 ± 15.2	229.1 ± 9.7	202.8 ± 29.9
Ultimate True Strain [mm/mm]	4.0 ± 0.1	3.8 ± 0.1	4.2 ± 0.05	3.7 ± 0.3
Energetic Toughness [J/mm <sup>3</sup> ]	297.9 ± 24.7	253.6 ± 22.8	361.5 ± 14.7	311.1 ± 50.4
α [MPa]	24.0 ± 0.2	24.9 ± 0.8	25.8 ± 0.2	24.2 ± 0.2
β [MPa]	-19.8 ± 0.7	-19.2 ± 1.2	-19.6 ± 0.4	-18.0 ± 0.6
γ	-29.3 ± 0.8	-29.9 ± 0.9	-28.9 ± 0.2	-27.6 ± 0.7

## Discussion:

This is the first study to provide a comprehensive mechanical testing analysis of contemporary formulations of UHMWPE and demonstrates the importance of defining a standard technique for characterizing the basic mechanical behavior of these orthopedic polymers. Additionally it was found that the Poisson's ratio can change with irradiation cross-linking and antioxidant additions to values above 0.5 which is possible for polymeric materials that exhibit anisotropy [6]. This work demonstrates the importance of a considered analytical approach in extracting linear values from the inherently nonlinear stress-strain relationship of UHMWPE when elastic properties are required for predicting deformation, fracture and fatigue of orthopedic implants.

## References:

- [1] Kurtz et al. Biomaterials 1998
- [2] Kurtz UHMWPE Handbook 2<sup>nd</sup> Edition 2009
- [3] Oral et al. Biomaterials 2006
- [4] Atwood et al. JMBBM 2011
- [5] Sobieraj et al. Biomaterials 2006
- [6] Bailey and Tsuruta Polymer Science 1984

# Clinical, Wear and Oxidative Performance of Long-Term Duration<sup>TM</sup> Polyethylene Acetabular Retrievals

Medel, F.J.<sup>1</sup>; Mateo, J.<sup>2</sup>; Canales, V.<sup>3</sup>; Panisello, J.J.<sup>2</sup>; Piñol, M.<sup>4</sup>; Gómez, J.<sup>5</sup>; Martín, C.<sup>2</sup>; Peleato, P.<sup>6</sup>

<sup>1</sup>Dpt. Mechanical Engineering, University of Zaragoza-ICMA (Spain)

<sup>2</sup>Department of Orthopaedic Surgery and Traumatology. Miguel Servet University Hospital (Zaragoza; Spain)

<sup>3</sup>Department of Orthopaedic Surgery and Traumatology. Royo Villanova Hospital (Zaragoza; Spain)

<sup>4</sup>Department of Organic Chemistry. University of Zaragoza-ICMA (Spain)

<sup>5</sup>Department of Orthopaedic Surgery and Traumatology. Lozano Blesa Clinic University Hospital (Zaragoza; Spain)

<sup>6</sup>Department of Orthopaedic Surgery and Traumatology. Hospital of Barbastro (Huesca; Spain)

fjmedel@unizar.es

**Introduction:** Duration<sup>TM</sup> Stabilized Polyethylene (Stryker Howmedica) has been the precursor of modern highly crosslinked polyethylenes in total hip joint arthroplasty [1]. Duration<sup>TM</sup> Polyethylene was subjected to gamma sterilization in low-oxygen blisters and post-irradiation annealing to promote crosslinking and free radical recombination [1-2]. Thus, Duration<sup>TM</sup> components were anticipated to exhibit enhanced oxidative stability and increased crosslink density -and therefore superior wear resistance- than historical, gamma-irradiated in air, components. Previous studies have reported lower *in vitro* and radiographic wear rates for Duration<sup>TM</sup> acetabular inserts [3-4]. However, it is unclear whether the wear reduction, with its potential benefit to bone stock, and the oxidative stability of Duration<sup>TM</sup> are maintained after long-term implantation. Our objective was to assess the clinical, wear and oxidative performance of Duration<sup>TM</sup> polyethylene acetabular inserts retrieved after long-term implantation.

**Methods and Materials:** As part of our multicenter retrieval program, 12 Anatomique Benoist Girard (ABG; Stryker Howmedica) polyethylene acetabular liners were collected after revision surgery (4 historical, ABG I, and 8 Duration<sup>TM</sup>, ABG II, polyethylene). The cementless, hydroxyapatite coated, ABG hip prosthesis was one of the first systems to evolve from a historical to a moderately crosslinked (Duration<sup>TM</sup>) polyethylene component [1, 3-7]. Clinical information was available for both patient cohorts, including implantation times, patient demographics, revision reason and the incidence of osteolysis. All the acetabular retrievals were clean and photodocumented. Loaded (superior) and unloaded (inferior) regions of the polyethylene liners were identified by visual inspection. The thicknesses of both superior and inferior regions were mapped using a digital point micrometer (resolution 0.001 mm). Femoral head penetration was computed as the difference between the average inferior and superior thicknesses. FTIR oxidation analysis was carried out on polyethylene sections (150-200 microns thick) microtomed from the retrieved acetabular inserts. To avoid the interference of absorbed lipids, polyethylene sections underwent heptane extraction (6 hours) prior to oxidation assessment. Maximum oxidation indexes were calculated per ASTM F2102 at the rim, bearing and backside of the acetabular

liners. Additionally, crystallinity contents were computed from infrared spectra to evaluate changes in microstructure triggered by oxidative chain scission. Crystallinity percentages were obtained applying the following formula:

$$\%C = \frac{\frac{A_{1897}}{A_{1303}}}{\frac{A_{1897}}{A_{1303}} + 1}$$

where  $A_{1897}$  and  $A_{1303}$  represent the areas under the peaks centered at the corresponding absorption frequencies [8]. As a measure of the progression of recrystallization processes, a recrystallization percentage was defined as the difference between the crystallinity percentages at the most and least oxidized areas for the regions of interest.

**Results:** Historical, ABG I, polyethylene liners were implanted for an average of 18.2 (14.0 – 21.3) years, whereas Duration<sup>TM</sup>, ABG II, polyethylene components were *in vivo* a mean of 12.3 (4.3 – 18.5) years. Reasons of revision of ABG I liners included polyethylene wear (n=1), pain (n=1), osteolysis (n=1), and loosening (n=1). In the case of retrieved ABG II acetabular inserts, loosening (n=3), pain (n=1), periprosthetic fracture (n=1), abscess (n=1), osteolysis (n=1) and polyethylene wear (n=1) motivated the revision surgery. Evidence of osteolysis was reported in three (n=3) of the patients implanted with historical ABG I acetabular liners and in five (n=5) of the patients implanted with Duration<sup>TM</sup> polyethylene components. All the historical polyethylene acetabular liners exhibited either rim damage or delamination near the loaded region of the insert. On the contrary, ABG II liners exhibited no sign of rim damage or delamination, except for one case. Historical ABG I polyethylene liners had higher femoral penetration ( $0.10 \pm 0.05$  mm/year) than Duration<sup>TM</sup> ABG II inserts ( $0.07 \pm 0.06$  mm/year). However, the difference in femoral penetration was not statistically significant ( $p=0.35$ ; Student's t-test). Oxidation results confirmed higher average maxima indexes for historical polyethylene in rim and bearing regions (Figure 1), although these differences were not statistically significant, except for the bearing inferior region ( $p=0.0013$ ). Nevertheless, some Duration<sup>TM</sup> acetabular retrievals exhibited high oxidation (OI > 3) at the rim near loaded areas and generally

increasing oxidation with implantation time (Figure 2). According to our FTIR crystallinity data, historical retrievals exhibited higher average crystallinity maxima in all regions. Likewise, recrystallization percentages were also higher in historical polyethylene retrievals (Table 1)

**Discussion:** Lower femoral penetration and the general absence of rim and delamination damage suggest Duration™ polyethylene inserts achieved superior wear resistance than historical components even in the long-term. However, this difference in wear performance was not significant as the power of our dataset was 14% and the least significant number of samples was 51. In addition, reasons of revision and the lower incidence of osteolysis in patients implanted with the Duration™ (ABG II) acetabular inserts also point out the deleterious effects of polyethylene wear were mitigated to some extent. Regarding oxidation, historical and Duration™ polyethylenes appear to have a similar behavior, as no significant differences were found in maxima FTIR oxidation indexes, except for the bearing inferior region. These findings suggest the post-irradiation annealing was not effective in providing Duration™ polyethylene liners with improved oxidative stability compared to historical components. However, FTIR crystallinity data indicate that recrystallization processes were dominant in historical, but not in Duration™ retrievals, even taking into account the difference in implantation time. The annealing strategy was also believed to promote additional crosslinking in Duration™ polyethylene, which could hinder microstructure rearrangements triggered by oxidation. Overall, Duration™ components appear to succeed as far as wear-related properties are concerned, but its success is limited regarding oxidative stability and oxidation-induced microstructure changes.

**Acknowledgements:** This study was funded by University of Zaragoza (Project JIUZ-2014-TEC-10) and Diputación General de Aragón (Project T40-Grupo Consolidado de Investigación en Biomateriales). We thank José Alberto Villuendas (Stryker Iberia) for his support to the retrieval program and María Povar and Encarna Sánchez for their technical assistance.

## References:

- [1] Manley M. *Highly Cross-Linked and Annealed UHMWPE*. In: *UHMWPE Biomaterials Handbook (Third Edition)*
- [2] Sun et al. *Non-oxidizing polymeric material*. United States Patent No.: 6,174,934 B1. Jan 16, 2001.
- [3] Geerdink et al. *Acta Orthopaedica* (2006) 77 (5): 719–725.
- [4] Geerdink et al. *Clin Orthop Relat Res* (2009) 467:979–984.
- [5] Gallo et al. *International Orthopaedics (SICOT)* 2010; 34:19–26.
- [6] Herrera et al. *The Journal of Arthroplasty* 2013; 28: 1160–1166.
- [7] Herrera et al. *BioMed Res Int* 2015; Art. ID 386461: 1–13.
- [8] Medel, Rimnac and Kurtz. *J Biomed Mater Res* 2009; 89A: 530–538.

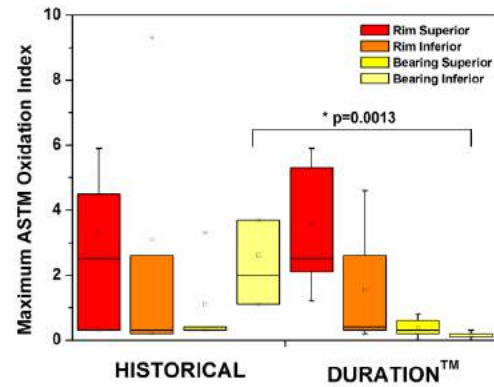


**Figure 1.** Maximum ASTM oxidation indices of historical and Duration™ polyethylene retrievals

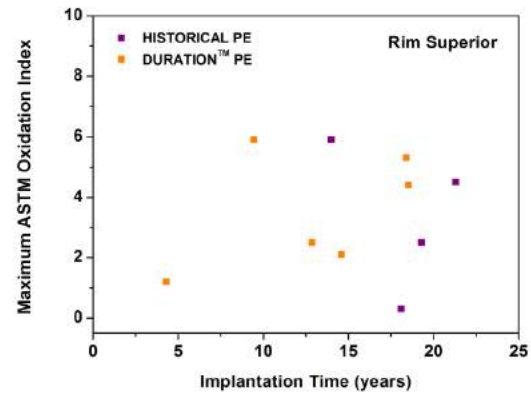


**Figure 2.** Evolution of oxidation with implantation time for acetabular polyethylene retrievals.

	RECRYSTALLIZATION (%)			
	Rim Superior	Rim Inferior	Bearing Superior	Bearing Inferior
Historical	10,4 ± 6,8	18,3 ± 11,0	16,7 ± 9,7	6,7 ± 4,7
Duration™	6,0 ± 8,1	7,0 ± 7,5	7,0 ± 9,0	4,5 ± 5,9

Table 1. Recrystallization percentages in retrieved historical and Duration™ polyethylene acetabular liners.

# In Vitro Wear and Particle Analysis Evaluation of Highly Cross-Linked UHMWPE and Vitamin E UHMWPE Thin Acetabular Liners and its Biological Effects

Satya Nambu<sup>1</sup>, Gary Hines<sup>1</sup>, Danny Chang<sup>1</sup>

<sup>1</sup>MicroPort Orthopedics, Arlington, TN-38002

satya.nambu@ortho.microport.com

**Introduction:** Many recent studies on polyethylene bearings including thin liners have demonstrated substantially lower wear for highly cross linked polyethylene (HXPE) liners when compared to conventional polyethylene (CPE) liners. Despite demonstrating excellent *in-vitro* and also *in-vivo* wear properties there are still some concerns about the incidence of osteolysis since few studies have published similar incidence of osteolysis for HXPE bearings at 15 years when compared to CPE liners (1). The findings from such studies corroborates that the incidence of osteolysis is not only dependent on the wear magnitude but also the particle characteristics (number/size/shape) and thus highlights the importance of evaluating and reporting the potential biological activity of wear debris along with the wear magnitude.

Vitamin E highly cross linked polyethylene (VEXPE) has recently been used in hip and knee bearings since its ability to prevent oxidation leading to even lower wear than HXPE bearings and thus hypothetically eliminating osteolysis. In the current study the wear and biological activity index of thin acetabular liners fabricated from VEXPE liners are compared against the thin liners fabricated from HXPE liners.

**Methods and Materials:** Hip wear testing was performed on 28-day aged 44 mm HXPE (7.5 MRad) and VEXPE (blended Vitamin E, 10 MRad) acetabular liners with 44 mm metal (CoCr) femoral head bearings. All the liners were terminally subjected to Eto sterilization. Testing was conducted in two conditions for both groups (a) normal conditions where both articulating surfaces are in pristine condition and (b) aggressive conditions where femoral heads were roughened using a diamond indenter. Six bearing couples were tested for VEXPE group while three bearing couples were tested for HXPE group. Prior to and after the conclusion of the testing, the surface roughness, diameter and sphericity of each liner were measured. Prior to testing, the liners were soaked in test lubricant for 48 hours. The liners were then removed from the test lubricant, cleaned, weighed and marked as a pre-test weight. All bearings were tested in both 6 and 12 station Shore Western orbital bearing hip wear test machine in the anatomically oriented position with the liners above and heads below. A simulated triple peak Paul gait-type loading profile with a minimum and maximum force of 200 N and 2000 N was applied to the bearings. The frequency was set to 1 Hz. The lubricant used for the test was 600 ml of 25% bovine serum with 0.2 % sodium azide, 20 mmol EDTA and DI water as per ISO 14242-3:2009. The lubricant was maintained at room temperature. The test was interrupted at regular intervals

of 0.5 Mc from 0-1Mc and thereafter for every 1 Mc for gravimetric assessment of the bearing wear. Lubricant volume and concentration was maintained by periodic addition of DI water to compensate for the evaporation of water during the tests. The lubricant was changed every 500k cycles.

Following wear testing, fluid (serum) from wear specimens were taken at one and five million cycles (Mc) for wear particle/debris morphological analysis. The wear particles were processed and isolated per ASTM F1877. The wear particles were then characterized using laser diffraction (Low Angle Laser Light Scattering, LALLS) and scanning electron microscopy (SEM) to obtain measures of particle size, shape and composition SEM number based analysis was performed on tif images at 100x, 1,000x and 10,000x magnification. The software program, Scion Image, was used to evaluate area, perimeter, ellipse major axis, ellipse minor axis for each particle on the image.

**Results and Discussion:** Figure 1 shows the results from the wear testing. VEXPE liners exhibited lower wear than the HXPE liners under both testing conditions (i.e., normal and aggressive wear conditions)

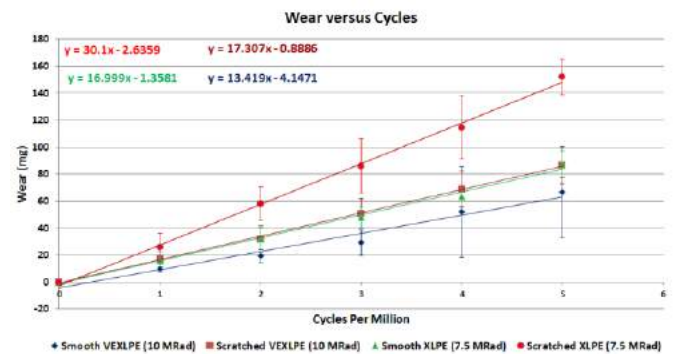


Figure 1: Cumulative Wear of aged bearing couples per million cycles

The particle morphology from the current study demonstrated particle aspect ratio, circular shape factor and equivalent circular diameter all within the range of *in vivo* particle characteristics for both VEXPE and HXPE groups in both normal and aggressive wear conditions. The results from the study demonstrate the wear magnitude lower than threshold required for osteolysis which is reported to be 80 mm<sup>3</sup>/Mc (2)

The particle biological activity characterization was conducted as per the previously published work by Fisher et al., and compared to smooth and rough head explants (3). The particles was first classified in three groups (i) <

1, (ii)1.0-10 and (iii)> 10  $\mu\text{m}$  ranges. The B(r) for each of these size ranges were 1.0, 0.17 and 0.04. The specific biological activity index (SBA) was then evaluated by integration of the product of the B(r) and volumetric wear. The functional biological activity index was then evaluated by multiplying the SBA and volumetric wear rate (Table's 1, 2 and 3).

Table 1: Biological Activity Index for 3 size ranges of polyethylene particle

Size Range of particle	0.1-1.0 $\mu\text{m}$	1.0- 10 $\mu\text{m}$	10-100 $\mu\text{m}$
B[r] mean (range)	1	0.17 (0.01 -0.44)	0.04 (0-0.34)
Smooth-XLPE C(r)	0.75	0.22	0.04
Smooth - VEXPE C(r)	0.82	0.17	0.01
<b>Roughened-XLPE C(r)</b>	0.70	0.29	0.00
Roughened-VEXPE C(r)	<b>0.78</b>	<b>0.21</b>	<b>0.02</b>

Table 2: SBA and FBA index for HXPE and VEXPE groups

Groups	SBA	Volumetric wear rate	FBA index
Smooth-XLPE	0.11	17.3	1.9
Smooth - VEXPE	0.07	13.4	0.99
<b>Roughened-XLPE</b>	0.08	30.1	2.42
Roughened-VEXPE	<b>0.08</b>	<b>17.0</b>	<b>1.44</b>

**Conclusions:** The results from the testing demonstrate that VEXPE thin liners generate lower wear than the HXPE liners. However substantial differences were more evident when comparing FBA indices indicating the importance of particle characteristics when presenting the wear data.

#### References:

1. Tsukamoto et al., J.Arthroplasty, 2017, Jan;32 (1):161-165
2. Oparaugo et al., Acta Orthop Scand 2001;72(1):22-28
3. Fisher et., 46<sup>th</sup> ORS, 0588, 2000

## Safe and efficacious release of pain medication from UHMWPE

Suhardi VJ<sup>1,2,3</sup>, Bichara DA<sup>1,2</sup>, Freiberg AA<sup>2</sup>, Bedair H<sup>1,2</sup>, Muratoglu OK<sup>1,2</sup>, Oral E<sup>1,2,+</sup>

<sup>1</sup>Massachusetts General Hospital; <sup>2</sup>Harvard Medical School; <sup>3</sup>Massachusetts Institute of Technology  
[eoral@mgh.harvard.edu](mailto:eoral@mgh.harvard.edu)

**Introduction:** The use of narcotic medications to manage postoperative pain after TJA has been associated with impaired mobility, diminished capacity to engage in rehabilitation, and lower patient satisfaction [1]. In addition, side effects including respiratory distress, constipation, dizziness, nausea, vomiting and urinary retention can prolong post-operative hospital stays. Intraarticular administration of local anesthetics such as bupivacaine reduces pain and lowers patients' length of stay [2]. We present a total joint arthroplasty bearing surface eluting pain medication for at least 2 weeks.

**Methods and Materials:** Medical grade UHMWPE was mixed with bupivacaine hydrochloride (BH) or bupivacaine free base (FB) and consolidated. Another construct was prepared with FB-blended UHMWPE layered with 1 mm-thick BH-blended UHMWPE (Bupi-PE) before compression molding (~10 mm-thick). Cylindrical pins were machined and wear tests were performed as previously described [3]. Strips (3 × 5 × 20 mm) were eluted in phosphate buffered saline (PBS) at 37°C. Bupivacaine concentration was measured by UV spectroscopy at 263 nm. A total of *n*=5 male Sprague Dawley rats (250 g) were implanted with Bupi-PE plugs (2.5 mm diameter and 5 mm length) transchondylarly. Efficacy was determined by performing a walking track analysis using a Tekscan® sensor (VHR, 5101). Walking tracks were performed at baseline (pre-surgery) and every 24 hours for two weeks. A total of *n*=5 male Sprague Dawley rats (250 g) were implanted subcutaneously with control or bupi-PE plugs. After incision site closure, 5 × 10<sup>7</sup> cfu of bioluminescent *Staphylococcus aureus* were injected around the implants. Bioluminescent signal (photons/s) was measured daily.

**Table 1. Wear and mechanical strength of bupivacaine-eluting UHMWPE.**

Parameter	Layered Construct
Yield Strength	21.0 ± 2.6
Ultimate Tensile Strength (MPa)	24.5 ± 2.5
Elongation to Break (%)	322 ± 53
Impact Strength (kJ/m <sup>2</sup> )	112 ± 4.9
Wear Rate (mg/million cycle)	4.2 ± 0.9

**Results:** Different elution profiles were feasible by changing the hydrophobicity of bupivacaine in UHMWPE (**Figure 1**). Burst release was decreased and bupivacaine release was sustained for at least 2 weeks by using a layered construct. Wear rates of bupivacaine-eluting UHMWPE with and without radiation crosslinking were in the range for clinically used UHMWPE bearing surfaces (**Table 1**). After the implantation of a UHMWPE plug transchondylarly, rats with the Bupi-PE implant

loaded both the operated and non-operated hindlimbs similarly for the duration of the study.

**Antibacterial activity:** Two control rats expired presumably due to sepsis. None of the Bupi-PE rats expired during the study. Significantly less bacterial load (indicated by bioluminescence) was observed in rats receiving Bupi-PE starting at 24 hr post implantation until the end of study (**Figure 2**).

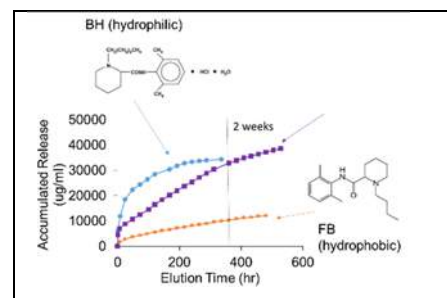


**Figure 1.** The in-vitro elution profile of bupivacaine from UHMWPE.

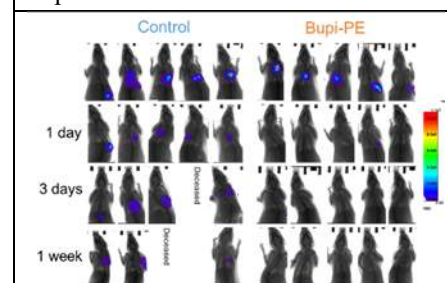


**Figure 2.** The bioluminescence signal in the dorsum of rats implanted with bupivacaine-eluting UHMWPE and inoculated with bioluminescent *Staphylococcus aureus* (Xen 29) as a function of time.

controlled release formulation (Exparel™, Pacira Pharmaceuticals, San Diego, CA) [4].

Bupivacaine-eluting UHMWPE also effectively reduced *S. aureus* load in the murine subcutaneous dorsum. The wear rate of the material was well within the range of clinically used UHMWPEs. This material is promising for use as infection prophylaxis and pain management after TJA.

**References:** [1] Tsukada, S et al. J Bone Joint Surg Am, 2014. 96(17): p. 1433-8. [2] Barrington JW et al., Orthop Clin North Am, 2015. 46(4): p. 469-77. [3] Oral E et al. J Biomed Mater Res 2016. 104B: p. 316-322. [4] Nadeau MH et al. Aesthetic Surgery Journal 2016. 36(2): p. NP47-NP52. [5] Domb BG et al. BMC Musculoskeletal Disorders 2014. 15:310.

**Discussion:** Bupivacaine was successfully loaded into UHMWPE bearing surfaces to elute at a clinically relevant concentration for at least 2 weeks. Efficacy was confirmed functionally *in vivo*. A bupivacaine-eluting UHMWPE surface has the potential of addressing pain for a longer time than the currently used

## Rifampin and vancomycin-eluting UHMWPE for long-term infection treatment

Suhardi VJ<sup>1,2,3</sup>, Bichara DA<sup>1,2</sup>, Freiberg AA<sup>2</sup>, Rubash HE<sup>2</sup>, Malchau H<sup>1,2,4</sup>, Muratoglu OK<sup>1,2</sup>, Oral E<sup>1,2,+</sup>

<sup>1</sup>Massachusetts General Hospital; <sup>2</sup>Harvard Medical School; <sup>3</sup>Massachusetts Institute of Technology; <sup>4</sup>Sahlgrenska University Hospital  
[eoral@mgh.harvard.edu](mailto:eoral@mgh.harvard.edu)

**Introduction:** The gold standard for peri-prosthetic joint infection (PJI) treatment is two-stage surgery [1] which is a prolonged procedure where the patient is mainly immobilized during treatment. Developing an antibiotic-eluting UHMWPE bearing surface has the potential of addressing a biofilm infection in a single stage. In this study, we incorporated rifampin and vancomycin into UHMWPE to investigate its elution characteristics, the mechanical properties as a bearing surface and its efficacy against a biofilm infection in a pre-clinical animal model.

**Methods and Materials:** Rifampin and vancomycin hydrochloride were incorporated into UHMWPE by blending and consolidating via layering a 1 mm layer of the antibiotic-containing UHMWPE on UHMWPE without any antibiotics. For drug elution, blocks were placed in 1 ml of phosphate buffered saline (PBS) and the eluted concentration of rifampin and vancomycin was measured by UV-Vis spectroscopy at 450 nm and 280 nm, respectively. Impact strength was tested according to ASTM D256. For antibacterial efficacy *in vivo*, skeletally mature adult male New Zealand White rabbits received either two non-antibiotic eluting UHMWPE plugs (control, n=5), bone cement (40 g) containing vancomycin (1 g) and tobramycin (3.6 g) (VTBC) or rifampin and vancomycin-eluting UHMWPE (RVPE, n=5) (3 mm in diameter and 6 mm length) in the patellofemoral groove. All rabbits received a beaded titanium rod in the tibial canal (4 mm diameter and 12 mm length) with a fully grown bioluminescent *Staphylococcus aureus* biofilm (Xen 29, Perkin Elmer 119240). None of the animals received any intravenous antibiotics for this study. Bioluminescence signal (photons/second) of the affected knee was measured when the rabbits expired, or at the study endpoint (day 21).

**Results:** Rifampin and vancomycin elution was sustained for over 35 weeks (>8 months). Vancomycin elution was higher than rifampin elution at all times during elution (Figure 1). The impact strength of the layered construct before sterilization was  $138 \pm 4$  kJ/m<sup>2</sup>. In our lapine acute biofilm infection model using bioluminescent *S. aureus*, knees treated with UHMWPE without antibiotics and bone cement containing vancomycin and tobramycin had significantly higher bioluminescence compared to those treated with RVPE (Figure 2).

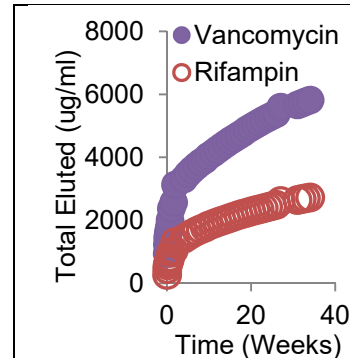


**Figure 1.** The elution of rifampin and vancomycin from RVPE.

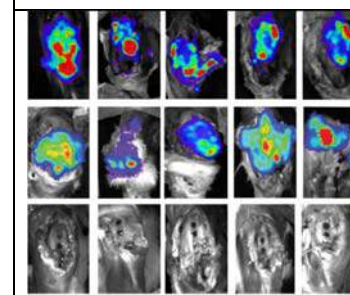


**Figure 2.** Knees inoculated with *S. aureus* treated with UHMWPE without antibiotics (control), bone cement with vancomycin and tobramycin (VTBC) and VPE.

**Discussion:** The total amount of rifampin and vancomycin and their ratio was optimized based on the preferred trough concentrations [2, 3]. Vancomycin concentration was higher than the rifampin concentration at all times during elution, which was designed to prevent the development of bacterial resistance to rifampin. A layered construct was devised to enable antibiotic elution without compromising the mechanical properties or the wear resistance of a long-term implant. Efficacy against a full grown biofilm was shown *in vivo*; the elimination of biofilm was also possible when using RVPE only compared to VTBC. Thus, these preliminary results suggest that a rifampin and vancomycin-eluting UHMWPE bearing surface designed with state-of-the-art wear resistance is feasible and is promising as an alternative treatment modality for peri-prosthetic joint infection in a single stage surgery.

**References:** [1] Zimmerli W. Journal of Internal Medicine, 2014. **276**: p. 111-119; [2] Garnham JC et al. Br. J. Clin. Pharmacol, 1976, 3, 897-902; [3] Liu C et al. Clin. Infect. Dis. 2011, 52, 1-38.

## Vancomycin-eluting UHMWPE bearing surface for acute PJI

Suhardi VJ<sup>1,2,3</sup>, Bichara DA<sup>1,2</sup>, Freiberg AA<sup>2</sup>, Rubash HE<sup>2</sup>, Malchau H<sup>1,2,4</sup>, Muratoglu OK<sup>1,2</sup>, Oral E<sup>1,2,+</sup>

<sup>1</sup>Massachusetts General Hospital; <sup>2</sup>Harvard Medical School; <sup>3</sup>Massachusetts Institute of Technology; <sup>4</sup>Sahlgrenska University Hospital; [eoral@mgh.harvard.edu](mailto:eoral@mgh.harvard.edu)

**Introduction:** The standard for peri-prosthetic infection (PJI) treatment uses antibiotic-loaded bone cement spacers, which are limited in load bearing; fracture and displacement are common occurrences [1]. Developing an antibiotic-eluting UHMWPE bearing surface can improve the mechanical properties of spacers and improve the quality of life of patients. Vancomycin is commonly used due to its activity against *Staphylococcus aureus* and *Staphylococcus epidermidis*, which constitute the infecting organisms in a majority of PJI cases [2]. We incorporated vancomycin into UHMWPE to investigate its elution characteristics, mechanical properties and its in-vivo efficacy against an acute PJI.

**Methods and Materials:** Vancomycin hydrochloride (4-10 wt%) was incorporated into UHMWPE by blending and consolidating. For drug elution, blocks were placed in 1 ml of phosphate buffered saline (PBS) and the eluted concentration of vancomycin was measured by UV-Vis spectroscopy at 280 nm. Tensile mechanical properties were tested according to ASTM D638 and impact strength was tested according to ASTM D256. For antibacterial efficacy *in vivo*, skeletally mature adult male New Zealand White rabbits received either two non-antibiotic eluting UHMWPE (control, n=5), bone cement (40 g) containing vancomycin (1 g) and tobramycin (3.6 g) or vancomycin-eluting UHMWPE (n=5) (3 mm diameter and 6 mm length) in the patellofemoral groove. All rabbits received a beaded titanium rod in the tibial canal (4 mm diameter and 12 mm length). All groups received two doses of  $5 \times 10^7$  cfu of bioluminescent *S. aureus* (Xen 29, PerkinElmer 119240) in 50  $\mu$ L 0.9 % saline in the following sites: (1) distal tibial canal prior to insertion of the rod; (2) articular space after closure of the joint capsule. None of the animals received any intravenous antibiotics for this study. Bioluminescence signal (photons/second) of the affected knee was measured when the rabbits expired, or at the study endpoint (day 21).

**Table 1.** Wear and tensile mechanical properties. Cross-linked: 100-kGy irradiated and melted.

	Wear rate (mg/MC)	UTS (MPa)	Impact Strength <sup>2</sup> (kJ/m <sup>2</sup> )
Unirradiated	9.7±0.2	53.0±3.0	127±8
Cross-linked	1.2±0.3	42.7±0.6	57±1
VPE (7%)	9.6±1.2	35.5±2.6	67±1

**Results:** Vancomycin elution increased with increasing drug loading (**Figure 1**). Elution above MIC (2  $\mu$ g/ml) for

3 weeks and optimized mechanical properties (**Table 1**) were obtained at 6-7 wt% vancomycin loading. In our lapine acute infection model using bioluminescent *S. aureus*, knees with UHMWPE without antioxidants and bone cement containing vancomycin and tobramycin had higher bioluminescence compared to those treated with vancomycin-eluting UHMWPE (**Figure 2**).

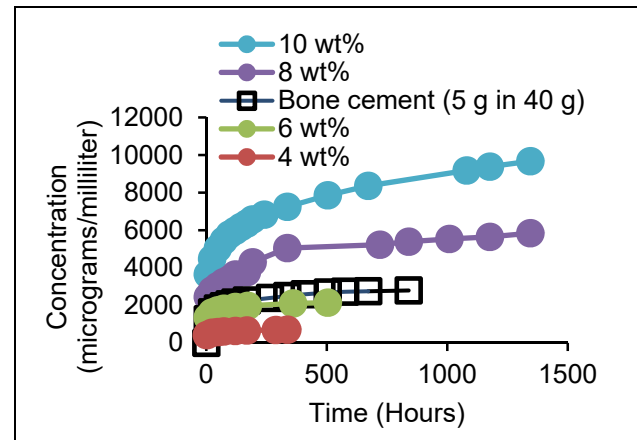


**Figure 1.** The elution of vancomycin from vancomycin-eluting UHMWPE and hand-mixed bone cement.

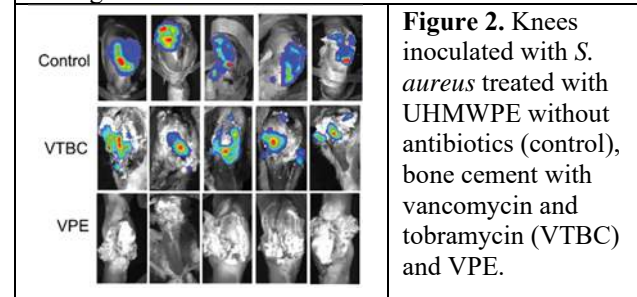


**Figure 2.** Knees inoculated with *S. aureus* treated with UHMWPE without antibiotics (control), bone cement with vancomycin and tobramycin (VTBC) and VPE.

**Discussion:** A vancomycin-eluting UHMWPE bearing surface, which could elute enough vancomycin to be effective against an acute *S. aureus* infection for at least 3 weeks with mechanical strength and wear resistance comparable to clinically available UHMWPEs was developed. In a lapine joint implantation model incorporating an acute planktonic infection, this UHMWPE showed higher efficacy against infection compared to bone cement containing vancomycin and tobramycin, a commonly used combination of antibiotics to treat PJI. These results suggest that an antibiotic-eluting UHMWPE spacer with acceptable properties as a bearing surface could be used to treat PJI in lieu of bone cement spacers. This could allow safer load bearing and a higher quality of life for the patients during treatment.

**References:** [1] Jung et al. International Journal of Medical Sciences, 6, 265-273 (2009). [2] Mittag et al. Acta Orthop Bras. 24(1): 43-47 (2016).

## **HXLPE with Covernox Antioxidant in Total Knee Arthroplasty: Risk and Reasons for Short-Term Revisions**

Mathew Kelly, Guy Cafri, Steven M. Kurtz, Elizabeth W. Paxton

**Introduction:** Highly crosslinked polyethylene (HXLPE) with Covernox antioxidant has been clinically introduced since 2014. Little is known about the clinical performance of TKAs with this novel type of antioxidant-containing HXLPE [1-4]. The purpose of this study was to compare the short-term risk and reasons for revision of TKAs incorporating HXLPE stabilized by Covernox versus other knee systems.

**Materials and Methods:** Using an integrated healthcare systems registry, 2,054 primary TKAs incorporating Covernox-stabilized HXLPE (Attune: DePuy Synthes, Warsaw, IN) were identified in the registry between 2001-2015. There were 142,360 primary knee systems identified in the registry (2001-2015). Age, gender, ASA scores, diagnoses, and revision surgery were obtained from the registry. The outcome of interest was cumulative percent revision and reasons for revision surgery.

**Results:** Mean follow-up was 1.10 years for COVERNOX-stabilized knees versus 5.12 for other knees. COVERNOX and the other knee group were similar in age, gender, and primary diagnosis. There were 19 COVERNOX and 3,797 other knee revisions during the study period. Two-year cumulative percent revision was 1.38% for COVERNOX (95% CI: 0.45%-2.8%) and 1.79% for other knees (95% CI: 1.67%-1.92%). The main reasons for ATTUNE revisions were infection (n=12, .6%), wound drainage (n=4, .2%), wound dehiscence (n=3, .1%) Instability (n=2, .1%), and hematoma-seroma (n=2, .1%).

**Conclusions:** Short-term results do not indicate a difference in revision rates for knee systems including Covernox-stabilized HXLPE versus other knee systems. Although previous studies have identified locking mechanisms and tibial baseplate loosening as potential concerns for the Attune design [1,2], such potential reasons for revision were not encountered by patients in the present study. Radiographic analyses, retrieval analyses, longer follow-up, and larger numbers are needed to better understand the clinical performance of knee systems incorporating Covernox-stabilized HXLPE.

### **References**

1. Bonutti PM, Khlopas A, Chughtai M, Cole C, Gwam CU, Harwin SF, Whited B, Omiyi DE, Drumm JE. Unusually High Rate of Early Failure of Tibial Component in ATTUNE Total Knee Arthroplasty System at Implant-Cement Interface. *J Knee Surg* 30(5): 435, 2017
2. Ay GR. Failure of Polyethelene Insert Locking Mechanism after a Posterior Stabilised Total Knee Arthroplasty- A Case Report. *J Orthop Case Rep* 6(3): 35, 2016
3. Martin JR, Jennings JM, Watters TS, Levy DL, McNabb DC, Dennis DA. Femoral Implant Design Modification Decreases the Incidence of Patellar Crepitus in Total Knee Arthroplasty. *J Arthroplasty* 32(4): 1310, 2017
4. Ranawat CS, White PB, West S, Ranawat AS. Clinical and Radiographic Results of Attune and PFC Sigma Knee Designs at 2-Year Follow-Up: A Prospective Matched-Pair Analysis. *J Arthroplasty* 32(2): 431, 2017

## Vitamin E-stabilized UHMWPE: evaluation of biological response on human osteoblasts to wear debris

Emanuela Galliera<sup>1,2</sup>, Vincenza Ragone<sup>4</sup>, Monica Gioia Marazzi<sup>1</sup>, Francesca Selmin<sup>5</sup>, Lorenzo Banci<sup>4</sup>, Massimiliano M.Corsi

Romanelli<sup>1,3</sup>

<sup>1</sup> Department of Biomedical Sciences for Health, Università degli Studi di Milano, Milan, Italy

<sup>2</sup> IRCCS Galeazzi Orthopaedic Institute, Milan, Italy.

<sup>3</sup> U.O.C SMEL-1 Patologia Clinica IRCCS Policlinico San Donato, San Donato, Milan, Italy.

<sup>4</sup> Research and Development Department, Permedica S.p.A. via como, 38 Merate (LC), Italy.

<sup>5</sup> Department of Pharmaceutical Science, Università degli Studi di Milano, Milan, Italy.

[Vincenza.Ragone@permedica.it](mailto:Vincenza.Ragone@permedica.it)

**Introduction:** Ultra High Molecular Weight Polyethylene (UHMWPE) wear debris stimulated a chronic inflammatory response, mainly mediated by infiltrating macrophages which are responsible of the phagocytosis of wear particles. UHMWPE doped with vitamin E was introduced as a method to provide oxidation resistance upon sterilization, without modifying UHMWPE mechanical property. During osteolytic process, osteoblasts have been shown to produce not only inflammatory mediators, but also osteoimmunological factors, such as RANKL and OPG and the inhibitors of Wnt pathway DKK-1 and Sclerostin. This study aimed to investigate in vitro how vitamin E-blended UHMWPE wear debris might modulate osteoblast mediated osteolysis, focusing in particular on the production of osteoimmunological markers RANKL, OPG, Sclerostin and DKK-1 compared to conventional UHMWPE wear debris.

**Methods and Materials:** UHMWPE wear particles were generated by four different types of UHMWPE articular inserts (raw material: GUR 1020): Material A) A moderately cross-linked vitamin E-blended UHMWPE (60 kGy electron-beam irradiated) (vitamin E concentration 0.1wt%) and EtO sterilized (*Vital-XE*<sup>®</sup>, Permedica, S.p.A.); Material B) standard UHMWPE (without vitamin E and not cross-linked) and EtO sterilized (Permedica, S.p.A.); Material C) vitamin E-blended UHMWPE (vitamin E concentration 0.1wt%) not cross-linked and EtO sterilized (*Vital-E*<sup>®</sup>, Permedica, S.p.A.); Material D) standard UHMWPE (without vitamin E and not cross-linked) and electron-beam sterilized (25 kGy) (Permedica, S.p.A.).

Human osteoblastic cell line SaOS2 were incubated with wear particles derived from UHMWPE doped and not doped and cellular response was evaluated in terms of gene expression and protein production of IL-6, RANKL; OPG, DKK-1, Sclerostin, compared to not treated cells

**Results:** RANKL, a bone erosion marker, resulted reduced, while OPG, as bone protective markers, resulted increased by the presence of vitamin E-blended UHMWPE compared to UHMWPE treatment. Sclerostin and DKK1 were not different from the control in presence of vitamin E-blended UHMWPE otherwise the two inhibitors of Wnt pathway resulted increased at different level in the conventional UHMWPE treatment group

**Discussion:** The present study focused for the first time on the osteo-inflammatory response of human osteoblast to vitamin E-blended UHMWPE, in order to evaluate whether vitamin E could protect from the inflammatory induced osteolysis through a modulation of the osteoimmunological response.

The majority of in vitro cell studies have dealt with commercial particles. In contrast, the present study focused on particles experimentally generated simulating the prosthetic joint wear, in order to produce UHMWPE particles more representative of the prosthetic wear debris occurred in vivo. In order to investigate the response of SaOs2 to wear particles of vitamin E-blended UHMWPE, we evaluated the production of different cytokines and osteoimmunological biomarkers that could be involved in the alteration of bone formation-resorption homeostasis, thus promoting aseptic loosening of the implant. The amount of IL-6 is far below the level of cytokines produced by osteoblasts in the presence of an inflammatory response [39], therefore it should be more referred to an initial response to the treatment with wear particles in order to induce a tissue remodelling process by stimulating, in turn, the production of osteoimmunological mediators.

OPG, a decoy receptor for RANKL, protects bone from excessive resorption by binding to RANKL and preventing it from binding to RANK. Thus, the relative concentration of RANKL and OPG in bone is a major determinant of bone mass and strength. Our results

suggest that vitamin E-blended UHMWPE strongly reduced RANKL production, thereby preventing osteoclasts activation and protecting from bone erosion. Similarly, standard UHMWPE debris has been reported to induce a suppression of OPG by human osteoblasts.

Taken together these results indicate that vitamin E-blended UHMWPE wear particles are able to influence the osteoimmunological response of SaOS2 cells, shifting the balance of RANKL-OPG production toward the bone protective role of OPG and suppressing the bone resorptive function of RANKL. Our results suggest that Sclerostin seems sensible to both vitamin E-blended UHMWPEs (cross-linked or not), while DKK-1 is more sensible to not cross-linked vitamin E-blended UHMWPE (Material C), which should have a higher protective effect from bone erosion than cross-linked vitamin E-blended UHMWPE. On the other hand E-beam sterilized standard UHMWPE (Material D) induced up-regulation of both inhibitors of the Wnt pathway (Sclerostin and DKK-1) suggesting that this material is the most prone to bone erosion.

Sclerostin and DKK-1 results confirm the indication of the canonical osteoimmunological biomarker RANKL-OPG, thereby suggesting that the presence of vitamin E-blended UHMWPE prevents the bone from erosion induced by UHMWPE alone.

Taken together these results indicated that in bone cells the vitamin E-blended UHMWPE induces an osteoimmunological response that positively affects the osteolysis induced by wear debris, thereby reducing the aseptic loosening of the implants.

# Estimating the osteolysis-free life of a total hip prosthesis with polyethylene bearings

Elke R<sup>1</sup> and Rieker CB<sup>2</sup>

<sup>1</sup>Merian Iselin Hospital, Basle, Switzerland

<sup>2</sup>Zimmer Biomet EMEA, Winterthur, Switzerland

*clauder.rieker@zimmerbiomet.com*

**Introduction:** Total Hip Arthroplasty (THA) is a well-established, cost-effective treatment for improving function and alleviating pain in patients who have disabling hip disease with excellent long-term results. Based on the excellent results, there is an ongoing trend for THA to be performed in younger and more active patients, having higher physical demands on their new total joints.

Polyethylene (PE) wear and its biological consequences are one of the main causes of implant failure in THA. Macrophages phagocytise PE wear particles and this will result in osteolysis and loss of periprosthetic bone<sup>1</sup>. The risk of these complications can be estimated in relation to the amount of volumetric wear based on two assumptions: firstly the number of PE particles dispersed in the periprosthetic tissues is controlled by the amount of PE wear; and secondly the development of osteolysis and the resulting aseptic loosening is triggered by these PE particles. Based on these two assumptions, a model was developed to estimate the osteolysis-free life of a THA, depending on the Linear Wear Rate (LWR) and femoral head size of the PE bearing.

**Methods and Materials:** An extensive review of the literature was conducted to provide an estimate of the radiologic osteolysis threshold based on the volumetric wear of the PE bearing. This review demonstrates that this radiologic osteolysis threshold is approximated 670 mm<sup>3</sup> for conventional PE. The osteolysis-free life of the THA was estimated by simply dividing this threshold volume by the annual Volumetric Wear Rate (VWR) of the bearing. The annual VWR is basically controlled by two parameters: firstly the annual LWR and secondly the head size. This annual VWR was calculated by using the Ilchmann formula<sup>2</sup>.

**Results:** For 28 mm, 36 mm, and 44 mm heads, following osteolysis-free life was determined in function of the annual LWR:

LWR	28 mm	36 mm	44 mm
10 µm/yr	116.61 yr	70.54 yr	47.22 yr
25 µm/yr	46.64 yr	28.21 yr	18.89 yr
50 µm/yr	23.31 yr	14.10 yr	9.44 yr
100 µm/yr	11.65 yr	7.05 yr	4.72 yr
200 µm/yr	5.82 yr	3.52 yr	2.36 yr

**Discussion:** The osteolysis-free life determined by this model is in good agreement with the clinical results of PE bearings having a 28 mm head size and demonstrates that extreme low LWRs are mandatory to assure a descent osteolysis-free life for THA (PE bearings) using large heads, such as 36 mm and 44 mm. For such head sizes, small variations of the LWR may have large impacts on the osteolysis-free life of the THA. For even larger head sizes, this analysis nicely confirms the bad clinical results (40% survival rate at eight years<sup>3</sup>) with resurfacing systems using conventional PE.

A limitation of the model is that the findings may not be readily generalizable to highly crosslinked polyethylene (XLPE), as the threshold volume for the latter is still to be determined. Furthermore, as different XLPEs are available on the market, the critical volume could be different for each specific brand. Even if this critical volume could be different from the 670 mm<sup>3</sup> seen for conventional PE, the influence of the two key parameters (linear wear rate and head diameter) also holds true for XLPE, and too large head sizes will still jeopardize the estimated osteolysis-free time of THA.

**Conclusions:** A model designed to determine the necessary wear resistance (LWR) for assuring good long-term results for UHMWPE bearings was presented and this model demonstrates that small variation in the LWR may have large clinical impacts, especially for large head sizes (≥ 36 mm).

Even if this model was not calibrated for XLPEs (unknown critical volume leading to osteolysis), we postulate that this model can be also be very useful for determining the maximum possible head size for articulations based on XLPE. However, further large-scale and long-term clinical outcome studies evaluating the effect of head size on the association between PE wear and osteolysis are warranted, especially for XLPE bearings.

<sup>1</sup> Willert et al / Reactions of the articular capsule to wear products of artificial joint prostheses / JBMR 11, 1977, p. 157

<sup>2</sup> Ilchmann et al / Estimation of the wear volume after total hip replacement / ME&P 30, 2008, p. 373

<sup>3</sup> Howie et al / Wagner Resurfacing Hip Arthroplasty / JBJS 72A, 1990, p. 708

# Evaluation of Batch-to-Batch Variability in Fracture Properties of Conventional, Highly Crosslinked, and Hindered Phenol Antioxidant UHMWPEs

Rimnac, C<sup>1</sup>, Bensusan, J<sup>1</sup>, Gupta, C<sup>2</sup>, Narayan<sup>2</sup>

<sup>1</sup>Case Western Reserve University, Cleveland OH; DePuy Synthes, Warsaw, IN, USA  
clare.rimnac@case.edu

**Introduction:** The static and cyclic fracture properties of UHMWPE in the presence of stress concentrations are important to characterize (in addition to oxidation and wear resistance) [1]. It is unclear how much batch-to-batch variation in fracture properties may occur. Thus, the objective of this study was to characterize the batch-to-batch variations in static fracture resistance (via the J-Integral test) and fatigue crack propagation resistance for 5 formulations of UHMWPE, from conventional, to first-generation highly crosslinked, to second-generation hindered phenol antioxidant.

**Methods and Materials:** All materials were provided by DePuy Synthes. Three batches each of the following materials were evaluated (Table 1): GVF (vacuum barrier gamma sterilized), Marathon, XLK, AltrX, and AOX.

*Static fracture resistance (J-R curves):* To generate the J-R curve, J Integral testing was conducted on 9-12 three-point bend specimens per batch for each material group using the multiple specimen test method described in ASTM Standard D 6068. At least 48 hours prior to testing, the notch was sharpened with a razor using a custom-built apparatus that displaces the razor at a constant displacement speed (1.0 micron/sec) to minimize damage at the crack tip. Tests were conducted in ambient air on an Instron closed-loop servo-hydraulic test machine at a displacement rate of 0.85mm/s. Stable crack extensions to different amounts in each specimen were created and load v. deflection was recorded.  $J$  (kJ/m<sup>2</sup>) was determined from the load-deflection curves according to:  $J = (2A)/(Bb)$ , where  $A$  is the area under the load-deflection curve,  $B$  is the specimen thickness, and  $b$  is the length of the unfractured ligament.  $J$  was corrected for indentation at the loading points, as per the standard. After unloading, the specimens were soaked in liquid nitrogen and then broken open at a high strain rate so as to clearly demarcate the crack extension that occurred during the test. The crack extension  $\Delta a$ , was determined directly from the fracture surface of each specimen using high resolution digital photography and computer image analysis (ImageJ).  $J$  v.  $\Delta a$  was fit with a power law regression to describe the J Integral resistance (J-R) curve ( $J = C_1 \Delta a^{C_2}$ ). For comparison between materials, an estimate of  $J$  at early crack initiation was ( $J_{init}$  at  $\Delta a = 0.5\text{mm}$ ) was also determined.

*Fatigue crack propagation (FCP):* FCP tests were conducted on an Instron servo-hydraulic testing machine following ASTM E647 as a guide. At least 3 specimens from each batch of each material were tested. All specimens were razor sharpened to a depth of 2mm and a minimum of 16 hours prior to testing. A sinusoidal waveform of 3 Hz and R ratio of 0.1 (minimum load/maximum load) was used for all cycling. An air jet

was used to cool the specimens during loading. Cycling was interrupted and the crack length measured for every 0.2mm of crack extension. Specimens were tested to failure (full fracture or until extensive opening of the specimen inhibited taking crack length measurements). Fatigue crack growth rate ( $da/dn$ ), and cyclic stress intensity factor ( $\Delta K$ ) were calculated. Linear regression of the log-log data was used to determine the exponent ( $m$ ) and coefficient ( $C$ ) of the Paris relationship ( $da/dn = C \Delta K^m$ ). The Paris regime was defined as the range of data from a crack growth rate ( $da/dn$ ) of 10<sup>-4</sup> mm/cycle to 10<sup>-2</sup> mm/cycle.  $\Delta K_{inception}$  was estimated based on visual inspection of the pooled  $da/dn$  vs  $\Delta K$  curves.

**Results:** All materials showed excellent consistency in J-R fracture (Table 2) and fatigue (Table 3) properties between batches. For comparison, DePuy provided impact toughness (double notch IZOD) results for all materials (Table 2); the results are consistent with the trend noted for J-R fracture results. As examples of batch behavior, the J-R curve behavior and the FCP behavior of the three AOX batches are shown in Figures 1 and 2, respectively. Comparing the five materials in terms of J-R behavior (Figure 3) suggests that static fracture resistance is diminished with increasing molecular weight and crosslinking gamma radiation dose. In contrast, cyclic fracture resistance (Figure 4) supports that AOX has better FCP than the other highly crosslinked formulations.

**Discussion:** For materials selection and design purposes, it is important to know how much batch-to-batch variation in mechanical properties, including fracture, might occur between batches of material. In this study, we found little variation in J-R static fracture and FCP resistance between 3 batches for five UHMWPE materials, including conventional, highly crosslinked and antioxidant-containing formulations.

Limitations of this study include that the tests were conducted in ambient laboratory conditions; however, similar consistency in properties would be expected in vivo, though likely altered from the ambient state.

The superior fatigue crack propagation resistance of the AOX material compared with the other highly crosslinked formulations is likely due to the absence of the need to thermally process the material for post-irradiation stabilization. As-such, there is better preservation of the crystalline regions of the material, which confers improved fatigue crack growth resistance. The comparable static fracture resistance of the AOX to Marathon and AltrX suggests that crack initiation is more influenced by crosslinking than by crystallinity.

The findings of this study are part of a large database at DePuy Synthes cataloging batch-to-batch variations in

physical, chemical, and mechanical properties of various formulations of UHMWPE. Such a database is invaluable for reference conditions of these implant materials.

**Acknowledgements:** This study was conducted with financial support from DePuy Synthes.

#### References:

[1] Atwood et al., JMBBM, 2011.

**Table 1.** Description of Materials. Vacuum packaged.

Material	Resin	$\gamma$ -radiation Crosslinking Dose	Post-irradiation stabilization	Sterilization Method
GVF	GUR 1020	None	None	$\gamma$ -radiation
Marathon	GUR 1050	50 kGy	Melt: 155C Anneal: 120C	Gas plasma
XLK	GUR 1020	50 kGy	Melt: 155C Anneal: 120C	Gas plasma
AltrX	GUR 1020	75 kGy	Melt: 155C Anneal: 120C	Gas plasma
AOX*	GUR 1020	80 kGy at sterilization step	None	$\gamma$ -radiation

\*contains 0.075% (w/w) hindered phenol antioxidant

**Table 2.** J-R Curve coefficients (mean and SD),  $J_{init}$  (J @  $\Delta a = 0.5\text{mm}$ ), and double notch IZOD (mean and SD). N = 3 pooled curves for each material. N = 30 for double notch IZOD.

Material	$C_1$	$C_2$	$J_{init}$ , kJ/m <sup>2</sup>	Impact toughness kJ/m <sup>2</sup>
GVF	66.35 (3.24)	0.71 (0.04)	40.66	106.39 (1.98)
Marathon	46.90 (0.32)	0.65 (0.01)	29.92	70.55 (1.33)
XLK	53.72 (0.40)	0.61 (0.04)	35.23	83.00 (2.49)
AltrX	45.84 (0.52)	0.68 (0.02)	28.69	71.06 (1.65)
AOX	46.25 (2.15)	0.69 (0.00)	28.67	73.09 (2.98)

**Table 3.** FCP curve coefficients (mean and SD) and  $\Delta K_{inception}$ . N = 9 curves pooled for each material.

Material	C	m	$\Delta K_{inception}$ , MPa(m) <sup>0.5</sup>
GVF	$5.22 \times 10^{-8}$ ( $2.89 \times 10^{-8}$ )	11.26 (0.45)	1.63-1.72
Marathon	$9.32 \times 10^{-6}$ ( $2.27 \times 10^{-6}$ )	9.52 (0.13)	1.07-1.10
XLK	$2.29 \times 10^{-6}$ ( $0.67 \times 10^{-6}$ )	9.98 (0.50)	1.16-1.24
AltrX	$7.64 \times 10^{-6}$ ( $0.96 \times 10^{-6}$ )	9.14 (0.11)	1.10-1.12
AOX	$1.84 \times 10^{-7}$ ( $1.03 \times 10^{-7}$ )	10.65 (0.36)	1.51-1.57

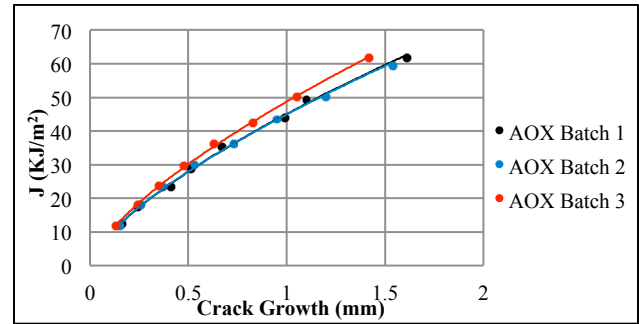


**Figure 1.** Example Batch J-R curves for AOX.

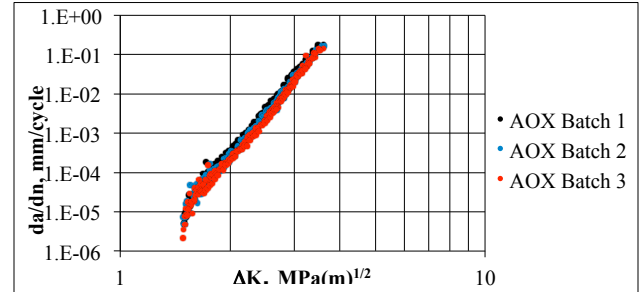


**Figure 2.** Example batch FCP behavior for AOX.

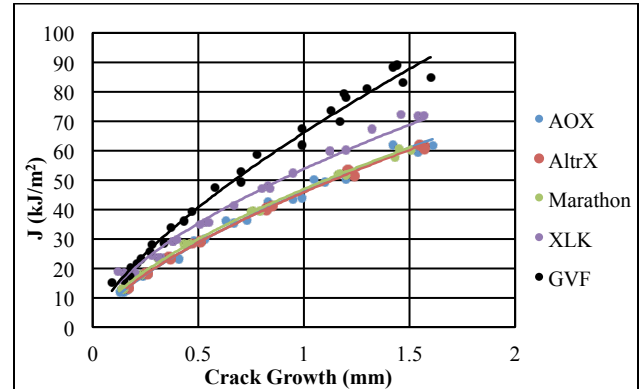


**Figure 3.** Comparison of the pooled batch J-R behavior for each of the 5 materials.

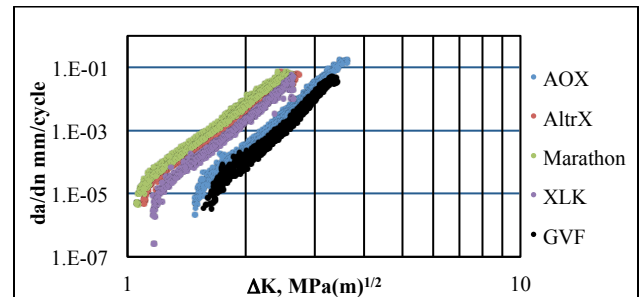


**Figure 4.** Comparison of the pooled batch FCP behavior for each of the 5 materials.

# Long-Term In Vivo Degradation of 1<sup>st</sup> Generation Highly Crosslinked Polyethylene in THA

<sup>1</sup>Schachtner, JT; <sup>1</sup>MacDonald, DW; <sup>3</sup>Klein, GR; <sup>4</sup>Chen, AF; <sup>5</sup>Kraay, M; <sup>6</sup>Malkani A; <sup>7</sup>Mont MA; <sup>5</sup>Rimnac, CM; <sup>1,2</sup>Kurtz, SM

<sup>1</sup>Drexel University, Philadelphia, PA; <sup>2</sup>Exponent, Philadelphia, PA; <sup>3</sup>Hartsham Center for Hip and Knee Replacement, Paramus, NJ; <sup>4</sup>Rothman Institute, Philadelphia, PA; <sup>5</sup>Case Western Reserve University, Cleveland, OH; <sup>6</sup>Jewish Hospital and St. Mary's Health Care, Louisville, KY <sup>7</sup>Sinai Hospital of Baltimore, Baltimore, MD  
jts338@drexel.edu

**Introduction:** Debris generated from ultra high molecular weight polyethylene (UHMWPE) wear in total hip arthroplasty can lead to osteolysis, component loosening, and ultimately revision surgery [1]. Highly crosslinked ultra high molecular weight polyethylene (HXLPE) was clinically introduced to reduce wear [1] however, the irradiation of UHMWPE to induce cross-linking also produces residual free radicals. Post-irradiation thermal processing, annealing or remelting, was introduced to stabilize HXLPE [1]. Annealing yields a HXLPE material with a low amount of residual free radicals while residual free radicals are undetectable in remelted HXLPE [2]. Recent studies have shown positive material performance for HXLPEs, but cohorts are small and/or do not evaluate implants with a long period of implantation [3-5]. The purpose of this study was to investigate the performance of HXLPE acetabular liners implanted for 5 or more years and determine if any differences exist between the of annealed and remelted HXLPE.

**Methods and Materials:** Between 2000 and 2017, 1,112 HXLPE hip components were collected as a part of an IRB approved, multi-institutional retrieval analysis program during routine revision surgery. Of the 1,112 components, 128 were 1<sup>st</sup> generation HXLPE, implanted for 5 or more years. Five liners were excluded from the study due to site restrictions, bone cement coating, and device design. The components were fabricated from two different materials: annealed HXLPE (n = 50; Crossfire, Stryker Orthopaedics, Mahwah, NJ), and remelted HXLPE (n = 73; Longevity, Zimmer Biomet, Warsaw, IN). Patient BMI, age, gender, and activity levels were similar (p>0.4; Table 1). The annealed cohort was implanted for a longer period of time, on average, when compared to the remelted cohort (Mean Difference = 1.4, p = 0.008, Table 1).

**Table 1:** Summary of patient demographics for the HXLPE cohorts. With the exception of gender, all values are reports as mean ± standard deviation.

Cohort	Number	Age (years)	Gender (%F)	BMI (kg/m <sup>2</sup> )	Implantation Time (years)	Max UCLA Score
Annealed	50	56 ± 16	54	30.5 ± 6.3	9.4 ± 3.0	6 ± 2
Remelted	73	56 ± 15	53	29.7 ± 6.3	8.0 ± 2.1	6 ± 2
p-value		p = 0.70	p = 0.94	p = 0.45	p = 0.01	p = 0.008

Wear was assessed through linear femoral head penetration using digital micrometers, where the thickness of the liners was measured in the loaded and unloaded

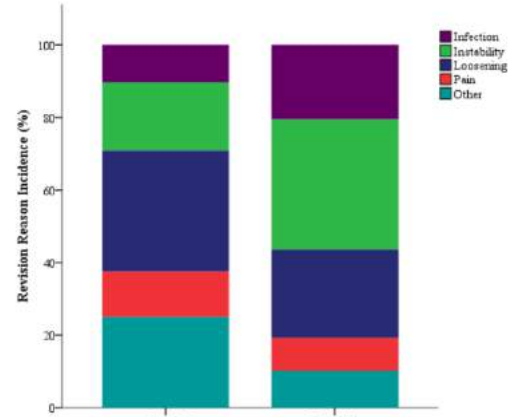


**Figure 1:** Reasons for revision for the acetabular liners by stabilization process.

regions. The measured head penetration was divided by the implantation time for the average penetration rate (mm/year).

To examine the oxidation properties, thin HXLPE slices (~200 µm) were taken from the superior/inferior axis of the revised liner. The HXLPE slices were boiled in heptane for six hours to extract lipids absorbed *in vivo*. Using transmission Fourier transform infrared spectroscopy (FTIR), 3-mm line profiles were taken perpendicular to regions of interest (ROI), according to ASTM F2102. ROI for the revised liners were the rim, locking mechanism, backside, and bearing surface.

**Results:** The principal revision reasons were infection, instability, pain, and loosening (Fig.1). There were 28 cases of osteolysis recorded, 12 of these were in the annealed cohort, while 16 were in the remelted cohort. The annealed components had higher oxidation indices than the remelted liners at the bearing surface (mean difference = 0.57, p < 0.001), backside (mean difference =

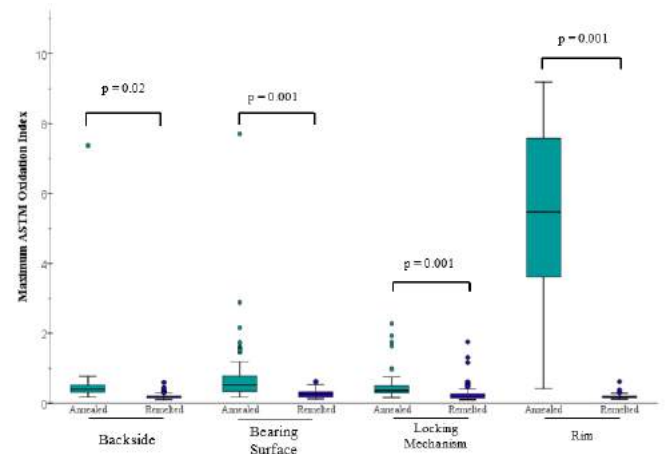


**Figure 2:** Oxidation indices for annealed and remelted cohorts.

0.37,  $p < 0.001$ ), locking mechanism (mean difference = 0.24,  $p < 0.001$ ), and rim (mean difference = 5.10,  $p < 0.001$ ).

Regional differences were observed within both cohorts (Fig. 2). In the remelted cohort, the bearing surface had the high oxidation indices then the backside, locking mechanism, and the rim (mean differences = 0.08, 0.00, and 0.08,  $p = <0.001$ , 0.003, and  $<0.001$ , respectively). The remelted liners retained consistent oxidation at the rim, backside, and locking mechanism ( $p > 0.11$ ). The greatest amount of oxidation occurred at the rim of annealed liners (median OI = 5.37,  $p < 0.001$ ). Oxidation was lowest at the backside (median OI = 0.29) and locking mechanism (median OI = 0.26), while slightly higher at the bearing surface (median OI = 0.43). Oxidation was not correlated with implantation time at any ROIs in either the remelted or annealed cohorts ( $p > 0.19$ ). There was no difference in linear penetration rate between the two cohorts ( $p = 0.11$ ).

**Discussion:** This study analyzed the oxidative stability and wear performance of long-term retrieved 1<sup>st</sup> generation HXLPE in THA. The results show that remelted long term HXLPE retains low oxidation indices (OI) with regards to all ROIs (median OI = 0.08). Annealed HXLPE did not retain such oxidative stability with the highest OI occurring at the rim (median OI = 5.37). This study shows that there is a significant difference in oxidative properties between the two stabilization processes. However, none of the Annealed components were revised for rim related failures and the linear penetration rates were similar between the two cohorts.

## References:

[1] Wannomae KK, et al. *JOA*, 2006; [2] Capello WN, et al. *CORR*, 2011; [3] Kurtz SM, et al. *JOA*, 2005; [4] Babovic N, et al. *JOA*, 2013; [5] Kurtz SM, et al. *CORR*, 2011;

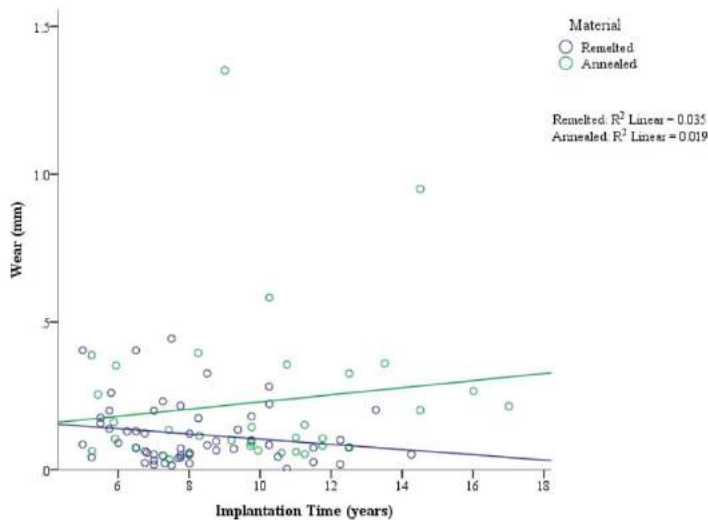


**Figure 3:** Wear of annealed and remelted cohorts over time.

## A Comparison of Short-Term Anti-Oxidant and Remelted HXLPE in THA

<sup>1</sup>Schachtner, JT; <sup>1</sup>MacDonald, DW; <sup>3</sup>Klein, GR; <sup>3</sup>Kraay M; <sup>2</sup>Rinnac, CM; <sup>1,2</sup>Kurtz SM

<sup>1</sup>Drexel University, Philadelphia, PA; <sup>2</sup>Exponent, Philadelphia, PA; <sup>3</sup>Hartsham Center for Hip and Knee Replacement, Paramus, NJ; <sup>4</sup>Case Western Reserve University, Cleveland, OH  
jts338@drexel.edu

**Introduction:** In the late 1990s, 1<sup>st</sup> generation highly crosslinked polyethylene (HXLPE) was introduced to increase wear resistance [1]. However, the mechanical, and oxidative properties of 1<sup>st</sup> generation HXLPE are still limited, as thermal processing is necessary for the reduction of free radicals caused by irradiation needed for polymer crosslinking. To address the deficiencies, manufacturers incorporated anti-oxidant vitamin E to the polymer for the preservation of mechanical properties and reduction of free radicals. There are two methods for incorporating Vitamin E with the polymer, (1) to diffuse it after the polymer has been consolidated (E1, Zimmer Biomet) or (2) to blend it with the polymer before consolidation (Vivacit-E, Zimmer Biomet) [1]. Second generation HXLPE has demonstrated improved oxidative and mechanical properties [2-4], however it has not been directly compared with 1<sup>st</sup> generation HXLPE. The purpose of this study was to compare the performance of wear properties and oxidative stability between retrieved 1<sup>st</sup> and 2<sup>nd</sup> generation HXLPE liners in THA.

**Methods and Materials:** Between 2010 and 2017, 49 anti-oxidant HXLPE acetabular liners were collected as part of an IRB approved, multi-institutional retrieval analysis program during routine revision surgery. Six liners were excluded as they were a dual mobility design. The acetabular liners were fabricated from two materials: anti-oxidant Diffused HXLPE (n = 25, E1, Biomet) and anti-oxidant blended (n = 18; Vivacit-E, Zimmer). To evaluate the efficacy of anti-oxidant HXLPE, the components were matched to 1<sup>st</sup> generation remelted HXLPE. The components were matched with these top criteria, listed in order of importance: implantation time (p = 0.91), patient BMI (p = 0.33), gender (p = 0.34), age (p = 0.69), and activity level (p = 0.22). The 1<sup>st</sup> generation HXLPE liners were fabricated from 1 material: remelted HXLPE (n = 43; Longevity, Zimmer). The anti-oxidant and 1<sup>st</sup> generation HXLPE components were both implanted for  $0.8 \pm 1.0$  years (Range: 0.0 – 4.75y).

To examine the oxidation properties, thin HXLPE slices (~200  $\mu$ m) were taken from the superior/inferior axis of the revised liner. The HXLPE slices were boiled in heptane for six hours to extract lipids absorbed *in vivo*. Using transmission Fourier transform infrared spectroscopy (FTIR), 3-mm line profiles were taken perpendicular to regions of interest (ROI), according to ASTM F2102. ROI for the revised liners were the rim, locking mechanism, backside, and bearing surface. Wear was assessed through linear femoral head penetration using point tipped digital micrometers, where the thickness of the liners was measured in the loaded and

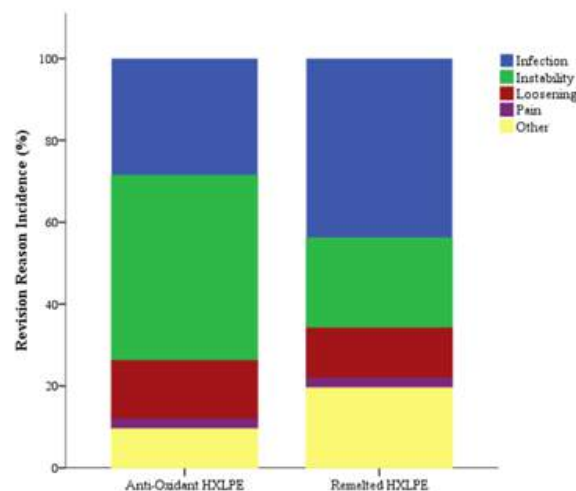


**Figure 1:** Reasons for revision for the anti-oxidant and remelted liners.

unloaded regions. The measured head penetration was divided by the implantation time for the average penetration rate (mm/year). All specimens implanted for under a year were excluded as creep is dominant during this period.

**Results:** The principal revision reasons were infection, instability, and loosening (Fig. 1). Oxidation was found to be highest at the rim of the anti-oxidant liners (mean = 0.18). Within the remelted HXLPE liners the oxidation was highest at the locking mechanism (mean = 0.19). Oxidation was not found to be significantly different between the two cohorts at any location (Fig. 2). The anti-oxidant liners had a mean linear penetration rate of 0.019 mm<sup>3</sup>/year whereas the mean rate was 0.024 mm<sup>3</sup>/year in the remelted cohort. There was no significant difference in linear penetration rates between the two cohorts (p = 0.31).

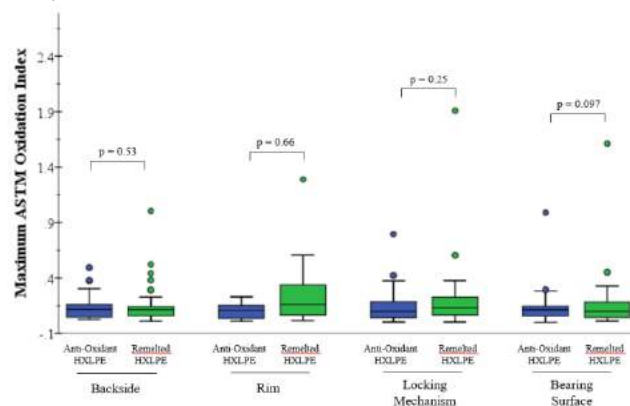


**Figure 2:** Oxidation indices for the anti-oxidant and remelted cohorts.

**Discussion:** This study reviewed the reasons of revision, oxidative stability, and linear penetration of short-term 1<sup>st</sup> and 2<sup>nd</sup> generation HXLPE. The results of this study show that 2<sup>nd</sup> generation HXLPE had lower mean levels of oxidation, and linear penetration rates but no significant difference was able to be detected between the two materials, likely due to the sample size. Because this study was limited by short implantation times, the results can only communicate to the lack of failure within the first years of implantation. Although these results support the continued use of this material, further research is required to describe the long term clinical performance.

**References:** [1] Yamamoto K. et al., *JOS*, 2017; [2] Nebergall AK. Et al., *BJJ*, 2017; [3] Salemyr M. et al., *IO*, 2015; [4] Costa L et al., *PDS*, 2009

# Delamination resistance of vitamin E blended and highly cross-linked ultra-high molecular weight polyethylene evaluated by novel accelerated test method

Sakoda, H<sup>1</sup>, Osaka, Y<sup>2</sup>, Uetsuki, K<sup>2</sup>, Okamoto, Y<sup>1</sup> and Haishima Y<sup>1</sup>

<sup>1</sup>National Institute of Health Sciences, Tokyo, Japan

<sup>2</sup>Teijin Nakashima Medical Co., Ltd., Okayama, Japan

sakoda@nihs.go.jp

**Introduction:** One of common destruction modes found in ultra-high molecular weight polyethylene (UHMWPE) is delamination, which can be found at the articulating surface of artificial knee joints, shoulder joints and at the rim of the acetabular components. Although there are many reports that reproduced delamination *in vitro* using a knee joint simulator it is difficult to make comparison between the results of these studies since parameters such as component design, applied joint motion and applied joint load are different. Moreover, the component design affects joint motion and loading. Therefore, *in-vitro* tests to compare the different UHMWPE is also important because they allow direct comparisons of materials without the added complexities and variability associated with the individual design of the components and kinetic and kinematic environment *in vivo*. However, conventional *in-vitro* ball-on-flat wear tests using simple reciprocation cannot evaluate delamination resistance of contemporary materials because it can reproduce delamination only on oxidized materials. In the present study, we employed unique U-shape motion that has been shown to accelerate the reproduction of delamination, to make direct comparison of delamination resistance of contemporary UHMWPEs.

**Methods and Materials:** Materials used in this study are summarized in Table 1. Highly crosslinked UHMWPE (HXLPE) were prepared by gamma irradiation at 100 kGy in inert followed by either remelting at 160 °C for 2 h (G100-R2) or annealing at 110 °C for 2–168 h (G100-Ax) in vacuum. VEPE was prepared by direct compression molding of UHMWPE powder blended with 0.3% vitamin E. VE-Ex was prepared by e-beam irradiation of VEPE at 120, 150 and 300 kGy in an inert atmosphere, followed by annealing at 110 °C for 72 h in vacuum. Accelerated aging (AA) was carried out at 80 °C for 21 days in air. Compulsory aging (CA), employed for VEPE and VE-Ex as a test under severe conditions, was carried out by gamma irradiation at 25 kGy in air, followed by AA at 80 °C for 21 days in air.

Table 1 Materials used in this study.

Name	Description
Virgin	UHMWPE as received
G25	Conventional, irradiated in inert
G25air	Historical, irradiated in air
G100-R2	HXLPE remelted at 160 °C for 2 h
G100-Ax	HXLPE annealed at 110 °C x: annealing time in hours
VEPE	0.3% vitamin E blended UHMWPE
VE-Ex	Vitamin E blended HXLPE x: e-beam irradiation dose in kGy

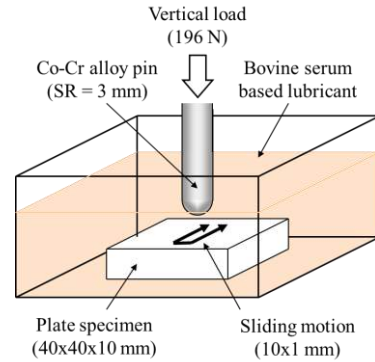


Fig. 1. Schematic diagram of the delamination test setup used in this study.

Thin specimens with a thickness of 100–200 µm were analyzed using Fourier transform infrared (FTIR) microscopy to obtain the oxidation index (OI) [1] and crystallinity index (CI). CI was calculated according to:

$$CI = (A_{1896}/A_{1305}) / (A_{1896}/A_{1305} + 0.25) \times 100$$

where  $A_{1896}$  and  $A_{1305}$  are the peak area for the crystalline band at 1896 cm<sup>-1</sup> and that for the amorphous band at 1305 cm<sup>-1</sup>, respectively [2].

Delamination tests were conducted using plate specimens with dimensions of 40×40×10 mm [3] (Fig. 1). A U-shaped sliding motion of 10×1 mm with a sliding velocity of 30 mm/s was applied to the specimen using a two-dimensional pin-on-plate wear test machine. A load of 196 N was applied through a metal pin with a hemispherical end having a radius of 3 mm. Bovine serum based lubricants was used and changed every week. The tests were periodically stopped to visually inspect the occurrence of delamination. The tests lasted until either delamination was observed or 1 million cycles were reached. The delamination score was defined as shown in Table 2. Three specimens of each material were tested.

Fatigue crack growth tests were conducted according to ASTM E647 with some modifications using compact tension specimens. Three specimens for each material were tested at 1 Hz. From the relation between the stress intensity factor range  $\Delta K$ , and the fatigue crack growth rate  $da/dN$ , the stress intensity factor range threshold  $\Delta K_{th}$  was calculated.

A Student's t-test for two-tailed distributions with unequal variance was used for statistical analysis. The difference was considered to be statistically significant at  $P < 0.05$ .

**Results:** The virgin UHMWPE, G25 and G100-A2 showed statistically significant increases in both maximum OI and CI due to AA, indicating potential of oxidative degradation of these materials. G100-R2 did not

show a statistically significant increase in maximum OI due to AA, which indicates good oxidation stability. Maximum OI of VEPE and VE-Ex increased slightly after CA, but CI of those were not affected by CA, indicating oxidation stability of these materials.

The virgin UHMWPE showed the delamination score of 2.7 and other materials that were not subjected to AA or CA exhibited better delamination resistance than the virgin UHMWPE as shown in Fig. 2. All three specimens of G100-A2, VE, VE-E300 and VE-E300-CA completed 1 million cycles without delamination, which gave an average delamination resistance score of 5. G25 and G100-A2 showed a significant decrease in the delamination resistance score after AA, while G100-R2, VE and VE-E300 showed excellent delamination resistance score irrespective of AA or CA.

$\Delta K_{th}$  for the virgin UHMWPE and VE were the highest, followed by those for G100-A168 and VE-E150, while those for G100-R2 and VE-E300 were the lowest as shown in Fig. 3. CA had no substantial effect on  $\Delta K_{th}$  for VEPE and VE-Ex.

Table 2 The definition of the delamination score.

Score	Description
5	No delamination until 1 million cycles
4	Delamination between 300,000 to 1 million cycles
3	Delamination between 100,000 to 300,000 cycles
2	Delamination between 10,000 to 100,000 cycles
1	Delamination between 1,000 to 10,000 cycles
0	Delamination before 1,000 cycles

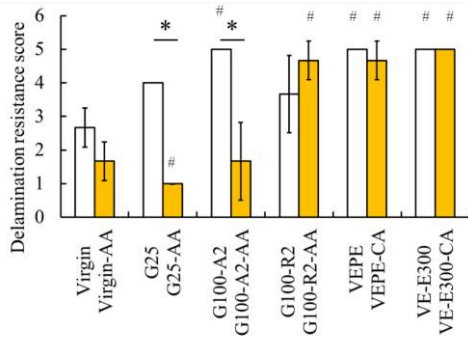


Fig. 2. Delamination resistance score obtained from delamination tests. \*: Significant difference between non-aged and aged specimens. #: Significant difference against the virgin UHMWPE.

**Discussion:** Conventional UHMWPE (G25) showed low delamination score after AA, which was consistent to the retrieval and joint simulator studies. Since delamination has not been observed on EOG sterilized UHMWPE [4, 5], it was considered that materials with delamination score of similar to or better than the virgin UHMWPE have little risk of delamination. G100A2-AA, representing aged annealed HXLPE had a delamination score lower than that of the virgin UHMWPE. Annealed

HXLPE has little experience in the knee prostheses. Instead, delamination of annealed HXLPE at the rim of hip acetabular liner has been reported [6], although the manufacturing process is not identical.

The results of the fatigue crack growth tests were inconsistent to those of the delamination tests. Delamination resistance of G100-R2 and VE-E300 were far better than that of the virgin UHMWPE although fatigue crack growth property of them were inferior to the virgin UHMWPE. This discrepancy could be explained by the complex mechanism of delamination, which consists of defects formation at consolidation, nucleation of new defects and growth of the defects under loading. Fatigue crack growth tests only evaluate the final step of the mechanism of delamination, ignoring the difference in the stress condition. Therefore, delamination resistance and fatigue crack growth property are independent properties and evaluation of both properties is required.

To the best of our knowledge, this is the first report that delamination was reproduced in materials which had not artificially been aged and this is the first report that made direct comparison of delamination resistance between contemporary materials. Fortunately, materials simulating contemporary UHMWPEs including HXLPEs, vitamin E blended UHMWPE and vitamin E blended HXLPE were found to have better delamination resistance than the virgin UHMWPE, indicating little risk of delamination *in vivo*. However, this does not mean that materials under development are also free from the risk of delamination. For instance, delamination in poly-ether-ether-ketone (PEEK) and carbon-fiber reinforced PEEK (CFR-PEEK) has been reported by the study using a knee joint simulator [7]. Thus, delamination resistance should be evaluated when new material is under development.

**References:** [1] ASTM F2102-01 [2] Costa 2001 Polym Test [3] Sakoda 2012 Japanese Journal of Clinical Biomechanics [4] Greulich 2012 J Arthroplasty [5] MacDonald 2012 Clin Orthop Relat Res [6] Currier 2007 J Bone Joint Surg Am [7] Brockett 2017 Wear

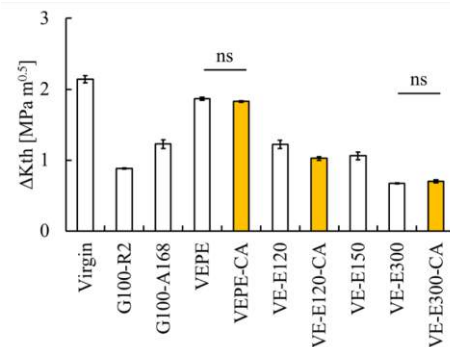


Fig. 3. Stress intensity factor range threshold ( $\Delta K_{th}$ ) obtained from fatigue crack growth tests. ns: No significant difference between non-aged and aged specimens.

**Title:****Influence of radiation conditions and aging duration on the wear behaviour of an vitamin E stabilized TKA bearing****Authors & affiliations:**

*J. Schwiesau<sup>1,3</sup>, B. Fritz<sup>1</sup>, I. Kutzner<sup>2</sup>, G. Bergmann<sup>2</sup>, T.M. Grupp<sup>1,3</sup>*

*<sup>1</sup>Aesculap AG, R&D, Tuttlingen, Germany.*

*<sup>2</sup>Charité-Universitätsmedizin, Julius Wolff Institut, Berlin, Germany.*

*<sup>3</sup>Ludwig-Maximilians-University- Campus Großhadern, Orthopedic Department, Munich, Germany.*

**Introduction:** The wear behaviour of total knee arthroplasty (TKA) bearings is dominated by abrasive wear and delamination. Bearing material properties and applied stresses affect the wear mode. With increasing stress caused by high demanding daily activities of the lower limbs and degraded material properties due to aging, delamination occurs more frequently. The bearing material properties can be stabilized by blending the Ultra High Molecular Weight Polyethylene (UHMWPE) with an aging inhibitor. Vitamin E is one substance that can reduce oxidation, the dominant aging process. In this study high demanding daily activities are simulated to evaluate the influence of radiation condition and duration of artificial aging on the wear behaviour of an TKA bearing material with vitamin E blending.

**Methods:** High flexion activities [Bergmann et al. 2014] predominate in the simulation (40% stairs ascending, 40% stairs descent, 10% level walking, 8% chair raising, 2% squatting). Five million test cycles are simulated with standard environmental conditions [ISO14243-1]. The tested TKA design was cruciate retaining with CoCr femoral components. Artificially aged [ASTM F2003-2] UHMWPE knee bearings with and without 0.1% vitamin E were tested. The gravimetric wear was evaluated according to ISO 14243-2. The wear mode was analysed optically.

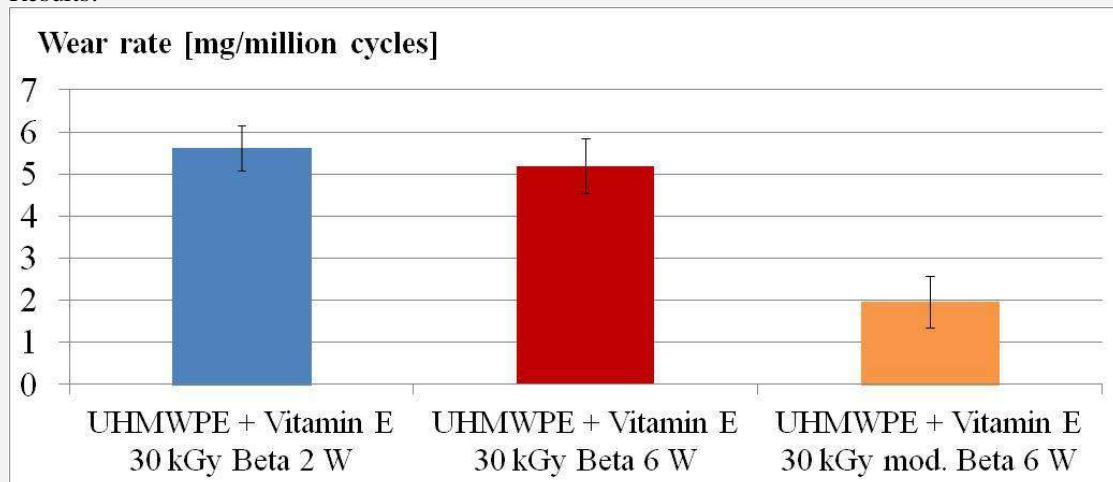
**Results:**

Fig.1: Average (n=3) weight reduction for the specimen.

Abrasion is the predominating wear mode. No case of delamination was observed.

**Discussion:** Based on the simulation of daily patient activities it was possible to differentiate the wear behaviour between the radiation conditions of the bearing materials. The influence on the wear rate was not significant for the duration of artificial aging.

## Biomimetic UHMWPE structures for restoration of osteochondral defects

Senatov F.S.<sup>1</sup>, Maksimkin A.V.<sup>1</sup>, Salimon A.I.<sup>1</sup>, Kaloshkin S.D.<sup>1</sup>, Anisimova N.Yu.<sup>1,2</sup>, Kiselevsky M.V.<sup>1,2</sup>, Zalepugin D.Yu.<sup>3</sup>

<sup>1</sup>National University of Science and Technology "MISIS", Moscow, Russian Federation

<sup>2</sup>N.N. Blokhin Russian Cancer Research Center, Moscow, Russian Federation

<sup>3</sup>State Plant of Medicinal Drugs, Moscow, Russian Federation

*Senatov@misis.ru*

**Introduction:** Biomaterials engineering is in need of tailored architected materials that ensure consistency between the structural anisotropy of the material and maximum functionality at all dimensional levels. A number of natural and engineering products based on such materials demonstrate the best combination of properties. Ultra-high molecular weight polyethylene (UHMWPE) is a widely used material for implantology because of its biocompatibility and high mechanical properties. On the other hand, extremely high molecular weight of the polymer does not allow using traditional methods of treatment. Experimental realization of complex architected structures can be achieved by the methods of material structuring: treatment in supercritical fluids, mechanochemical synthesis, gel-forming, etc. Combination of different methods allows creating materials with locally customized structure to simulate the complex architecture of biological tissues occurring in living organisms that were optimized as a result of natural evolution.

Reconstruction of the structural integrity of the damaged cartilage and bone tissue may appear as an urgent problem. Cartilage and bone tissue has a natural ability to regenerate, but in cases of large defects this ability is limited. The development of biomimetic scaffolds with the architecture of bone or cartilage tissue which are capable to function under the mechanical load is a promising direction for solving this problem.

The purpose of this work was the development of individualized biomimetic UHMWPE implants for restoration of osteochondral defects.

**Methods and Materials:** Two types of biomimetic UHMWPE structures were obtained: (1) multilayer UHMWPE scaffolds with nonporous bulk layer and porous layer which mimic cortical and cancellous bone architecture, and (2) oriented bulk UHMWPE which mimics surface layers of the cartilage of the joints.

Porous part of multilayer UHMWPE was obtained by mixing with NaCl powder and further thermopressing. The soluble filler was removed after thermopressing with subcritical water at a temperature of 120 °C and a pressure of 250 bar. Prepared multilayer UHMWPE scaffolds were designed as a simulation of tubular and plane bones as described in [1].

The obtained multilayer UHMWPE samples were studied with scanning electron microscopy (SEM) and tested for compressive strength and impact. Volume porosity and pore size distribution were studied. Porous UHMWPE samples were colonized with multipotent mesenchymal stromal cells from bone marrow and implanted into

osteochondral defects of experimental animals (mice, rats and dogs).

Oriented bulk UHMWPE were prepared to mimic surface layers of the cartilage of the joints. The multilayered wall carbon nanotubes (MWCNTs) by "Nanotechcenter Ltd" (Russia) were used as the filler. MWCNT fluorination was carried out. Introduction of FMWCNTs into UHMWPE matrix was performed using a planetary ball mill APF-3. FMWCNT concentration in UHMWPE was varied as 0.1, 0.5 and 1% wt. The synthesis of bulk oriented nanocomposites proceeded in accordance with the multi-stage process: hot pressing, stretching and hot pressing. A detailed description of this method is given in [2]. Comparative analysis of the tribological characteristics of canine joint cartilage and UHMWPE-based biomimetic materials was performed [3].

**Results:** The architecturing of the UHMWPE / FMWCNT material at the nano- and micro-level by means of orientation stretching resulted in the formation of an oriented nanofibrillar structure (Fig.1) simulating the surface layer of the cartilage of the joint, which resulted in significant reduction in the friction coefficient from 0.2 to 0.05 and increase of the tensile strength from 22 MPa to 130 MPa.

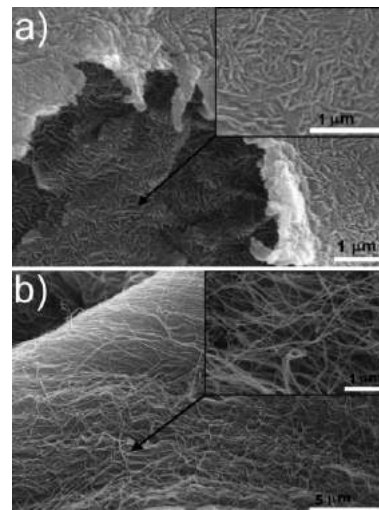


Figure 1 - (A) Lamellar structure of isotropic UHMWPE nanocomposites; (B) nanofibrillar structure of bulk oriented UHMWPE/MWCNT nanocomposites [4]

The combination of thermo-pressing and processing in a supercritical fluid led to the formation of a microporous structure in UHMWPE: a pore size of 50-800 μm, a porosity of 90 vol. %. The combination of a bulk and

porous layer of UHMWPE simulates the micro- and macrostructure of the trabecular and cortical bone (Fig.2).

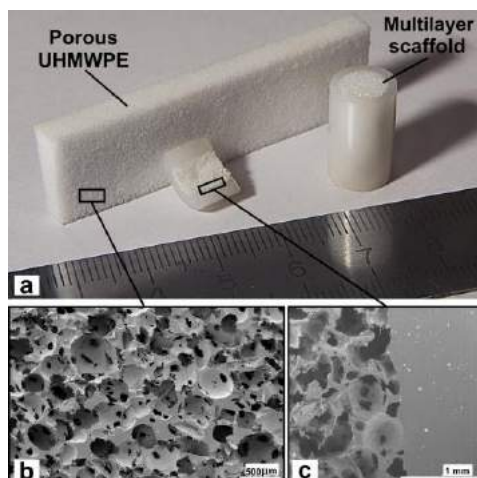


Figure 2 – (a) Porous UHMWPE and multilayer UHMWPE scaffold, (b) SEM of porous UHMWPE and (c) SEM of multilayer UHMWPE scaffold [1]

Histology of implanted porous UHMWPE samples and the surrounding tissues was studied. Important indicators are the state of the bone tissue that contacts with the implant and the motor activity of animals. Histological study of the implants demonstrated that the synthetic samples induced the formation of the thin layer of a fibrovascular tissue after subcutaneous implantation. Blood vessels were detected within porous part of the implanted multilayer scaffolds with complete filling of all pores by connective tissue, but with no signs of cellular infiltration by neutrophils (Fig.3A). There was documented a formation of the tissue layer on the scaffold's external surface (Fig.3B).

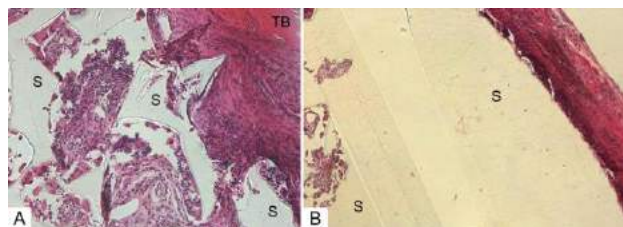


Figure 3 – Histological analysis of multilayer UHMWPE scaffolds (S) with surrounding tissue after 30-day of the implantation into rat tibia bone (TB). A – porous part of scaffold; B – tissue converted external surface layer of the nonporous bulk part of scaffold. Stained with HE, magnification  $\times 100$  [1]

**Discussion:** The architecturing of UHMWPE at the macro / micro / nanoscale by the methods of orientation stretching, thermopressing and processing in supercritical fluids makes it possible to form implants with structure that mimics the structure of native bone and cartilage.

The efficiency of porous scaffolds is largely determined by their architecture, which includes the type of porous structure, three-dimensional pore content and size distribution. Architecture of porous scaffold creates favorable conditions for the formation of new tissue.

The main idea of the suggested multilayer UHMWPE scaffold is determined by specific features of its design making it similar to tubular bones. There are two firmly adhered layers. The surface one is continuous and solid. This layer, just like a cortical layer of natural bones, makes the construction firm and provides support ability of extremity. The internal layer possesses the pores of the determined size and may be colonized by recipient's cells and thus accelerating intergrowth of this tissues into the construction and resulting fixing of the implant in the defect zone. These specific features of the construction determine the novelty of the suggested scaffold. The data obtained prove that the suggested multilayer scaffold is promising for creation of medical products: inner prostheses and bioimplants.

Mimicking of bone structures allows manufacturing a multilayered bioengineering scaffolds for regenerative surgery of flat and tubular bones. The orientation of the UHMWPE macromolecules allows imitating surface layers of the cartilage of the joints and producing acetabular cups for hip-joint implants based on nanocomposites with programmable characteristics. UHMWPE-based biomimetic materials are able to replace traditional materials due to the best combination of functional characteristics. Such biomimetic structures will be suitable for use in regenerative medicine and tissue engineering.

- [1] A.V. Maksimkin, F.S. Senatov, N.Yu. Anisimova, M.V. Kiselevskiy, D.Yu. Zalepugin, I.V. Chernyshova, N.A. Tilkunova, S.D. Kaloshkin. Multilayer porous UHMWPE scaffolds for bone defects replacement / Materials Science and Engineering: C 73 (2017) 366–372
- [2] A.P. Kharitonov, A.V. Maksimkin, K.S. Mostovaya, et al. Reinforcement of bulk ultrahigh molecular weight polyethylene by fluorinated carbon nanotubes insertion followed by hot pressing and orientation stretching / Compos Sci Tech, 120 (2015), pp. 26–31
- [3] A.V. Maksimkin, D.I. Chukov, F.S. Senatov, A.I. Salimon. Comparative analysis of the tribological characteristics of canine joint cartilage and UHMWPE-based biomimetic materials / Materials Letters Volume 191, 15 March 2017, Pages 105-107
- [4] A.V. Maksimkin, F.S. Senatov, V.D. Danilov, K.S. Mostovaya, S.D. Kaloshkin, M.V. Gorshenkov, A.P. Kharitonov, and D.I. Chukov. Transformation of the lamellar structure into nanofibrillar structure in the bulk oriented ultra high molecular weight polyethylene: mechanical and tribological properties / Mendelev Comm., 2016, 26, 350–352

# New Stabilization System for UHMWPE Based on Vitamin E and Tetracycline Antibiotic: Synergistic Increase in Oxidation Resistance

Slouf, M<sup>1</sup>, Krulis, Z<sup>1</sup>, Nevoralova, M<sup>1</sup>, Michalkova D<sup>1</sup>, Gohs, U<sup>2</sup>, Fulin, P<sup>3</sup>, Pokorny, D<sup>3</sup>

<sup>1</sup>Institute of Macromolecular Chemistry AS CR, Heyrovsky Sq. 2, 162 06 Prague 6, Czech Republic

<sup>2</sup>Institute of Polymer Research Dresden, Hohe Strasse 6, 01 069 Dresden, Germany

<sup>3</sup>1st Orthopedics Clinic of the 1st Faculty of Medicine UK, Hospital Motol, V Uvalu 84, 156 06 Prague 5, Czech Republic  
slouf@imc.cas.cz

**Introduction:** UHMWPE wear and oxidative degradation are the most important reasons of total joint replacement failures from the point of view of materials science [1]. The wear resistance is usually increased by radiation-induced crosslinking combined with thermal treatment. The oxidation resistance can be increased by addition of biocompatible stabilizers, such as vitamin E (or, more precisely, the most efficient antioxidant component of vitamin E, which is  $\alpha$ -tocopherol) [1]. In this contribution, we introduce a novel stabilization system for UHMWPE, which combines vitamin E and tetracycline antibiotic [2].

**Methods and Materials:** Samples were prepared from UHMWPE powder ( $M_w = 3 \times 10^6$  g/mol; bought from Sigma-Aldrich), which was dry mixed (i.e. dry blended) with 0.15 wt. % of stabilizer(s) and compression molded (hot press at 190 °C). For each sample, the first part was unmodified (NN samples), while the other two parts were irradiated with accelerated electrons (100 kGy) and annealed (AN samples; hot press at 110°C/10min) or remelted (RM samples; hot press at 150°C/10min). Control samples were commercial Chirulen 1020 and Chirulen 1020E; all samples discussed in this contribution are summarized in Table 1; total number of the samples was ~30. All samples were prepared in laboratory scale and characterized by microscale methods: IR, DSC, TGA, SEM and microindentation hardness testing.

Sample ID	Description
Chirulen 1020	Control #1: medical grade UHMWPE
Chirulen 1020E	Control #2: like previous, with 0.1% vit.E
PE	Control #3: compression molded PE powder
PE+E	PE + 0.15% of vitamin E
PE+E+T (2:1)	PE + 0.15% of vit.E and tetracyclin (2:1)
PE+E+T (1:1)	PE + 0.15% of vit.E and tetracyclin (1:1)
PE+E+T (1:2)	PE + 0.15% of vit.E and tetracyclin (1:2)

Table 1. List of the prepared UHMWPE samples.

**Results:** IR measurements yielded oxidation index (OI), trans-vinylene index (VI) and crystallinity index (CI); which were within usual limits for crosslinked and thermally treated UHMWPE's [3]. Good correlation between IR/CI, DSC crystallinity and microhardness (Fig. 1) confirmed the correctness of our results. The most important result was the synergistic increase in oxidation resistance for crosslinked and thermally treated UHMWPE samples stabilized by combination of vitamin E and tetracycline (Fig. 2): their oxidation induction temperature (OIT) increased with the content of tetracycline up to vitamin E/tetracycline ratio (1:2).

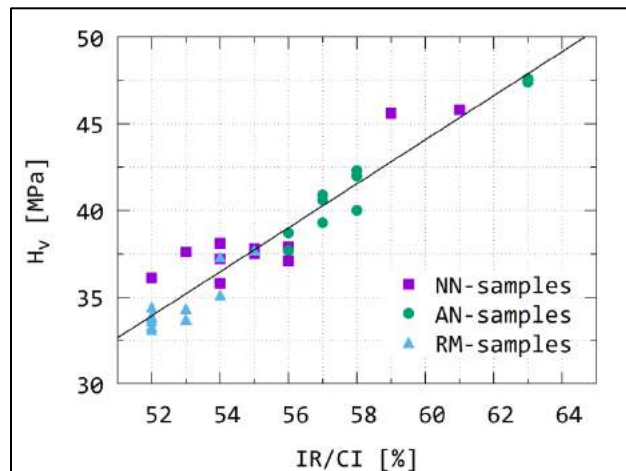


Fig. 1. Correlation between Vickers microhardness ( $H_v$ ) and crystallinity index determined from IR spectra (CI).

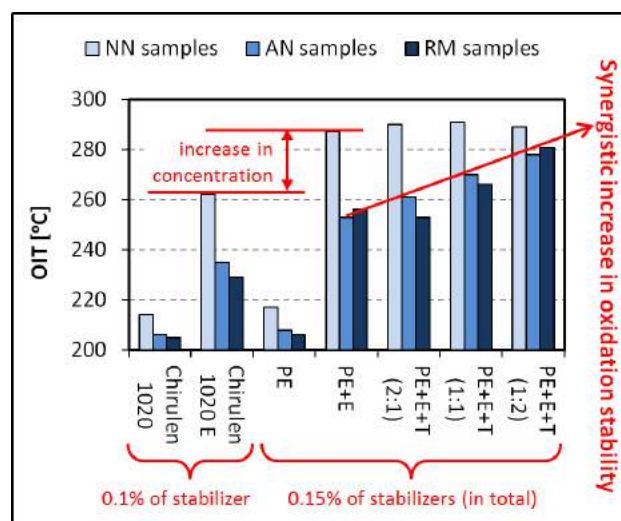


Fig. 2. Synergistic increase in oxidation induction temperature (OIT) for samples with different stabilizers.

**Discussion:** We have demonstrated that the stabilization system based on the combination of vitamin E and tetracycline increased the UHMWPE oxidation resistance more than vitamin E alone. The advantage of our solution consists in that both vitamin E and tetracycline antibiotics are approved for usage in human medicine.

## References

- [1] Kurtz SM: UHMWPE biomaterials handbook (2016).
- [2] Czech patent application CZ 2015-267 A3.
- [3] Slouf M et al.: Polymer Testing 41 (2015) 191–197.

**Acknowledgement:** NV15-31269A, TE01020118.

# UHMWPE Compounding with High Shear Polymer Modification, and Challenging Examples

Patel BS<sup>1</sup>, Shanahan SE<sup>1</sup>, Janse M<sup>1</sup>, Tapsak MA<sup>1,2</sup>

<sup>1</sup>Zzyzx Polymers LLC, Allentown, PA; <sup>2</sup>Bloomsburg University of Pennsylvania, Bloomsburg, PA  
*mtapsak@bloomu.edu*

**Introduction:** The high impact strength and abrasion resistance of UHMWPE has made it a preferred candidate for replacing metals and ceramics for a range of medical and industrial applications. While UHMWPE offers extreme physical properties, the market for UHMWPE is ultimately limited by its strength, stiffness, abrasion and thermal resistance. While polymeric materials are often reinforced with filler materials to meet the demands of high value applications, efforts to incorporate various fillers into UHMWPE have been hampered by the inherent processing and blending limitations of UHMWPE [1]. Further, because neat UHMWPE has intrinsically high strength and toughness, filler materials often improve one characteristic at the expense of another key property, such as reducing impact strength. High-shear polymer modification (HSPM) offers a means of incorporating filler materials into UHMWPE, while offsetting the negative effects fillers have on key physical properties.

The use of conventional fillers such as glass or carbon fibers, as well as natural fibers such as cellulose, has received much academic and commercial attention [1,2]. Indeed, it is well-known that the macroscopic properties of composite materials reinforced with micro-sized fillers depend upon many factors including; its composition, the characteristics of each component, the geometry of the filler, the filler dispersion, filler/filler and filler/matrix interactions and, in some cases, blending-induced changes to the matrix itself [3]. Of these factors, the potential property improvement of any UHMWPE-based composite depends heavily on effective dispersion and the degree of filler/matrix interaction. Both of these factors pose as major challenges for achieving practical UHMWPE blends.

The aim of this work is to demonstrate the use of HSPM processing for preparing effective UHMWPE/filler blends. Zzyzx Polymers LLC developed the HSPM process to modify the molecular weight distribution (MWD) of UHMWPE and other polymers. For example, it is known that for polyethylene, the shortest polymer chains reduce mechanical properties and that the longest chains reduce processibility. This is because the shorter polymer chains are not long enough to contribute to the connectivity within the material but merely act as a diluent [4]. The high relative number of end groups in these shorter chains also leads to crystalline defects [5]. In contrast, the longest polymer chains possess very low chain mobility such that coalescence across the UHMWPE particle interfaces is severely hindered [6]. To address these known limitations, the HSPM process preferentially cleaves the longest polymer chains near their midpoint. This selective chain scission results in two new chains that contribute to a more median chain length.

The HSPM process is also well suited for effectively dispersing fillers with UHMWPE through pulverization and selective mechanochemical actions. These operations allow for improved filler dispersion and promote more intimate filler/matrix interactions as compared to traditional melt processing technologies. Further, HSPM can be used to simultaneously optimize MWD for improved physical properties, offsetting negative effects of filler materials. In this research, some unusual materials were chosen for blending because extreme cases highlight the ability to disperse and compatibilize materials. For example, if unusual materials like as-received coffee and chicken feathers can be successfully compatibilized with UHMWPE, the authors believe it will better convey the idea that more typical fillers or additives, such as colorants, antioxidants or common fillers, can also be successfully blended with UHMWPE.

**Methods and Materials:** The UHMWPE base material used for this blending study was Lupolen UHM 5000 (Lyondell Basell). A range of filler materials were acquired to test the feasibility limits of HSPM-processed UHMWPE blends. Roasted coffee beans and feather pillows were purchased from WalMart (Bentonville, AR), PTFE was purchased from Inflon, graphite from Asbury Carbon, and titanium dioxide from Kronos. All powders, beans and feathers were used as received. No additional size reduction was performed prior to HSPM processing of any sample.

Test specimens were machined from compression molded sheets made in an electrically heated hydraulic press. Molding conditions were as follows; the temperature was raised to 420 °F and then a pressure of 725 psi was maintained at temperature for 25 minutes, then the pressure was increased to 915 psi and the mold was allowed to slowly cool to 160 F after which it was ejected from the mold. Mechanical properties were measured following standard ASTM or ISO procedures suitable for UHMWPE specimens.

**Results:** All UHMWPE blends prepared for this study were processed using a ZSK70 twin-screw extruder that has been modified for control of specific energy and thermal profiles to perform HSPM at a throughput rate of 200 lbs. per hour. This is a continuous, solvent-free technique that enables the controlled delivery of mechanical energy to the resin/filler mixture. The composition of each sample is outlined in **Table 1** below.

**Table 1.** Blend compositions prepared in this study. The base resin in all samples was Lupolen UHM 5000

Sample	Additive	Loading
1	Roasted coffee beans	2%
2	Feathers	2%
3	PTFE, Inoflon 210	5%
4	PTFE, Inoflon 210	10%
5	Graphite, Asbury Carbon 4827	0.5%
6	TiO <sub>2</sub> , KRONOS 2310	0.5%

**Discussion:** In this study, we demonstrate the use of HSPM for both the modification of the base UHMWPE while at the same time incorporating various fillers. Notably, samples 1 and 2 are novelty items, meant to demonstrate that effective pulverization and dispersion of the filler particles that can be accomplished in this continuous, single step process. These bio-based fillers are already known to be challenging to blend in conventional melt processing due to their sensitivity to thermal degradation. Furthermore, because the UHMWPE base resin is not required to melt during HSPM processing, its inherent melt-stability becomes an efficient processing aid. The solid UHMWPE particles better transfer mechanical energy into the filler to both reduce the particle size of the filler and effectively disperse it into the polymer resin.

Samples 3 through 6 incorporate more conventional polymer fillers. There even dispersion throughout the

UHMWPE base resin results in improved surface properties and uniform coloration. Mechanical data and microscopic images for all samples will be shared during the conference presentation.

Although some of the current samples discussed are novelty items they demonstrate the potential variety of UHMWPE blends that can be achieved with HSPM processing. Furthermore, HSPM processing can increase the utility of UHMWPE by expanding its use into higher value-added applications. For instance, antioxidants such as Vitamin E can be blended with UHMWPE with HSPM processing while simultaneously optimizing the MWD of the UHMWPE for a targeted application. Alternatively, additives that tend to agglomerate, such as carbon nanotubes and graphene, can be added without surface modification to realize mechanical properties for UHMWPE not achievable previously. Furthermore, additives which have traditionally hindered sintering may now yield novel UHMWPE-based concentrates suitable for other post-processing technologies. HSPM enables UHMWPE to finally achieve the customizability that has become commonplace for its lower molecular weight counterparts - LLDPE, LDPE and HDPE.

**Acknowledgements:** Research reported here was supported in part by the Division of Industrial Innovation and Partnerships of the National Science Foundation under award number 1434826. This study is also supported by the National Science Foundation under Grant # IIP-1059286 to the American Society for Engineering Education.

---

[1] Jang et al, *Appl. Polym. Sci.* **2010**

[2] Kumar et al, *Polymer* **2002**

[3] Pukanszky et al, In *Mineral Fillers in Thermoplastics I*; Springer: New York, **1999**

[4] Tervoort et al, *Macromolecules.* **2002**

[5] Ronca et al, *Ind. Eng. Chem. Res.* **2015**

[6] Hambir et al, *Bull. Mater. Sci.* **2000**

# Influencing UHMWPE Molecular Weight Distributions by High Shear Polymer Modification

Patel BS<sup>1</sup>, Shanahan SE<sup>1</sup>, Janse M<sup>1</sup>, Tapsak MA<sup>1,2</sup>

<sup>1</sup>Zzyzx Polymers, Allentown, PA; <sup>2</sup>Bloomsburg University of Pennsylvania, Bloomsburg, PA  
*mtapsak@bloomu.edu*

**Introduction:** The physical properties for commodity polyolefins have steadily improved over the course of the last 30 years. Some of these developments have been accomplished by optimizing structure-process-property relationships. For example, it is known that the longest of polymer chains can act as tie molecules between crystalline lamella, thereby increasing toughness but decreasing processability. It is also known that a balance of properties is often achieved by tuning a resin's molecular weight distribution (MWD) for a given application. There have also been improvements in single site catalysts that can be used either within the same reactor or within reactor cascades to better control the resulting MWD. Unfortunately, these improvements have not translated to new UHMWPE or HXLPE materials suitable for use in medical devices. Improvements developed for commodity polyolefins do not translate to polymerization control at the very high molecular weights. But this is critical for total joint replacement (TJR) bearing inserts that require superior impact and wear resistance.

Successfully modifying UHMWPE to meet growing demands for thinner and stronger TJR bearing inserts will require precise control over the entire distribution of the polymer chain lengths, extending therefore beyond those molecular weights for which most polymerization research has found commercial success. In fact, it is likely that UHMWPE having optimal properties will have a number-average molecular weight ( $M_n$ ) which is higher than what researchers have so far achieved. In addition, an improved UHMWPE should have a narrow MWD. This will help balance processability and key physical properties such as impact strength and abrasion resistance. In order to design such materials, we have developed a proprietary technology called High Shear Polymer Modification (HSPM).

The HSPM process has evolved from a technology first developed to blend otherwise-immiscible or comingled polymers. The blending process was pioneered at Northwestern University, USA. Zzyzx Polymers expanded upon that work to develop a first principles understanding of the MWD modification mechanisms achieved by HSPM. For example, it is known that for polyethylene, the shortest polymer chains reduce mechanical properties and that the longest chains reduce processability. This is because the shorter polymer chains are not long enough to contribute to the connectivity within the material but merely act as a diluent [1]. The high relative number of end groups in these shorter chains also leads to crystalline defects [2]. In contrast, the longest polymer chains possess very low chain mobility such that coalescence across the UHMWPE particle interfaces is severely hindered [3]. To address these known limitations, the HSPM process preferentially cleaves the longest polymer chains near their midpoint. This selective chain

scission results in two new chains that contribute to a more median chain length.

Typically, polymer chemists work in a bottom-up manner to modify polymer properties by way of improvements to catalysts. There is a significant and ongoing effort to develop new polymerization schemes and catalysts for ethylene [4,5,6]. Researchers have even synthesized narrow molecular weight UHMWPE using single site catalysts [7,8]. However, the use of single site catalysts has been limited to lab-scale production. Also, the development of new catalysts for the precise control of polymer synthesis traditionally has a very slow path to commercialization because it sometimes requires special reactors and the optimization of costly catalyst materials. Furthermore, the newer single site catalyst systems tend to produce short chain branching (SCB), especially at the highest of molecular weights [9]. This is problematic because SCB causes crystal imperfections in UHMWPE, an issue which is known to reduce performance in TJR bearing components [10]. Alternatively, the HSPM process is an innovative, continuous commercial-ready top-down approach for improving the material properties of UHMWPE.

**Methods and Materials:** Gel Permeation Chromatography (GPC) was performed in close accordance with ASTM D6474-12 using a Waters GPCV2000 system. NMR spectra were obtained on a Bruker Avance 400 MHz two-channel, multinuclear NMR spectrometer equipped with an Oxford magnet. FTIR spectra were collected on a Perkin-Elmer Spectrum 400 FT-IR/FT-NIR spectrometer fitted with a universal ATR sampling accessory.

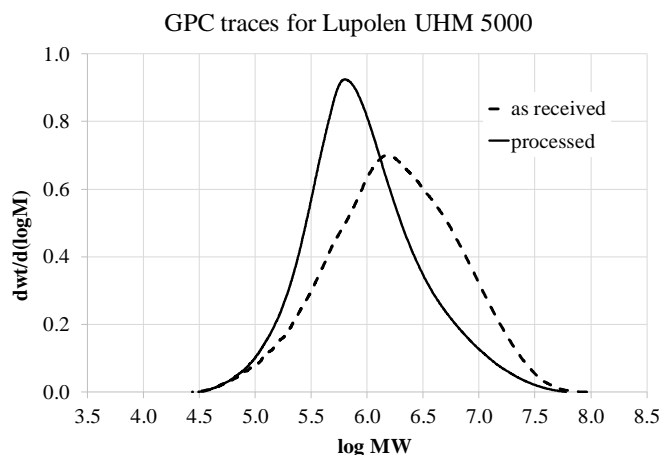
The UHMWPE materials used for this study were GUR 4022 (Celanese), U090LH (Korean Petrochemical Industry), Lupolen UHM 5000 (Lyondell Basell), and UTEC 6541 (Braskem). The UHMWPE powders were used as received.

Izod impact testing was performed according to ASTM D4020-11 guidelines. Test specimens were machined from compression molded sheets made in an electrically heated hydraulic press. Molding conditions were as follows; raise pressure to 1875 psi for two minutes, reduce pressure to 930 psi, maintain pressure and temperature at 420 °F for 45 minutes, then cool mold slowly with water for 40 minutes, eject sheet from mold.

**Results:** UHMWPE samples for this study were processed using a ZSK70 twin-screw extruder outfitted to perform HSPM at a throughput rate of 100-200 lbs. per hour. This is a continuous, solvent-free, additive-free technique that enables the efficient delivery of mechanical energy to the resin.

**Table 1.** GPC data for as received and HSPM processed UHMWPE.

Sample		M <sub>n</sub>	M <sub>w</sub>	M <sub>peak</sub>	M <sub>z</sub>	M <sub>w</sub> /M <sub>n</sub>
GUR 4022	As received	808,000	3,678,000	2,014,000	5,936,000	4.55
	Processed	465,000	1,552,000	1,023,000	4,740,000	3.33
U090LH	As received	1,697,000	5,658,000	2,774,000	16,480,000	3.33
	Processed	1,013,000	4,016,000	1,425,000	15,640,000	3.96
Lupolen UHM 5000	As received	737,000	3,785,000	1,754,000	12,230,000	5.14
	Processed	516,000	1,988,000	717,000	8,898,000	3.86
UTEC 6541	As received	1,785,000	5,903,000	1,931,000	18,310,000	3.31
	Processed	672,000	2,881,000	1,280,000	11,570,000	4.29

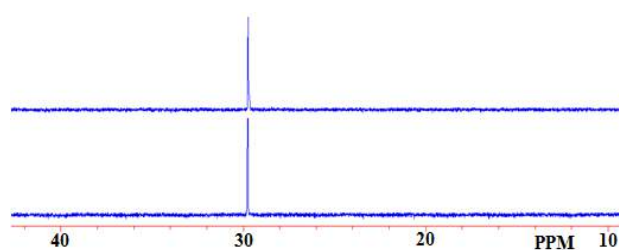
**Figure 1.** GPC traces of as received (dash line) and SSSP processed UHMWPE (solid line).

Processed material was then characterized using GPC, NMR, FTIR and Izod impact strength. **Table 1** lists the GPC data as calculated using the following calibration equation:

$$\text{Log MW} = 2.36 - 2.82V + 0.151V^2 - 0.003V^3$$

where V is the elution volume in mL. The R<sup>2</sup> value for the calibration curve was 0.9988. **Figure 1** displays an example set of as received and processed GPC traces for one of the four specimens of this study, Lupolen UHM 5000. **Figure 2** shows an expanded region of 10 to 45 PPM of the same specimens. The absence of peaks in this region indicate the scarcity of short chain branches.

**Table 2** provides Izod impact data for the Lupolen UHM 5000 samples. The 10% improvement for the HSPM processed specimen is attributed to the narrower PDI as compared to the as-received material.

**Figure 2.** <sup>13</sup>C NMR spectra for Lupolen UHM 5000 specimens.**Table 2.** Izod impact strength data on as received and SSSP processed Lupolen UHM 5000.

Sample	Impact Strength (kJ/m <sup>2</sup> )
As received	134+/-2.8
SSSP-processed	148+/-4.4

**Discussion:** In this study, we demonstrate the MWD modification of four separate UHMWPE samples using HSPM. Clear changes in molecular weight are detected by GPC, without the introduction of branching as observed by NMR or FTIR.

Furthermore, we show that some samples display a narrowing of PDI and improvement in Izod impact strength. In all cases we observed a qualitative improvement on processability. Therefore, we suggest that HSPM will serve as a useful tool for determining how UHMWPE can be improved through MWD modification. This could then facilitate the development of improved HXLPE materials suitable for use in TJR bearings.

**Acknowledgements:** Research reported here was supported in part by the Division of Industrial Innovation and Partnerships of the National Science Foundation under award number 1434826.

- [1] Tervoort et al, *Macromolecules*. **2002**
- [2] Ronca et al, *Ind. Eng. Chem. Res.* **2015**
- [3] Hambir et al, *Bull. Mater. Sci.* **2000**
- [4] Ronellenfitch et al, *Macromolecules*. **2017**
- [5] Dai et al, *Macromolecules*. **2016**

- [6] Chen et al, *Organometallics*. **2016**
- [7] Yu et al, *J. Am. Chem. Soc.* **2008**
- [8] Reinartz et al, *Organometallics*. **2003**
- [9] Sturzel et al, *Chem. Rev.* **2016**
- [10] Sobieraj et al, *J. Mech. Behav. Biomed. Mater.* **2009**

# The Roles of Stress, Lipids, and Reactive Oxygen Species in the Oxidation of UHMWPE: In Vitro Results Support Retrieval Findings

Van Citters, DW; Herzig MS; Nagaraj N; Currier BH  
Dartmouth College, Hanover, NH 03755  
[dvancitters@dartmouth.edu](mailto:dvancitters@dartmouth.edu)

## Introduction:

Despite the success and worldwide acceptance of total knee arthroplasty, in vivo oxidation threatens to limit the longevity of implanted Ultra High Molecular Weight Polyethylene (UHMWPE) bearing components. Historically, polyethylene oxidation has been attributed to the existence of irradiation induced free radicals seen in conventional gamma-inert sterilized polyethylene. Highly cross-linked polyethylene was developed to eliminate free radicals, create an oxidation resistant polymer, and reduce wear rates. However, recent retrieval analysis has demonstrated the oxidation of these materials particularly in higher-stress regions, indicating the presence of an alternative in vivo oxidative pathway facilitated by stress. This study first uses retrieved knee components to explore whether implanted UHMWPE materials, regardless of free radical content, can become susceptible to oxidative degradation by organic species present in the synovial fluid. The second portion of this study examines the roles of stress, lipids, and ROS in the oxidation of HXL UHMWPE in vitro. It is hypothesized that organic species, in the presence of reactive oxygen species (ROS), will drive the oxidation reaction in the absence of polymer free radicals.

## Methods and Materials:

**Retrieval Analysis:** Retrieved tibial inserts representing three treatment groups (EtO: n=13; Remelted HXL: n=15; Gamma Barrier: n=10) were selected from an IRB-approved retrieval database. FTIR spectroscopy was used to determine the maximum ketone (1713-1718 cm<sup>-1</sup>), ester (1735-1740 cm<sup>-1</sup>), conjugated carbonyl (1666-1686 cm<sup>-1</sup>), and average trans-vinylene index (TVI) (950-980 cm<sup>-1</sup>) in each retrieved insert. Peak heights were normalized to 1368 cm<sup>-1</sup>. Multiple scans were performed on each insert to identify regions of highest oxidation. Three eight-hour hexane extractions were conducted to evaluate the organic content in the articular, bulk, and non-articular region of each retrieval type. Extracted lipid components were derivatized with tetramethylammonium hydroxide yielding fatty acid methyl esters that were amenable to separation and detection by gas chromatography-mass spectrometry (GC/MS).

**In vitro simulation:** Based on retrieval analysis, the effects of stress, lipids, and ROS on the oxidation of GUR 1020 UHMWPE (virgin and 75 kGy irradiated/remelted) were examined individually and in various combinations. These included stress and ROS; lipids and ROS; and stress, lipids, and ROS. Stress was modeled using a previously developed rolling/sliding tribotester and a cobalt-chrome femoral head fixed to a reciprocating linear oscillator. ROS were experimentally modeled using

H<sub>2</sub>O<sub>2</sub> or O<sub>3</sub>. Mixtures of fatty acids and their methyl esters and cholesterol were used to examine the effect of lipids. Oxidation was assessed by the ketone index observed on FTIR microscopy.

## Results:

**Retrieval Analysis:** Subsurface oxidation was detected at elevated levels at the articular region in all three retrieval groups. Only the gamma barrier samples showed elevated oxidation at regions distant from the articular surface (i.e. the anterior or posterior edge). Ester was detected at increased concentrations at the articular region of all treatment groups, and was significantly lower at non-stressed regions. GC/MS revealed increased lipid content throughout the polymer (e.g. Octadecanoic acid, methyl ester), with some sterols. These were more readily found at the articular surface.

**In vitro simulation:** In isolation, stress, lipids, or ROS did not lead to an oxidation level associated with a clinically significant decline in mechanical properties. Limited oxidation was observed in the presence of H<sub>2</sub>O<sub>2</sub> alone. Oxidation was more rapid when ROS and lipids were present in solution. The combined effect of lipids and ROS was shown to be more rapid than the sum of their individual effects, indicating a synergistic reaction between the two species ( $p < 0.001$  for comparison to all other slopes). Oxidation was even more rapid when ROS, lipids, and stress acted in combination. Moreover, the FTIR ester absorbance was greater under locations of maximum stress, indicating the increased absorbance of lipids. Correspondingly, oxidation was also greater under areas of higher stress.

## Discussion:

It is well characterized that the irradiation dependent pathway produces primary radicals and secondary radicals throughout a tibial insert via scission of C-C and C-H bonds. The high concentration of free radicals leads to creation of trans-vinylene bonds and cross-links. Due to their high reactivity, allylic hydrogens are susceptible to abstraction, resulting in further radical propagation. In the absence of free radicals (e.g. remelted materials and EtO sterilized materials) ROS in the synovial fluid may directly abstract hydrogens from polyethylene chains to form a secondary radical. The GC/MS results demonstrate that lipids from the synovial fluid can enter the polyethylene surface and it is proposed that these may also react with ROS to create a secondary radical.

The results of the in vitro experiments were used to further our understanding of the oxidation kinetics. Since ROS and lipids reacted together synergistically, it is

proposed that these two species together initiate the radical pathway. Specifically, ROS may abstract hydrogen from lipids to yield alkyl and allyl radical species. In the presence of oxygen, these may react to yield peroxy radicals. Lipid peroxy and alkyl radicals may then abstract hydrogen from UHMWPE to yield a macroradical. UHMWPE macroradicals may also be generated by the action of ROS independently, although this pathway is slower. Macroradicals formed by either mechanism react via a peroxy radical intermediate to produce ketones, esters, and aldehydes. The oxidation of this peroxy radical yields an additional UHMWPE radical, leading to chain reaction propagation and the observed exponential oxidation with time in vivo.

Stress alone, and with ROS, do not result in the highest oxidation rates of UHMWPE in this work. However, in the presence of ROS and lipids, oxidation is maximum under areas of high stress, consistent with in vivo findings. Elevated ester absorbance in stressed UHMWPE suggests that stress enhances the diffusion of lipids into the polymer. These, in turn, enable more rapid oxidation.

The findings presented here represent an experimentally-validated mechanism for the oxidation of HXL UHMWPE that advances the work of prior investigators. A complete understanding of the mechanism by which this polymer degrades could inform the development of more stable polymers for total joint arthroplasty.

## **Vitamin E-Polyethylene and Non E-Polyethylene have similar short term total knee arthroplasty revision rates**

Matthew Kelly<sup>a</sup>, Guy Cafri<sup>b</sup>, Robert Namba<sup>d</sup>, Brian Fasig<sup>b</sup>, Elizabeth W. Paxton<sup>b</sup>

**Introduction:** Oxidation can lead to accelerated wear, osteolysis and implant failure following total knee arthroplasty (TKA). In vitro studies suggest decreased wear with Vitamin E-Polyethylene (E-Poly), in vivo survivorship data is lacking. The purpose of this study was to compare the risk of TKA revision when using E-Poly versus Non E-Poly.

**Materials and Methods:** Using an integrated healthcare systems registry, 805 primary TKAs with E-Poly and 1,248 without E-Poly from the same manufacturer were identified (2001-2014). The outcome of interest was time to revision surgery. Comparison of groups was based on a between-within mixed-effects semi-parametric survival model with propensity score weight. Diagnosis, ASA score, fixation, exposure, posterior stabilized, race, approach, diabetes, height, BMI, operative time, gender, age, bilateral were adjusted for as confounders in the multivariate analyses.

**Results:** There were 12 and 19 revisions for the E-Poly and Non E-Poly groups, respectively. Two year cumulative revision rates were 1.6% for E-Poly (95% CI: 0.9%-2.9%) and 1.2% for Non E-Poly (95% CI: 0.7%-2.0%). After adjusting for confounders, the HR did not reach significance (HR= .63: 95% CI=.24, 1.68, p=.358). E-Poly reasons for revision included: Arthrofibrosis (1), Failed TKA (2), Infection (7), Instability (2), and Other (1). Reasons for Non E-Poly revisions included: Arthrofibrosis (1), Aseptic Loosening (5), Failed TKA (3), Infection (9), Instability (3), and Pain (5).

**Conclusions:** Short-term results do not indicate a difference in revision rates for Vitamin E-Poly versus Non E-Poly. Longer follow-up and larger numbers are needed to determine if E-Poly is more effective than Non E-Poly.

## GUR® 1001 – A New Injection Moldable GUR to Extend the Celanese Medical Materials Portfolio

Blumoer, Frank; Cano, Camilo; Schmid, Christina; Verrocchi, Anthony; Walkenhorst, Rainer<sup>1</sup>

<sup>1</sup>Celanese Services Germany GmbH, Engineered Materials; Am Unisys-Park 1, 65843 Sulzbach (Taunus), Germany  
Rainer.walkenhorst@celanese.com

### Introduction:

Aside from other medical materials like e.g. Hostaform/Celcon POM, Celanex PBT or Vectra LCP, Celanese has offered a number of UHMW-PE grades for medical applications for decades: GUR® 1020 and GUR® 1050 as well as the analogous vitamin E containing grades GUR® 1020-E and GUR® 1050-E. All these GUR® grades are primarily used for orthopedic implant applications, namely total joint replacements. The reason for using GUR® UHMW-PE in these applications is its extraordinary wear resistance and low friction properties which are accompanied by very good mechanical properties like impact strength. GUR® 1020 and GUR® 1050 exhibit an extremely high melt viscosity due to their ultra-high molecular weights. For this reason, melt processing via screw extrusion or injection molding is not possible. The final parts are typically machined out of compression molded or ram extruded pre-forms.

To extend the Celanese portfolio for medical applications, a new grade with the name of GUR® 1001 is presented. GUR® 1001 is a low molecular weight linear polyethylene material that can be injection molded. This allows more efficient production of parts in different shapes.

### Methods and Materials:

GUR® 1001 is a newly developed injection moldable polyethylene implant grade. The properties are shown in Table 1 in comparison to GUR® 1020.

In addition, an extensive set of biocompatibility data will be presented as well as an injection molding processing guideline. It will be shown that, despite its still relatively high molecular weight, injection molding of GUR® 1001 can be done without degrading the material and that the resulting properties of molded parts are comparable to compression molded parts of GUR® 1001.

Furthermore, e-beam irradiation at different dosages has been performed to analyze property changes.

### Results:

Due to its lower molecular weight compared to GUR® 1020 and GUR® 1050, the mechanical properties of GUR® 1001 do not reach the same level of an ultra-high molecular weight polyethylene, but in certain medical applications the extraordinary wear resistance and impact strength are not required to the extent the two UHMW-PE grades offer.

Property	Unit	Test Method	GUR® 1001	GUR® 1020
Elongational stress	MPa	ISO 11 542-2	< 0,05	0,23
Average molecular weight	g/mol	Calculated from VN using Margolies equation	0,6*10 <sup>6</sup>	4,7*10 <sup>6</sup>
Average molecular weight	g/mol	Calculated from VN using ASTM equation	0,5*10 <sup>6</sup>	3,3*10 <sup>6</sup>
Density	g/cm <sup>3</sup>	ISO 1183 method A	0,95	0,93
Mass melt-flow rate MFR 190/21.6	g/10 min	ISO 1133	1,1	< 0,1
Viscosity number (VN)	ml/g	ISO 1628, part 3	500	2300
Intrinsic viscosity (IV)	ml/g	ISO 1628, part 3	500	2000
Bulk density	g/cm <sup>3</sup>	ISO 60	0,45	0,45
Impact strength (Charpy) (double 14° V-notch)	kJ/m <sup>2</sup>	ISO 11542, part 2	45	240
Wear by sand-slurry method (GUR 4120 = 100)	none	internal test method	250	100
Tensile modulus E <sub>t</sub>	MPa	ISO 527, part 1/2; test speed 1 mm/min	1150	690
Tensile stress at yield $\sigma_y$	MPa	ISO 527, part 1/2; test speed 50 mm/min	27	20
Tensile strain at yield $\epsilon_y$	%	ISO 527, part 1/2; test speed 50 mm/min	9	13
Tensile stress @ 50% strain $\sigma_{50}$	MPa	ISO 527, part 1/2; test speed 50 mm/min	18	19
Tensile stress at break $\sigma_b$	MPa	ISO 527, part 1/2; test speed 50 mm/min	no break @ 500%	> 44
Nominal elongation at break $\epsilon_b$	%	ISO 527, part 1/2; test speed 50 mm/min	> 500	> 450
Average particle size (d50)	µm	Laser scattering	110	140
2nd melting crystallinity	%	DSC	65	49
Ash content	ppm	ISO 3451-1	52	44

Table 1

### Discussion:

Celanese offers GUR® 1001 as an addition to its well established medical materials portfolio. GUR® 1001 can be injection molded, so that it offers an alternative to GUR® 1020 and GUR® 1050 for implant applications in the medical field.

# Preparation of Medical Ultra High Molecular Weight Polyethylene Fiber via Dry Spinning

Xinwei WANG<sup>1,2,3</sup>, Yongfei SUN<sup>1,2,3</sup>, Jianlong LI<sup>1,2,3</sup>

<sup>1</sup>State Key Laboratory of Polyolefins and Catalysis, Shanghai, China;

<sup>2</sup>Shanghai Research Institute of Chemical Industry Co., Ltd., Shanghai, China;

<sup>3</sup>Shanghai Key Laboratory of Catalysis Technology for Polyolefins, Shanghai, China;

w\_xv@hotmail.com

**Introduction:** Ultra High Molecular Weight Polyethylene (UHMWPE) fiber is well known as one of high performance fibers together with carbon fiber and Kevlar. With high strength, high flexibility and biocompatibility, UHMWPE fibers were widely used medical field such as shoulder fixation, knee ligament and meniscus repair. Currently, two routes are applied in UHMWPE fibers production. Decalin is used as solvent in dry route, while mineral oil is used in wet route. Comparing to wet route, dry route has advantages of short process, less solvent residual rate, fast spinning, good product quality, directly recycled solvent and environment friendly, which is more favorable used in the field of medical fiber. Wet route is widely researched in labs, on the other hand, research of dry route is relatively scarcity.

**Methods and Materials:** In this paper, high-performance UHMWPE fibers with 4 million molecular weight were prepared by advanced dry route pilot line, which was designed independently by Shanghai Research Institute of Chemical Industry (SRICI). The mechanical properties, thermal properties and microstructure of UHMWPE fibers with different draw ratio were characterized by electronic testing machine, SEM and DSC.

**Results:** Fig.2 showed that crystallinity degree of UHMWPE fibers increased from 49.57 percent to 72.17 percent with increasing drawing ratio. Comparing to as-spun fiber, well-drawn fiber's breaking strength increased from 2.35 cN/dtex to 31.53 cN/dtex, as well as 15.68 cN/dtex to 1054.78 cN/dtex improvement in breaking modulus (As shown in Fig.3). Fig.4 showed that solvent residual rate decreased from 626 ppm to 95 ppm with increasing drawing ratio.

**Discussion:** In the process, the disorder macromolecular chains was straightened, and amorphous regions turned into crystalline regions gradually, which resulted in well-ordered and compact micro-structure. Highly crystallized fiber showed better mechanical performance because uniform chains required more energy to break.

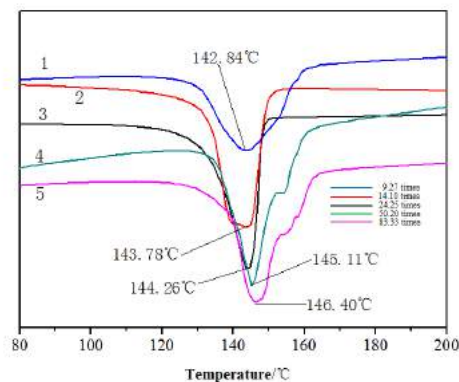


Fig.2 DSC graph of different fibers draw ratio

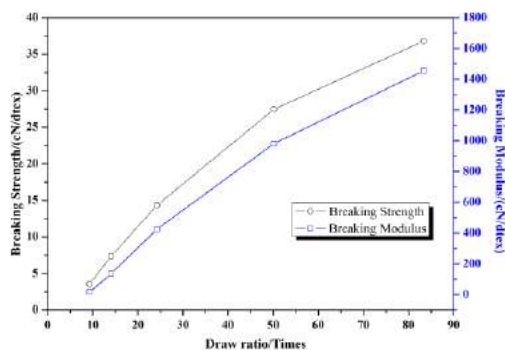


Fig.3 Mechanical properties of different fibers draw ratio

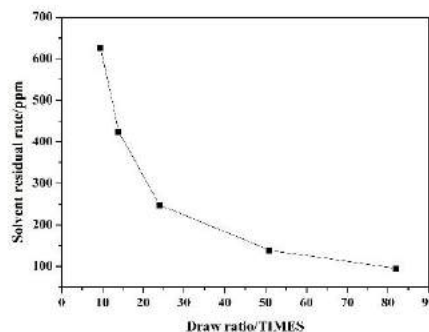


Fig.4 Solvent residual rate of different fibers draw ratio

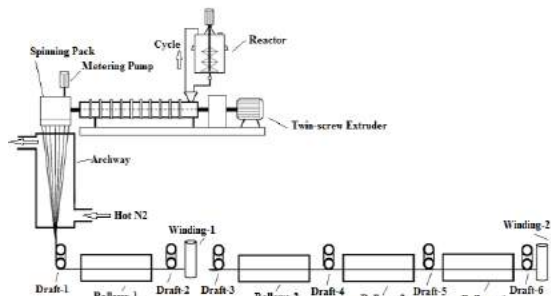


Fig.1 Flowchart of UHMWPE fiber production by Dry Spinning (SRICI)

## Antioxidant Stabilized Highly Crosslinked Polyethylene in TKA: A Retrieval Analysis

Ponzio DY, Weitzler L, deMeireles A, Esposito CI, Wright TM, Padgett DE  
Hospital for Special Surgery, New York, NY  
*wright@hss.edu*

**Introduction:** Antioxidants have been introduced into highly cross-linked polyethylene (XLPE) tibial inserts with the intentions to increase resistance to oxidation and potentially improve wear resistance. In vitro studies of antioxidant stabilized XLPE (A-XLPE) components showed higher wear resistance, less damage to articular surfaces, and lower oxidative degradation when compared to standard XLPE. Unfortunately, such in vitro pre-clinical tests may not accurately predict the oxidative resistance in total knee arthroplasty (TKA) patients, since the tibial component experiences highly complex stresses when articulating with the metallic femoral component. We evaluated surface damage, crosslink density, and oxidation levels in retrieved antioxidant stabilized XLPE (A-XLPE) inserts and compared the results to those from a matched cohort of standard remelted XLPE inserts.

**Methods:** From 2011 to 2016, nineteen A-XLPE tibial inserts were retrieved during revision TKA after a mean time in vivo of  $15 \pm 10$  months and matched to nineteen XLPE on the basis of age, BMI, length of implantation (LOI), and indication for revision. The inserts were mapped to calculate the percent areas of different damage modes on their articular surfaces. Crosslink density of the polyethylene was calculated through swell ratio testing, and Fourier transform infrared spectroscopy was used to calculate oxidation at both loaded and unloaded regions of the inserts (Fig. 1).

**Results:** Overall, A-XLPE and XLPE inserts showed low levels of damage to their articular surfaces (Fig. 2), with total mean percent damage modes of 61% and 51%, respectively (out of a potential maximum score of 700%). A-XLPE inserts had higher rates of burnishing ( $p = 0.02$ ) and abrasion ( $p = 0.004$ ) and lower rates of pitting ( $p = 0.01$ ) compared to XLPE, but no difference in crosslink density ( $p > 0.05$ ) was found at loaded and unloaded regions. A-XLPE showed higher oxidation indices at the unloaded surface region when compared to XLPE ( $p < 0.01$ ); however, there were no differences in oxidation levels at the loaded regions ( $p > 0.05$ ).

**Conclusion:** Despite theoretical benefits and added cost, retrieval analysis of A-XLPE did not find a clinically relevant difference in articular surface damage, crosslink density, or oxidation levels compared to standard XLPE tibial inserts.

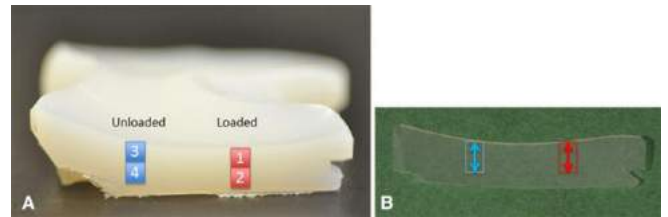


Fig. 1 Regions at which crosslink density (left) and Fourier transform infrared spectroscopy measurements were made on each insert.

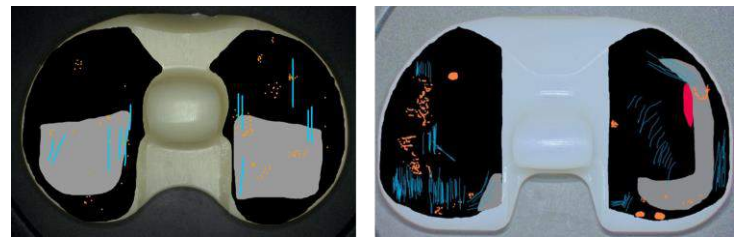


Fig. 2 Damage maps for (left) A-XLPE (Biomet E1 Vanguard with LOI of 17 mos) showing more burnishing and less pitting compared to (right) XLPE (Zimmer Prolong NexGen PS with LOI of 16 mos) that has more deformation.

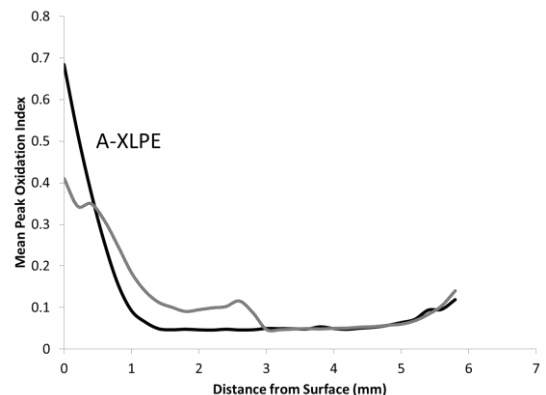


Fig. 3 Oxidation index as a function of distance from the surface for both types of polyethylene materials.

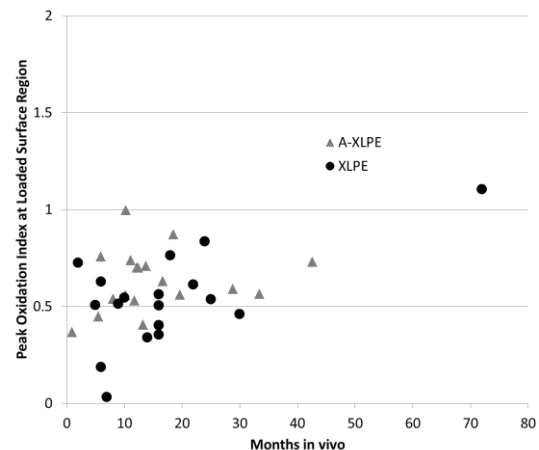


Fig. 4 Peak oxidation index as a function of months in vivo at the loaded surface region for both polyethylene materials.

## Surface Damage and Oxidation are Reduced in Highly Crosslinked Polyethylene Tibial Inserts at Midterm Follow-up

Stavrakisa A, Weitzler L, Wright T, Padgett D

Hospital for Special Surgery, New York, NY

wright@hss.edu

**Introduction:** Background: Highly crosslinked ultrahigh-molecular weight polyethylene (XLPE) has been associated with reduced wear in total hip arthroplasty when compared to net compression molded polyethylene (compPE); however, minimal research evaluating polyethylene damage in XLPE tibial components in total knee arthroplasty exists. The purpose of this study was to evaluate damage and material properties in these components at midterm (minimum of 2.5 years) follow-up.

**Methods:** Nineteen XLPE tibial inserts with a minimum 30 months in vivo use were identified in our IRB-approved implant retrieval system. Insert matching with 19 compPE retrieved inserts was done based on age at index surgery, BMI, sex, and length of implantation. Articular surface damage was assessed using a subjective grading system. Crosslink densities (measured by swell ratio testing) were obtained for the XLPE inserts, and oxidation indices (OI, measured by Fourier transform infrared spectroscopy) were measured at loaded and unloaded surface and subsurface regions for both groups (Fig. 1).

**Results:** The compPE group had a significantly higher overall damage score than the XLPE group ( $54 \pm 14$  versus  $41 \pm 11$ ,  $p=0.002$ ), primarily due to greater damage to the post-cam interface of posterior stabilized inserts in the compPE group ( $p<0.001$ ). Crosslink density of the XLPE group was significantly lower at the loaded surface ( $0.159 \text{ mol/dm}^3$ ) region than either of the unloaded regions ( $0.183 \text{ mol/dm}^3$ ) ( $p<0.05$ , Fig. 2). CompPE peak OI was 1.67 and 1.38 in the loaded and unloaded surface regions, respectively. These values were greater than XLPE peak OI in both loaded (0.61) and unloaded (0.46) regions of the surfaces ( $p<0.001$ ).

**Conclusion:** Our findings suggest that XLPE experiences less damage and oxidation at mid-term (minimum of 2.5 years) follow-up when compared to compPE. A peak OI greater than 1.0 in the compPE group suggests that some degradation in mechanical properties had occurred, possibly explaining the greater damage in the compPE group when compared to the XLPE group. Information from longer term retrievals will determine whether these trends continue and be associated with polymer degradation.

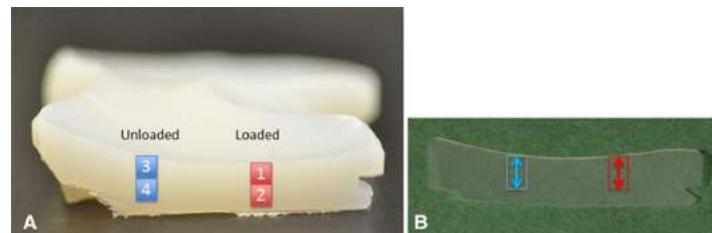


Fig. 1 Regions at which crosslink density (left) and Fourier transform infrared spectroscopy measurements were made on each insert.

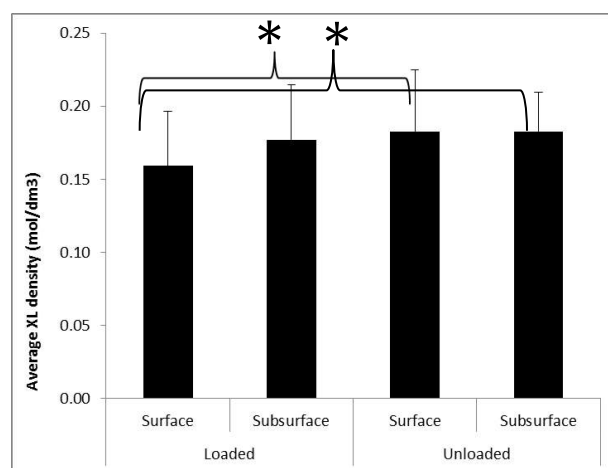


Fig. 2 Crosslink density measurements obtained in the loaded and unloaded regions shown in Figure 1 (\*= $p<0.05$ ).

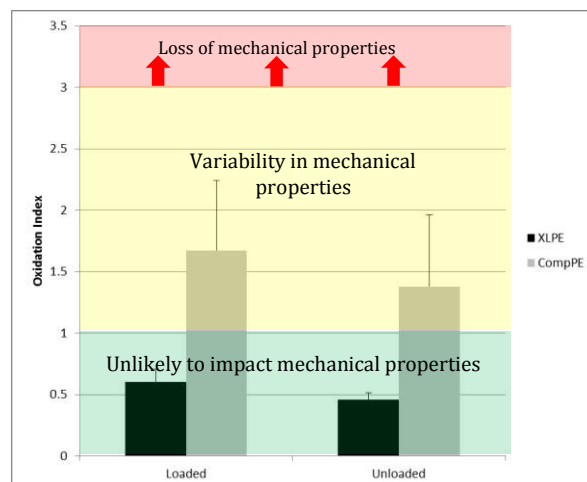


Fig. 3 Oxidation index measurements obtained in the loaded and unloaded regions shown in Figure 1.

## Development and optimization of a model to measure in vitro cellular response to UHMWPE wear debris

Yarrow, LE<sup>1</sup>; Williams, S<sup>1</sup>; Hewitt, E<sup>2</sup>; Tipper, JL<sup>1,2</sup>

<sup>1</sup>Institute of Medical and Biological Engineering, School of Mechanical Engineering, University of Leeds, Leeds, UK;

<sup>2</sup>Faculty of Biological Sciences, University of Leeds, Leeds, UK.

mnley@leeds.ac.uk

### Introduction:

Inert polyethylene wear debris, produced by metal (and ceramic) on polyethylene gold standard hip replacements, stimulates a foreign body response but is unable to be chemically broken down. The subsequent frustrated macrophage response leads to osteolysis and aseptic loosening (Green et al, 1998). Osteolysis and aseptic loosening are the leading causes of hip replacement revision surgery (National Joint Registry 13<sup>th</sup> Annual Report 2016). In order to reduce the volume of UHMWPE wear debris produced, polyethylene can be crosslinked. Crosslinking is achieved by gamma irradiation, which can alter the polymers mechanical properties if all free radicals are not terminated during the process. Antioxidants can be added to quench free radicals to prevent oxidative embrittlement (Bladen et al, 2013a). Furthermore, the addition of antioxidants appears to reduce the inflammatory response to UHMWPE wear debris (Bladen et al, 2013b). If these anti-inflammatory properties can be more fully understood then the longevity of total joint replacements may be improved in the future.

Peripheral blood mononuclear cells (PBMNC's) cultured on agarose gel encapsulating UHMWPE wear debris is the model often used to evaluate cellular responses to UHMWPE wear debris. UHMWPE debris must be encapsulated, as it is less dense than water. The agarose can be centrifuged to create a 2D surface layer of debris (Green et al, 1998) or left uncentrifuged with particles randomly dispersed to create a 3D model (Liu et al, 2015). The model has been optimised by increasing cell seeding density, increasing the gel volume, decreasing the concentration of agarose in the gel and increasing particle volume (Gowland, 2014). However the model still has major drawbacks. Most cells do not penetrate the gel and, as the gelation of agarose is heat dependent, the cells cannot be added to the gel beforehand to create a truly 3D model. Additionally, as PBMNC's are primary cells, there is poor reliability of data due to donor variation. There is also a limit to how many cells can be obtained per donor. There is therefore a need to improve the current model in terms of cell type and the type of gel used. This study investigated the use of RAW 264.7 murine macrophages in collagen gel. RAW 264.7 murine macrophages are a cell line and therefore it is easy to obtain large cell numbers whilst donor variation is not an issue unlike PBMNC's. Collagen is pH dependent rather than heat dependent; allowing cells and particles to be encapsulated simultaneously creating a truly 3D model. The aim of this study was to assess the viability of this cell type in collagen gel and to assess whether this combination of cell type and gel type was capable of supporting a reliable

cytokine output in response to model polyethylene particles.

### Methods and Materials:

#### *Cell culture:*

RAW 264.7 murine macrophages were grown in vitro in supplemented Dulbecco's Modified Eagles Medium (DMEM).

#### *Gel preparation:*

Collagen gels were prepared by mixing 80% (v/v) collagen and 10% (v/v) 10X Minimum Essential Medium (MEM); the phenol red pH indicator acts as a colorimetric measure indicating when gelation has occurred. Sodium hydroxide (1.94M) was added dropwise to the mixture until a peachy pink colour was achieved. The cells/media/particles (4.2% (v/v)) was then added before the gel was pipetted into 48 well plates – 200 µl per well.

#### *Viability studies:*

Cells were seeded in type I collagen. Cells were seeded at densities of  $1 \times 10^5$ ,  $5 \times 10^4$  and  $1 \times 10^4$  cells per well ( $n=4$ ) and the viability of each combination was assessed over 3 days using the ATP-lite assay (Perkin-Elmer). Media only negative controls and cells plus dimethyl sulfoxide (DMSO – 17% (v/v)) positive controls were used.

#### *Cytokine output studies:*

Ceridust®, a low molecular weight polyethylene powder, was suspended in DMEM and filtered into the following size ranges:  $>10\mu\text{m}$ ,  $1 - 10\mu\text{m}$  and  $0.1 - 1\mu\text{m}$ . Fluospheres ( $0.2\mu\text{m}$ ), spherical latex particles with a fluorescent tag that induce a defined inflammatory response, and Ceridust® were then combined with collagen gel (along with  $1 \times 10^5$  cells per well). The viability of the cells was measured using the ATP-lite viability assay (Perkin-Elmer) at 12 hours. The culture supernatants at these time points were harvested and frozen at  $-80^\circ\text{C}$  until used in Enzyme-Linked Immunosorbant Assay (ELISA). ELISA assessed TNF- $\alpha$  output at 12 hours. A cells only negative control and a cells plus Lipopolysaccharide (LPS) ( $200 \text{ ngml}^{-1}$ ) positive control were included.

#### *Statistical analysis:*

The data from both assays was analysed using the student's T test. Statistical significance was displayed at  $p<0.05$ . Data was scaled up for both assays to reflect the full volume of cells/supernatant per well.

### Results:

#### *Viability studies:*

RAW 264.7 murine macrophages exhibited an overall increase in viability when cultured in collagen over the course of 3 days (Fig. 1). For the lower cell seeding densities of  $1 \times 10^4$  cells per well and  $5 \times 10^4$  cells per well, this increase continued over the course of the entire assay whereas, for the highest cell seeding density of  $1 \times 10^5$  cells per well, the viability increased until day 3 after

which the viability decreased. Cells treated with DMSO clearly showed poor cell viability, which decreased rapidly over the course of the assay.

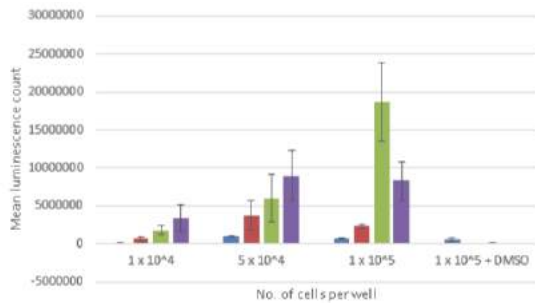


Figure 1. RAW 264.7 murine macrophage viability in collagen.

#### Cytokine output studies:

RAW 264.7 murine macrophages cultured with Ceridust® and fluospheres in collagen gels produced a measurable TNF- $\alpha$  cytokine output to all conditions (Fig. 2). The cells only condition produced a background of approximately 200 pg.ml<sup>-1</sup> TNF- $\alpha$  and the response to 1 – 10 $\mu$ m ceridust was lower than this. All other particle conditions produced significantly higher TNF- $\alpha$  release than the cells only negative control. The cells plus LPS positive control showed an output of approximately 4600 pg.ml<sup>-1</sup> of TNF- $\alpha$  after 12 hours (not shown here).

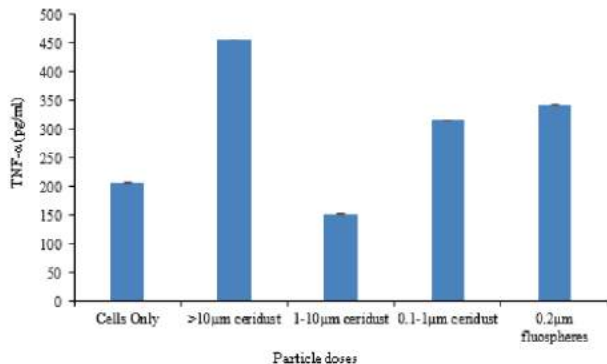


Figure 2. TNF- $\alpha$  cytokine output from RAW 264.7 murine macrophages cultured with Ceridust® and fluospheres in collagen after 12 hours of culture.

#### Discussion:

There was a general upwards trend in viability over the course of 3 days for  $1 \times 10^4$  and  $5 \times 10^4$  cells per well, however the students T test showed the differences in viability over the 3 days were not significant. The cells seeded at  $1 \times 10^5$  cells per well also increased in viability – this was significant – but experienced a significant decrease in viability after 3 days. Since cytokine release tends to be measured after 24 hours, this decrease in viability should not be relevant to any future studies as cells will not be used beyond 24 hours. Additionally, the positive control group clearly showed a significant decrease in viability in response to DMSO. It therefore

appears that, overall, collagen gel has no adverse effect on the viability of RAW 264.7 murine macrophages.

RAW 264.7 murine macrophages were able to produce a significant TNF- $\alpha$  response to all but one particle condition. A study by Green et al (1998) showed C3H murine peritoneal macrophages released similar levels of TNF- $\alpha$  in response to culture with Ceridust® particles in agarose gels. This implies that this combination of cell type and gel type shows some promise as a potential improved 3D model for generating a reliable cytokine response to UHMWPE wear debris.

#### Conclusion:

From the data present, it appears that RAW 264.7 murine macrophages in collagen may be suitable for modeling the 3D in vitro response to UHMWPE wear debris as the cells are able to produce a reliable cytokine response to known model particles. Further work into a combination of various cell and gel types to improve the reliability and accuracy of the existing model should also be carried out to find the most suitable combination for the task.

#### Future Work:

The author is currently conducting a larger study comparing multiple cell types - PBMC's, U937 human histiocytes and RAW 264.7 murine macrophages – and multiple gel types – agarose and collagen. U937 human histiocytes are a reliable cell line alternative to PBMC's (Matthews et al, 2001) however they lack the sensitivity of murine macrophages (Matthews et al, 2000). The aim of this study is to assess the viability of the cells in both gel types and to assess whether the various combinations of cells and gels are capable of exhibiting a reliable cytokine output in response to model polyethylene particles; the goal being to produce a reliable, reproducible in vitro cellular model of osteolytic response.

#### References:

- National Joint Registry 13<sup>th</sup> Annual Report – 2016
- T.R. Green, J. Fisher, M. Stone, B. M. Wroblewski and E. Ingham. (1998). Polyethylene particles of a 'critical size' are necessary for the induction of cytokines by macrophages in vitro. *Biomaterials*. 19 (24), pp. 2297 – 2302.
- C.L. Bladen, L. Tzu-Yin, J. Fisher and J.L. Tipper. (2013a). In vitro analysis of the cytotoxic and anti-inflammatory effects of antioxidant compounds used as additives in ultra high-molecular weight polyethylene in total joint replacement components. *Journal of biomedical materials research Part B*. 101B, pp. 407-413.
- C.L. Bladen, S. Teramura, S.L. Russell, K. Fujiwara, J. Fisher, E. Ingham, N. Tomita and J.L. Tipper. (2013b). Analysis of wear, wear particles, and reduced inflammatory potential of vitamin E ultrahigh-molecular-weight polyethylene for use in total joint replacement. *Journal of biomedical materials research Part B, Applied biomaterials*. 101 (3), pp. 458-66.
- A. Liu, L. Richards, C. L. Bladen, E. Ingham, J. Fisher and J. Tipper. (2015). The biological response to nanometer-sized polymer particles. *Acta Biomaterialia*. 23, pp. 38 – 51.
- N. Gowland. (2014) Ph.D Thesis. University of Leeds.
- J. B. Matthews et al. Comparison of the response of primary murine peritoneal macrophages and the U937 human histiocyte cell line to challenge with in vitro generated clinically relevant UHMWPE particles. *Biomed Mater Eng*. 2000: 10(3-4), pp. 229 – 240.
- J. B. Matthews, T. R. Green, M. H Stone, B. M. Wroblewski, J. Fisher and E. Ingham. Comparison of the response of three human monocytic cell lines to challenge with polyethylene particles of known size and dose. *Journal of materials science: materials in medicine*. 2001: 12 (3), pp. 249 – 258.